Lunar and Planetary Laboratory
Department of Planetary Sciences

West Texas: Kilbourne Hole, Sierra Madera and Odessa Crater Complex

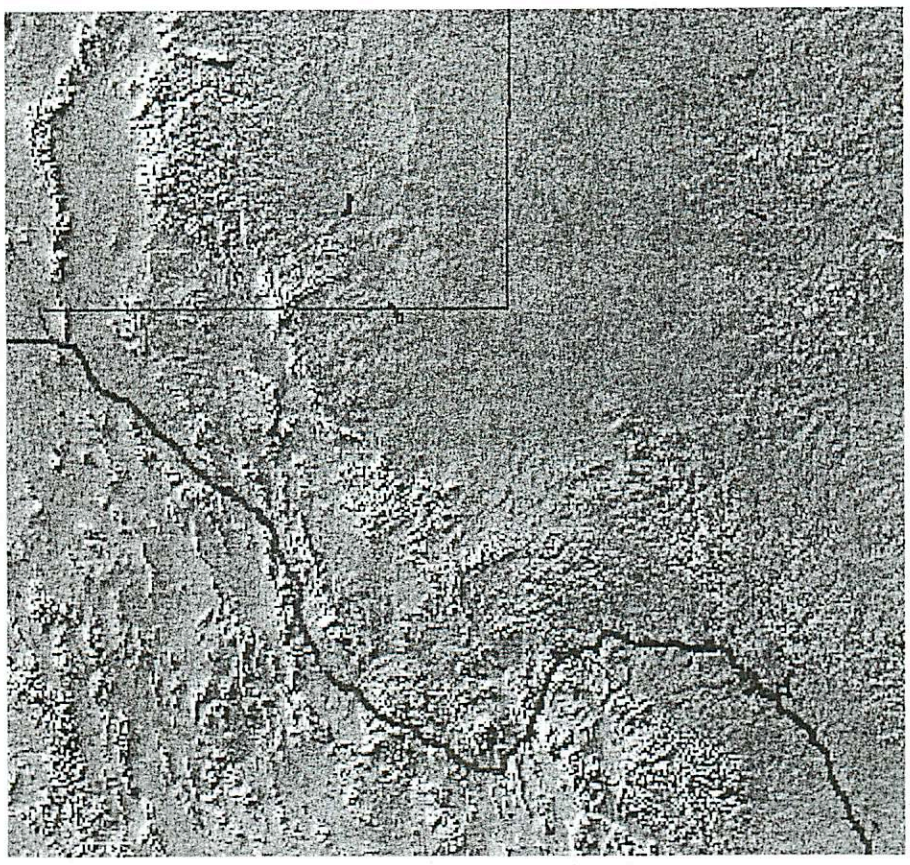

Planetary Geology Field Practicum
PTYS 594A
March 31 – April 4, 2004

The University of Arizona
Tucson, Arizona

Table of Contents

West Texas: Kilbourne Hole, Sierra Madera and Odessa Crater Complex

Planetary Geology Field Practicum
PTYS 594a
March 31 – April 4, 2004

Itinerary
PtyS 594a - Spring 2004
Kilbourne Hole, Sierra Madera Crater, & Odessa Crater

Wednesday - March 31

Drivers pick up vehicles from UA Motor Pool (beginning at 6 am)
Drivers pick up radios and road emergency kits from Gould-Simpson locker
(One or two drivers can agree to do this, rather than all drivers)
Drivers arrive at LPL loading dock no later than 7:30 am.

7:30 am — Load vehicles at the LPL loading dock.

8:15 am — Vehicles begin rolling
Campbell/Kino south to I-10
I-10 east, towards El Paso

12:00 pm — Lunch in vicinity of Deming, New Mexico

12:45 pm — Vehicles begin rolling again; continue east on I-10

Routes to Kilbourne Hole:
From I-10, between Deming and Las Cruces
Turn S on frontage road at exit 116
Follow road B4 to intersection with A17
Turn S to vicinity of Kilbourne Hole

From La Union, New Mexico
Proceed to NW edge of town
At the fork, take Dona Ana County Road A-020 on the left of fork
Proceed W on A-020 to the RR tracks
Cross RR tracks, turn right at the T
Proceed NW
Cross 2 cattle guards, then turn left on the second road, Dona Ana County Road A-011
Proceed W on A-011
Pass A-016 and A-015 intersections; Continue W to Kilbourne Hole

From El Paso, Texas
0.0 mi Mesa St. (Route 20) and I-10
Drive W on Mesa St., which becomes Country Club Rd.
Stay on TX-260 at fork with TX-20 (2.5 mi)
2.5 mi State line. Continue straight on Route 1884, entering NM (0.7 mi)
3.2 mi At junction with NM-273, turn right (1.6 mi)
4.8 mi Turn left at junction with Santa Teresa Aeropuerto; Dona Ana County NM A-17 (2.6 mi)
7.4 mi Turn left on paved road at sign for John Nobles, Inc. (pink stripe on building) (0.3 mi)
7.7 mi Dirt road begins (0.1 mi)
7.8 mi Bear right at fork, just after RR tracks (0.85 mi)

8.65 m Jct. AC-3; bear right at fork; RR tracks on right (0.55 mi)
9.2 mi Cross cattleguard (4.8 mi)
14.0 m Cross cattleguard; turn left toward JCJ Ranch. Mount Riley and East Portillo Mountains ahead on the horizon until next turn (10.2 mi)
24.2 m Road passes over first flows of the Afton-Aden volcanic field (1.1 mi)
25.3 m Pass road on right (0.3 mi)
25.6 m Turn right towards Hunt's Hole on prominent dirt road; continue around left side on graded road (1.3 mi)
26.9 m Gate (close after passing through, if closed at approach) (1.0 mi)
27.9 m Push up lava flow on the right, ahead (1.7 mi)
29.6 m South end of Kilbourne Hole

~3:30 pm Arrive Kilbourne Hole
Examine base surge deposits on S rim of maar crater
Peter: Maar formation and surge deposits at Kilbourne Hole

5:00 pm Set up camp

Thursday - April 1

8:00 am Pack camp and prepare for hike **(water, sunscreen, etc.)**
8:30 am Hike partway around Kilbourne Hole, collecting crustal and mantle xenoliths
Back at camp, assemble a lithostratigraphic column with collected samples
Mandy: crustal xenoliths and implications for crustal evolution
Celinda: mantle xenoliths and implications for mantle evolution

11:30 am Lunch

12:15 pm Return to I-10, continue east through El Paso
Where I-10 and I-20 branch, take I-20 left (north) fork
Continue on I-20 through the town of Monahans

~6:45 pm Set up camp at Monahans Sandhills State Park
(NOTE: We lose an hour between Kilbourne Hole and Monahans due to time change)

Friday - April 2

7:30 am Rolling out of camp (**EARLY** start)
Take SR 18 south towards Fort Stockton

8:30 am Meet Mr. Lyda in Fort Stockton

8:45 am Take US 385 south to La Escalera Ranch and Sierra Madera *(complex)* impact crater

9:15 am Arrive at ranch and begin examining Sierra Madera impact crater
Surrounding uplifted hills
Gwen: What are the sizes of the transient and final craters? How has erosion modified the (apparent) size of the structure?
Maki: Discuss the age of the crater, its uncertainty, and how it might be

better determined in the future

North side of central uplift

Be prepared for hiking (water, sunscreen, etc.)

Tamara: Describe the impact breccias and discuss their formation

Abby: Describe shatter cones and discuss their formation

Oz: Discuss fault accommodation in the structural uplift/central peak and compare with that at Upheaval Dome

12:00 pm — Return to trucks for lunch

12:45 pm — Continue examining Sierra Madera impact crater

Southwest side of central uplift

Be prepared for hiking (water, sunscreen, etc.)

John: Describe shock-metamorphism in crystalline targets and compare with that seen here in sedimentary target material.

Jade: What was the environment like at the impact site at the time of impact? What were the environmental effects of this impact event?

Oleg: Was there any post-impact hydrothermal activity? If so, what type of evidence should one find? If not, what other target conditions or size of impact would be needed to generate hydrothermal activity?

4:00 pm — Begin drive back to Monahans Sandhills State Park

5:30 pm — Return to camp

Carl: Monahans meteorite fall and the significance of its halite

Saturday - April 3

8:30 am — Break camp

Travel east on I-20 towards Odessa

9:10 am — Arrive at Odessa *(simple)* impact craters

Examine the main crater and largest secondary crater

Jim: Describe the structures in the Odessa impact crater field

Curtis: Fragmentation of iron asteroids in the atmosphere and the formation of multiple crater fields

Jason: Formation of impact melt and impact melt spherules

Tamara: May have more to say about sedimentary breccias

Jani: Outline an exploration strategy for craters like those at Odessa and the ones at the Mars Exploration Rover landing sites

12:00 pm — BBQ lunch as guests of Mr. Rodman

1:15 pm — Begin return drive to Tucson

I-20 west towards Van Horn

Merge with I-10 west, continue through El Paso

6:00 pm — Camp at Kilbourne Hole or Aguirre Springs

Route to Aguirre Springs

I-10 west to Las Cruces

I-25 north towards Albuquerque
Before leaving Las Cruces, exit east onto US Route 70 (towards Organ)
After 15-20 miles, turn south onto road to Aguirre Springs NRS

(NOTE: We regain an hour of time between Odessa and the Las Cruces area)

Sunday - April 4

8:30 am Break camp
Return to Tucson (arriving mid-afternoon)

Route for West Texas field trip

← I-10 to and from Tucson

5

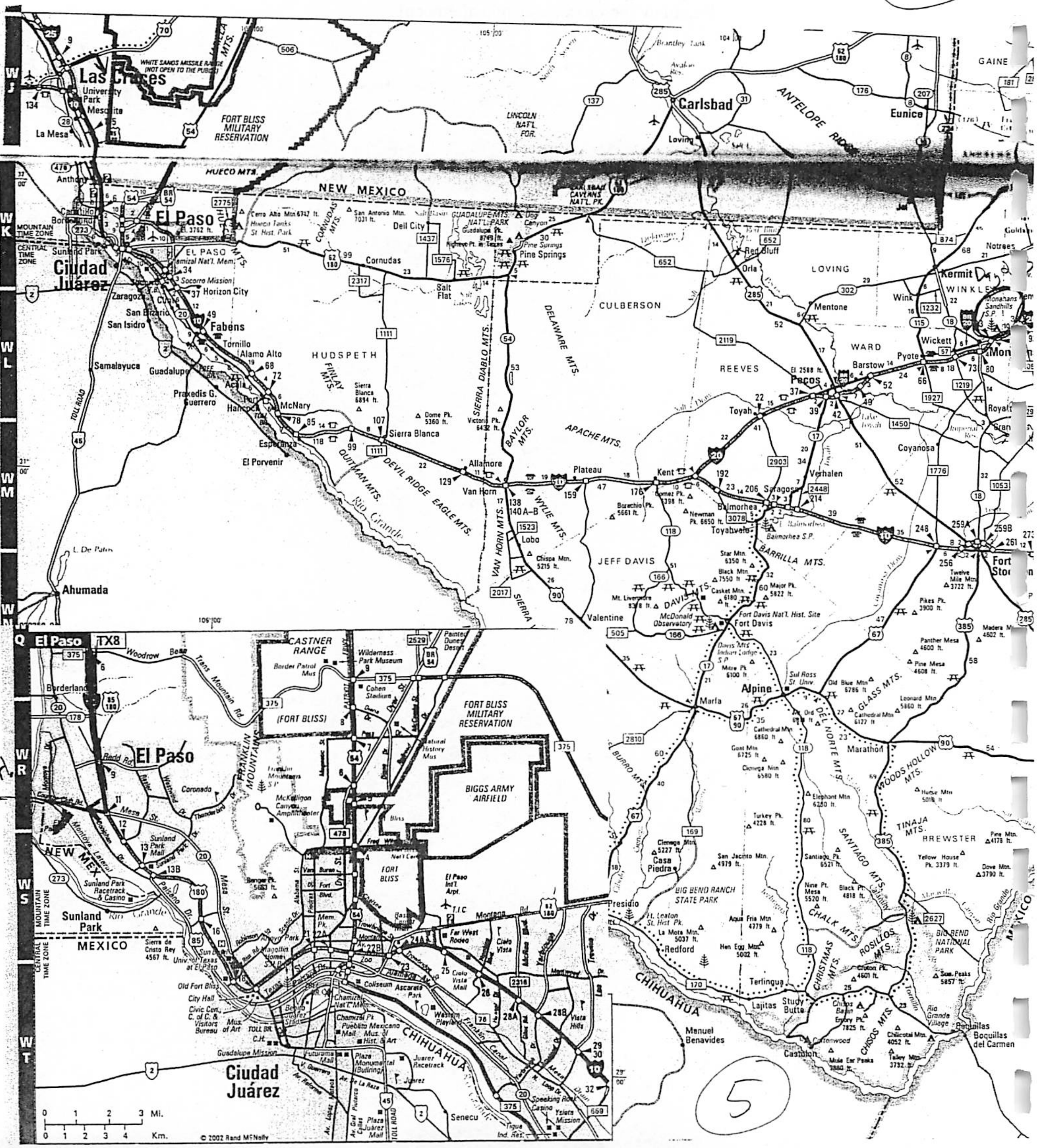

to K.H.

5

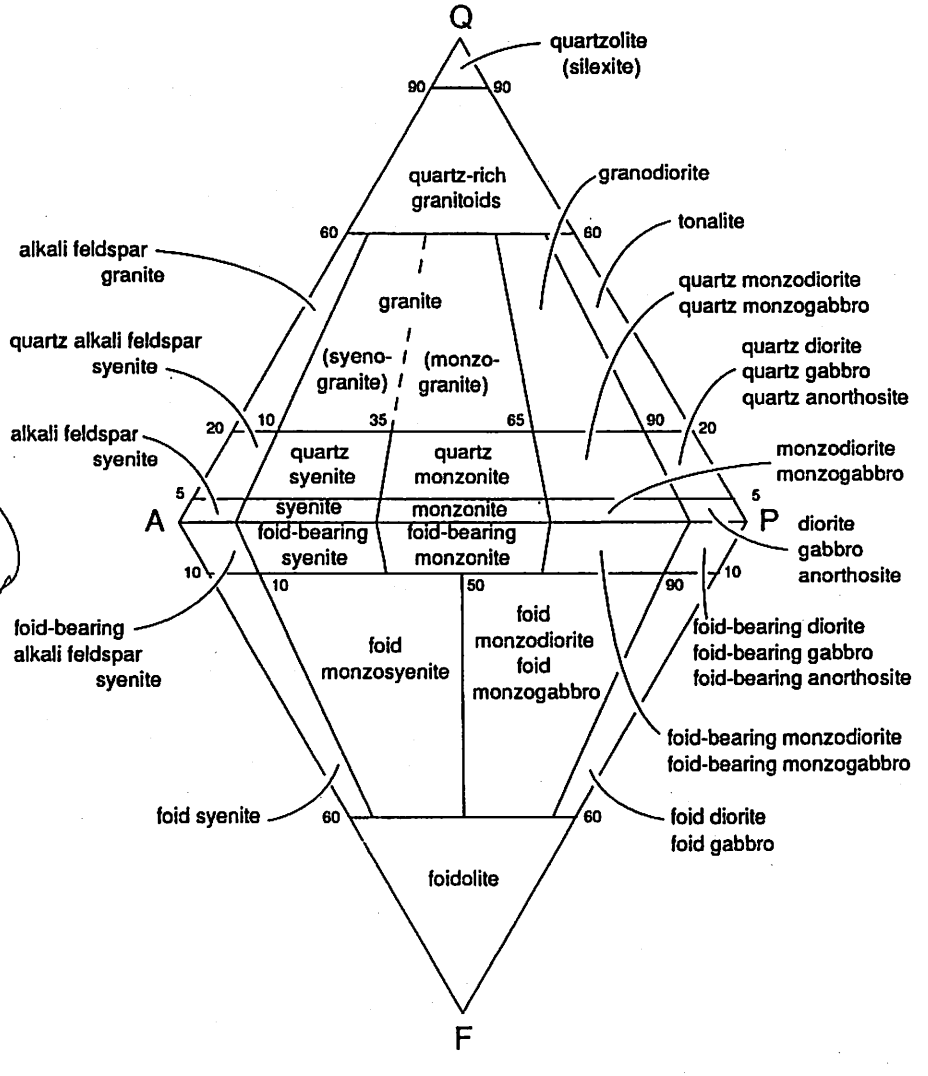

Fig. B.4. Classification and nomenclature of plutonic rocks according to their modal mineral contents using the QAPF diagram (based on Streckeisen, 1976, Fig. 1a). The corners of the double triangle are Q = quartz, A = alkali feldspar, P = plagioclase and F = feldspathoid. However, for more detailed definitions refer to section B.2. This diagram must not be used for rocks in which the mafic mineral content, M, is greater than 90%.

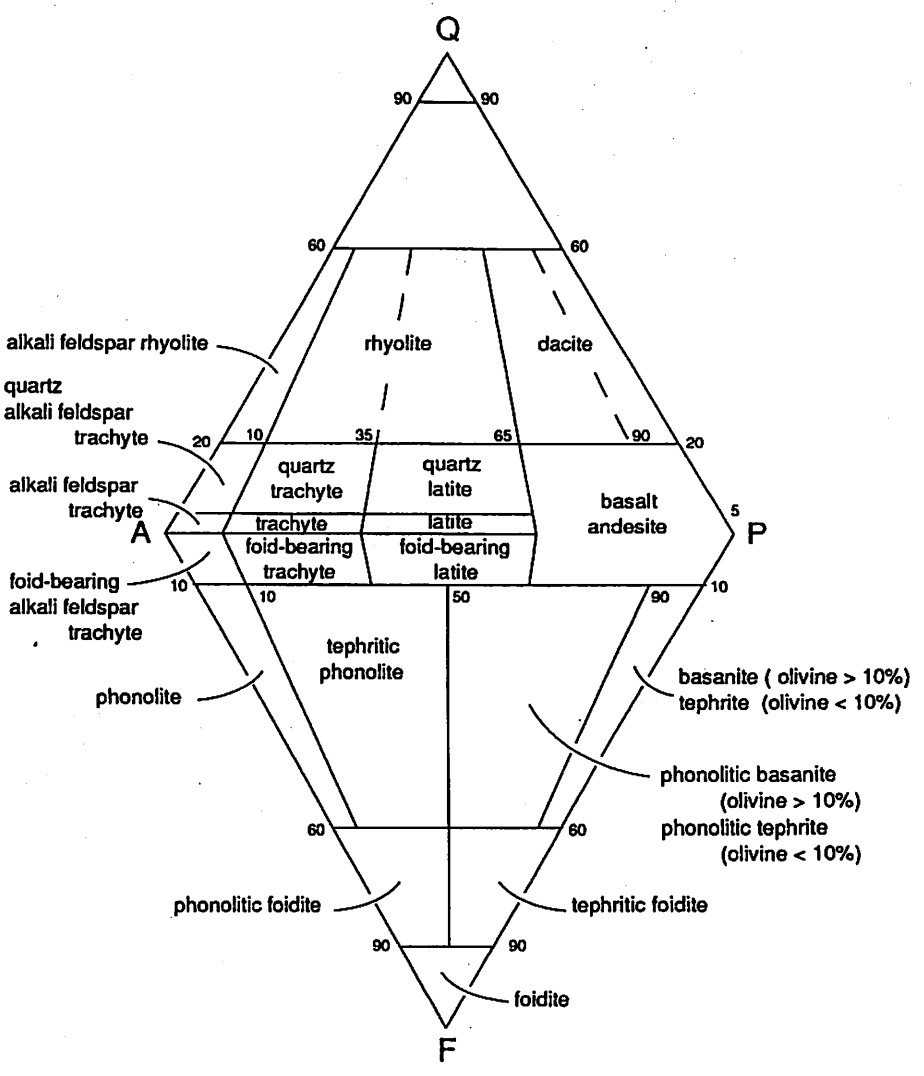

Fig. B.10. Classification and nomenclature of volcanic rocks according to their modal mineral contents using the QAPF diagram (based on Streckeisen, 1978, Fig. 1). The corners of the double triangle are Q = quartz, A = alkali feldspar, P = plagioclase and F = feldspathoid. However, for more detailed definitions refer to section B.2.

"Classification of Igneous Rocks and Glossary of Terms" Le Maitre, ed. Blackwell Scientific Publications (1989)

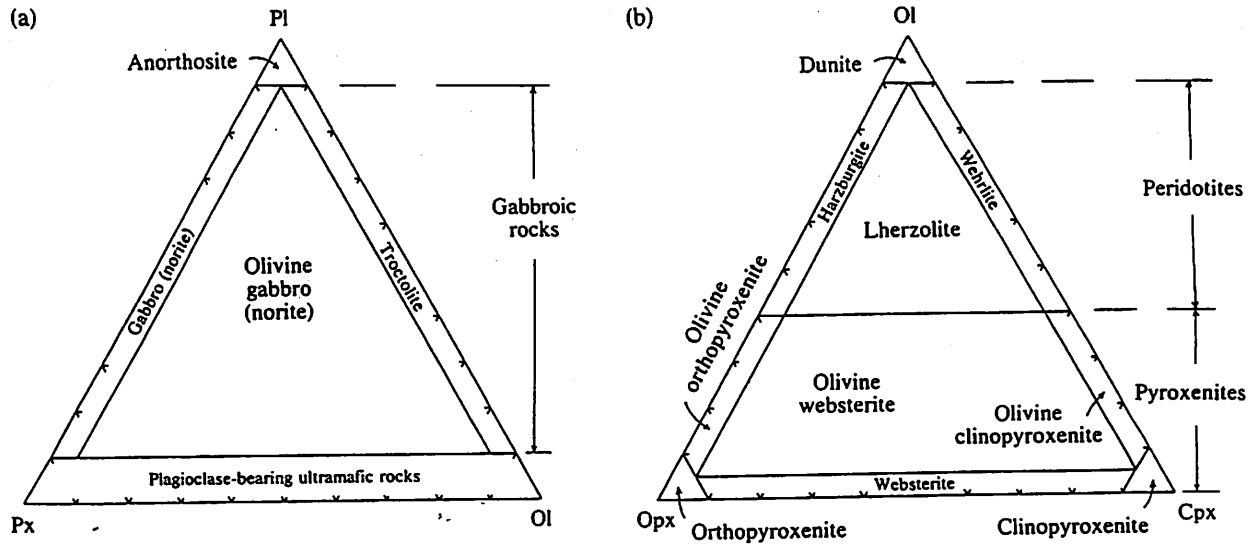

Figure 5-26 Classification of phaneritic rocks comprised of some combination of plagioclase, olivine, and pyroxene. (a) Rocks with major amounts of plagioclase (usually labradorite–bytownite). The field of gabbro is large and modifying prefixes are helpful, such as feldspathic gabbro, leuco-gabbro, olivine-rich gabbro, and so on. Gabbro in which the pyroxene is principally orthopyroxene can be called norite. (b) Classification of ultramafic phaneritic rocks comprised of olivine and pyroxenes. [After A. Streckeisen, 1979, Classification and nomenclature of volcanic rocks, lamprophyres, carbonatites, and melilitic rocks: Recommendations and suggestions of the IUGS Subcommission on the Systematics of Igneous Rocks, *Geology* 7.]

Best, "Igneous & Metamorphic Petrology"

FIG. 13.47. *(a)* Pyroxene compositions in the system $CaSiO_3$-$MgSiO_3$-$FeSiO_3$. General compositional fields are outlined. Representative tielines across the miscibility gap between augite and more Mg-Fe-rich pyroxenes are shown. The "augite" field is labeled with quotation marks because all augite compositions contain considerable Al which is not considered in this triangular composition diagram.

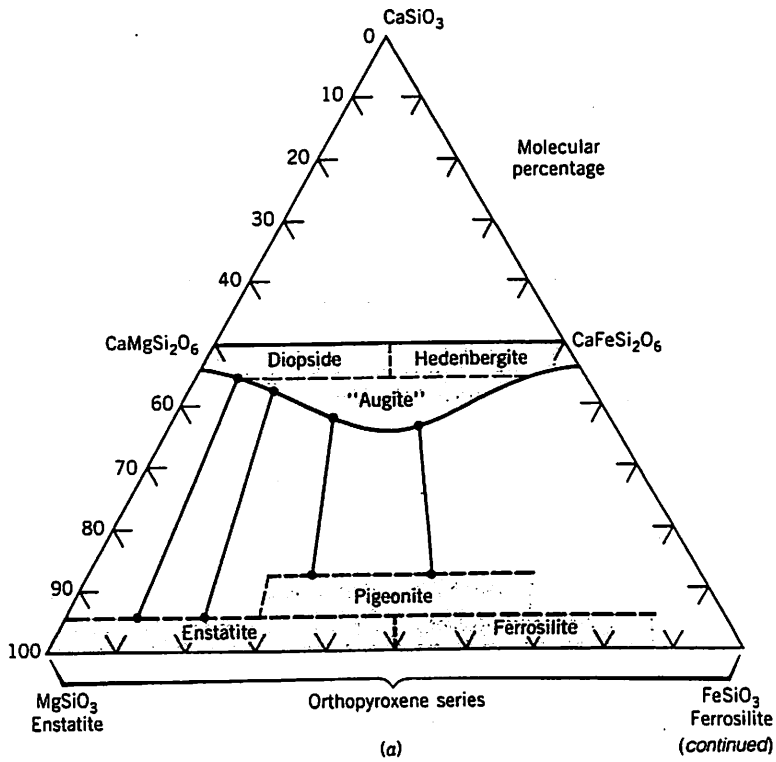

Klein & Hurlbut, "Manual of Mineralogy"

(continued)

7

MINERAL NAMES

Mineral	Formula
Åkermanite	$Ca_2MgSi_2O_7$
Alabandite	(Mn,Fe)S
Albite	$NaAlSi_3O_8$
Andradite	$Ca_3Fe_2Si_3O_{12}$
Anorthite	$CaAl_2Si_2O_8$
Apatite	$Ca_3(PO_4)_2$
Aragonite	$CaCO_3$
Armalcolite	$FeMgTi_2O_5$
Augite	$Mg(Fe,Ca)Si_2O_6$
Awaruite	Ni_3Fe
Baddeleyite	ZrO_2
Barringerite	$(Fe,Ni)_2P$
Bassanite	$CaSO_4 \cdot 1/2H_2O$
Bloedite	$Na_2Mg(SO_4)_2 \cdot 4H_20$
Brezinaite	Cr_3S_4
Brianite	$CaNa_2Mg(PO_2)$
Buchwaldite	$NaCaPO_4$
Calcite	$CaCO_3$
Carlsbergite	CrN
Caswellsilverite	$NaCrS_2$
Chalcopyrite	$CuFeS_2$
Chamosite	$Fe_6Mg_3[(Si_4O_{10})(OH)_8]_2$
Chaoite	C
Clinopyroxene	$(Ca,Mg,Fe)SiO_3$
Chlorapatite	$Ca_5(PO_4)_3Cl$
Chromite	$FeCr_2O_4$
Cohenite	$(Fe,Ni)_3C$
Copper	Cu
Cordierite	$Mg_2Al_4Si_5O_{18}$
Corundum	Al_2O_3
Cristobalite	SiO_2
Cronstedtite	$(Mg,Fe)_2Al_3Si_5AlO_{18}$
Cubanite	$CuFe_2S_3$
Daubreelite	$FeCr_2S_4$
Diamond	C
Diopside	$CaMgSi_2O_6$
Djerfisherite	$K_3CuFe_{12}S_{14}$
Dolomite	$CaMg(CO_3)_2$
Enstatite	$MgSiO_3$
Epsomite	$MgSO_4 \cdot 7H_2O$
Farringtonite	$Mg_3(PO_4)_2$
Fassaite	$Ca(Mg,Ti,Al)(Al,Si)_2O_6$
Fayalite	Fa_2SiO_4
Feldspar solid solution	
albite (Ab)	$NaAlSi_3O_8$
anorthite (An)	$CaAl_2Si_2O_8$
orthoclase (Or)	$KAlSi_3O_8$
Ferrosilite	$FeSiO_3$
Forsterite	Mg_2SiO_4
Gehlenite	$Ca_2Al_2SiO_7$
Gentnerite	$Cu_8Fe_3Cr_{11}S_{18}$
Graftonite	$(Fe,Mn)_3(PO_4)_2$
Graphite	C
Greigite	Fe_3S_4
Grossular	$Ca_3Al_2Si_3O_{12}$
Gypsum	$CaSO_4 \cdot 2H_2O$
Haxonite	$Fe_{23}C_6$
Heazlewoodite	Ni_3S_2
Hedenbergite	$CaFeSi_2O_6$
Heideite	$(Fe,Cr)_{1+x}(Ti,Fe)_2S_4$
Hematite	Se_2O_3
Hercynite	$(Fe,Mg)Al_2O_4$
Hibonite	$CaAl_{12}O_{19}$
Ilmenite	$FeTiO_3$
Kaersutite	$Ca_2(Na,K)(Mg,Fe)_4TiSi_6$-$Al_2O_{22}F_2$
Kamacite	α-(Fe,Ni)
Krinovite	$NaMg_2CrSi_3O_{10}$
Lawrencite	$(Fe,Ni)Cl_2$
Lonsdaleite	C
Mackinawite	FeS_{1-x}
Maghemite	Se_2O_3
Magnesiochromite	$MgCr_2O_4$
Magnesite	$(Mg,Fe)CO_3$
Magnetite	Fe_3O_4
Majorite	$Mg_3(MgSi)Si_3O_{12}$
Marcasite	FeS_2
Melilite solid solution	
åkermanite (Ak)	$Ca_2MgSi_2O_7$
gehlenite (Ge)	$Ca_2Al_2SiO_7$
Merrihueite	$(K,Na)_2Fe_5Si_{12}O_{30}$
Merrillite	$Ca_9MgH(PO_4)_7$
Mica	$(K,Na,Ca)_2Al_4[Si_6Al_2O_{70}]$-$(OH,F)_4$
Molybdenite	MoS_2
Monticellite	$Ca(Mg,Fe)SiO_4$
Montmorillonite	$Al_4(Si,Al)_8O_{20}(OH)_4Mg_6$-$(Si,Al)_8O_{20}(OH)_4$
Nepheline	$NaAlSiO_4$
Niningerite	(Mg,Fe)S
Oldhamite	CaS
Olivine	$(Mg,Fe)_2SiO_4$
Olivine solid solution	
fayalite (Fa)	Fe_2SiO_4
forsterite (Fo)	Mg_2SiO_4
Orthoclase	$KAlSi_3O_8$
Orthopyroxene	$(Mg,Fe)SiO_3$
Osbornite	TiN
Panethite	$(Ca,Na)_2(Mg,Fe)_2(PO_4)_2$
Pentlandite	$(Fe,Ni)_9S_8$
Perovskite	$CaTiO_3$
Perryite	$(Ni,Fe)_5(Si,P)_2$
Pigeonite	$(Fe,Mg,Ca)SiO_3$
Plagioclase	
albite	$NaAlSi_3O_8$
anorthite	$CaAl_2Si_2O_8$
Portlandite	$Ca(OH)_2$
Potash feldspar	$(K,Na)AlSi_3O_8$
Pyrite	FeS_2
Pyrope	$Mg_3Al_2(SiO_4)_3$
Pyroxene solid solution	
enstatite (En)	$MgSiO_3$
ferrosilite (Fs)	$FeSiO_3$
wollastonite (Wo)	$CaSiO_3$
Pyrrhotite	$Fe_{1-x}S$
Quartz	SiO_2
Rhönite	$Ca_4(Mg,Al,Ti)_{12}(Si,Al)_{12}O_{40}$
Richterite	$Na_2CaMg_5Si_8O_{22}F_2$
Ringwoodite	$(Mg,Fe)_2SiO_4$
Roaldite	$(Fe,Ni)_4N$

MINERAL NAMES *continued*

Mineral	Formula	Mineral	Formula
Roedderite	$(K,Na)_2Mg_5Si_{12}O_{30}$	Stanfieldite	$Ca_4(Mg,Fe)_5(PO_4)_6$
Rutile	TiO_2	Suessite	Fe_3Si
Sanidine	$KAlSi_3O_8$	Sulfur	S
Sarcopside	$(Fe,Mn)_3(PO_4)_2$	Taenite	γ-(Fe,Ni)
Scheelite	$CaWO_4$	Tetrataenite	FeNi
Schöllhornite	$Na_{0.3}(H_2O)$ $[CrS_2]$	Thorianite	ThO_2
Schreibersite	$(Fe,Ni)_3P$	Tridymite	SiO_2
Serpentine (or chlorite)	$(Mg,Fe)_6Si_4O_{10}(OH)_8$	Troilite	FeS
Sinoite	Si_2N_2O	Ureyite	$NaCrSi_2O_6$
Smythite	Fe_9S_{11}	V-rich magnetite	$(Fe,Mg)(Al,V)_2O_4$
Sodalite	$Na_8Al_6Si_6O_{24}Cl_2$	Valleriite	$CuFeS_2$
Sphalerite	(Zn,Fe)S	Vaterite	$CaCO_3$
Spinel	$MgAl_2O_4$	Whewellite	$CaC_2O_4 \cdot H_2O$
Spinel Solid Solution		Wollastonite	$CaSiO_3$
spinel	$MgAl_2O_4$	Yagiite	$(K,Na)_2(Mg,Al)_5(Si,Al)_{12}O_{30}$
hercynite	$FeAl_2O_4$	Zircon	$ZrSiO_4$
chromite	$FeCr_2O_4$		
magnesiochromite	$MgCr_2O_4$		
V-rich magnetite	$(Fe,Mg)(Al,V)_2O_4$		

"Meteorites & The Early Solar System" Kerridge & Matthews, ed. U of A Press (1988).

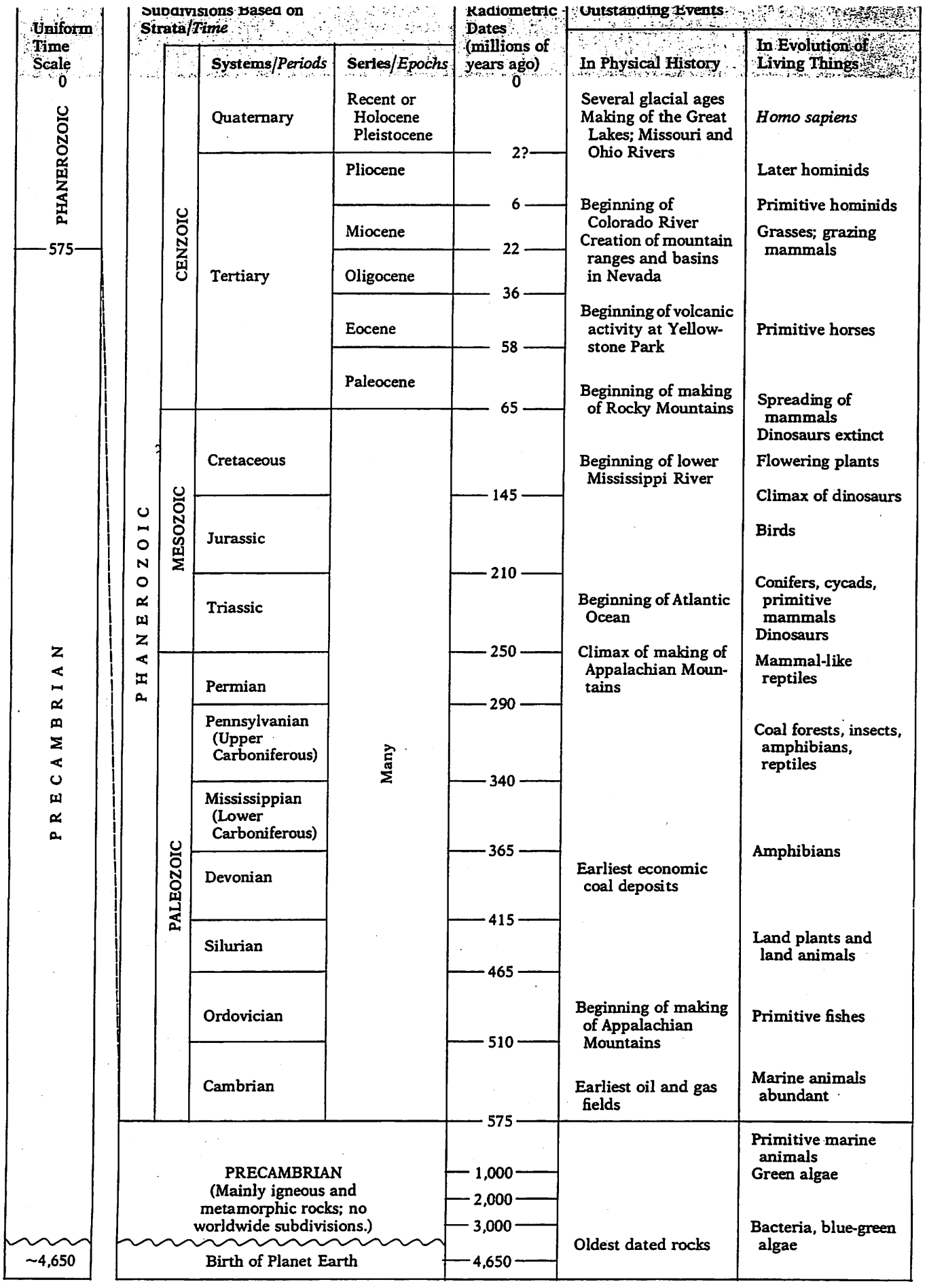

10

Flint & Skinner, "Physical Geology" 2 ed (1977)

TABLE 7-3 Classification of Chemical and Biochemical Sedimentary Rocks

Texture	Composition	Rock Name	
Clastic or crystalline	Calcite ($CaCO_3$)	Limestone (includes coquina, chalk, and oolitic limestone)	Carbonates
	Dolomite [$CaMg(CO_3)_2$]	Dolostone	
Crystalline	Gypsum ($CaSO_4 \cdot 2H_2O$)	Rock gypsum	Evaporites
	Halite (NaCl)	Rock salt	
Usually crystalline	Microscopic SiO_2 shells	Chert	
—	Altered plant remains	Coal	

TABLE 7-2 Classification of Detrital Sedimentary Rocks

Sediment Name and Size	Description	Rock Name	
Gravel (>2 mm)	Rounded gravel	Conglomerate	
	Angular gravel	Sedimentary breccia	
Sand (1/16–2 mm)	Mostly quartz	Quartz sandstone	
	Quartz with >25% feldspar	Arkose	
Mud (<1/16 mm)	Mostly silt	Siltstone	Mudrocks
	Silt and clay	Mudstone*	
	Mostly clay	Claystone*	

*Mudrocks possessing the property of fissility, meaning they break along closely spaced, parallel planes, are commonly called *shale*.

FIGURE 7-9 (*a*) Photomicrograph of a sandstone showing a clastic texture consisting of fragments of minerals, mostly quartz in this case. (*b*) Photomicrograph of the crystalline texture of a limestone showing a mosaic of calcite crystals.

(a)

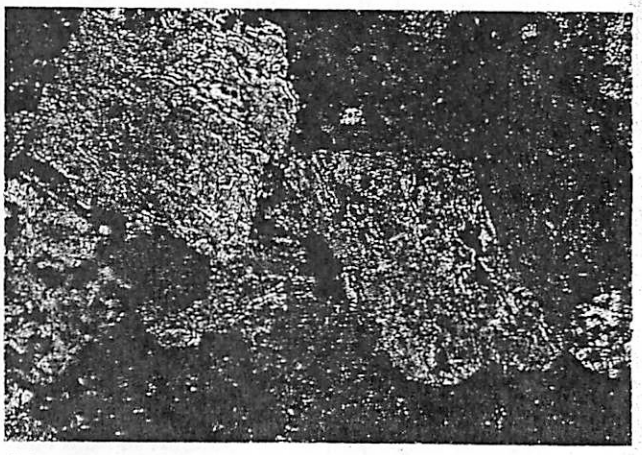

(b)

Physical Geology
Monroe + Wicander (1992)

11

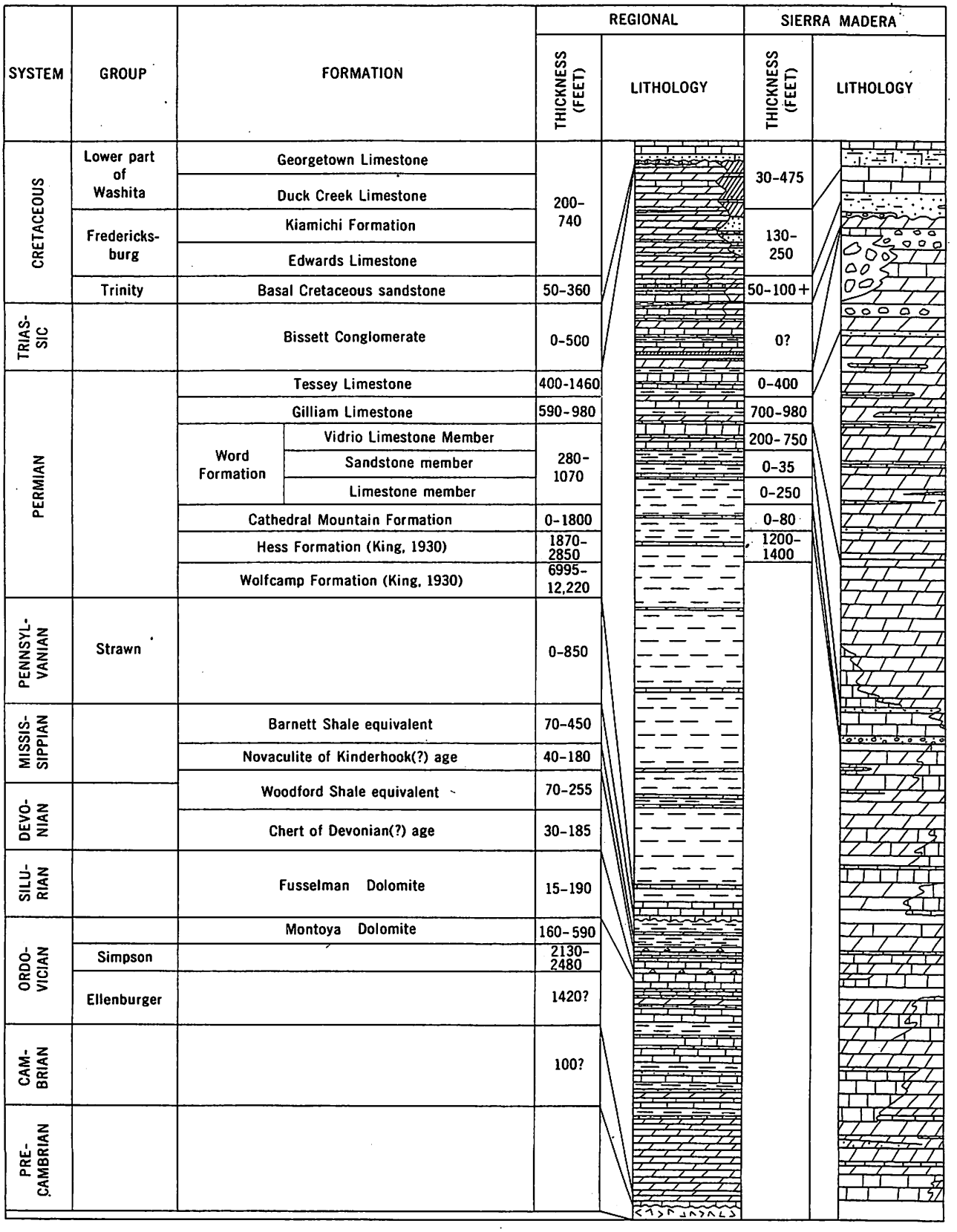

FIGURE 2.—Generalized stratigraphic column of Precambrian to Lower Cretaceous rocks at Sierra Madera (left column) and detailed stratigraphic column of rocks exposed at Sierra Madera (right column).

12

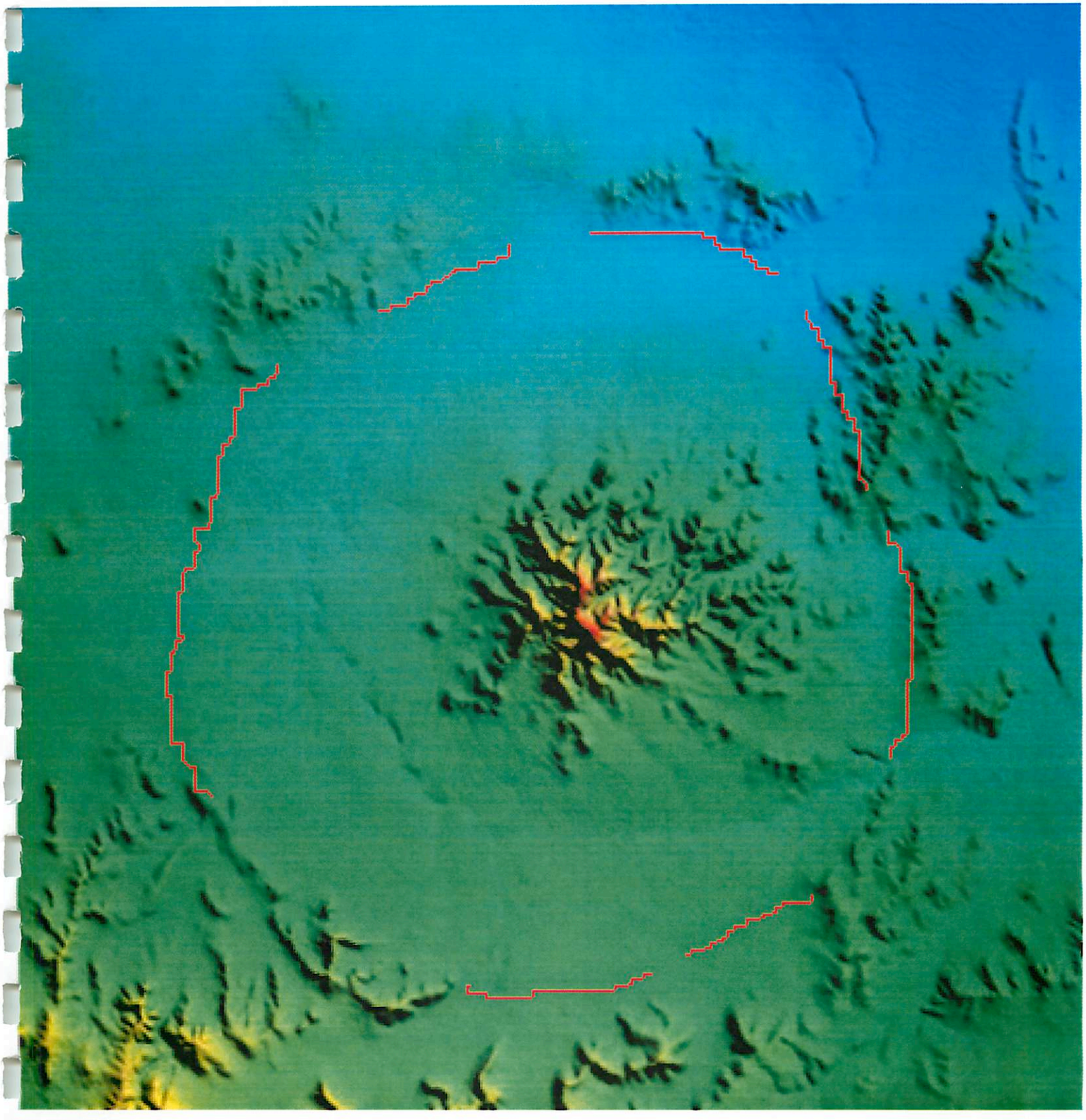

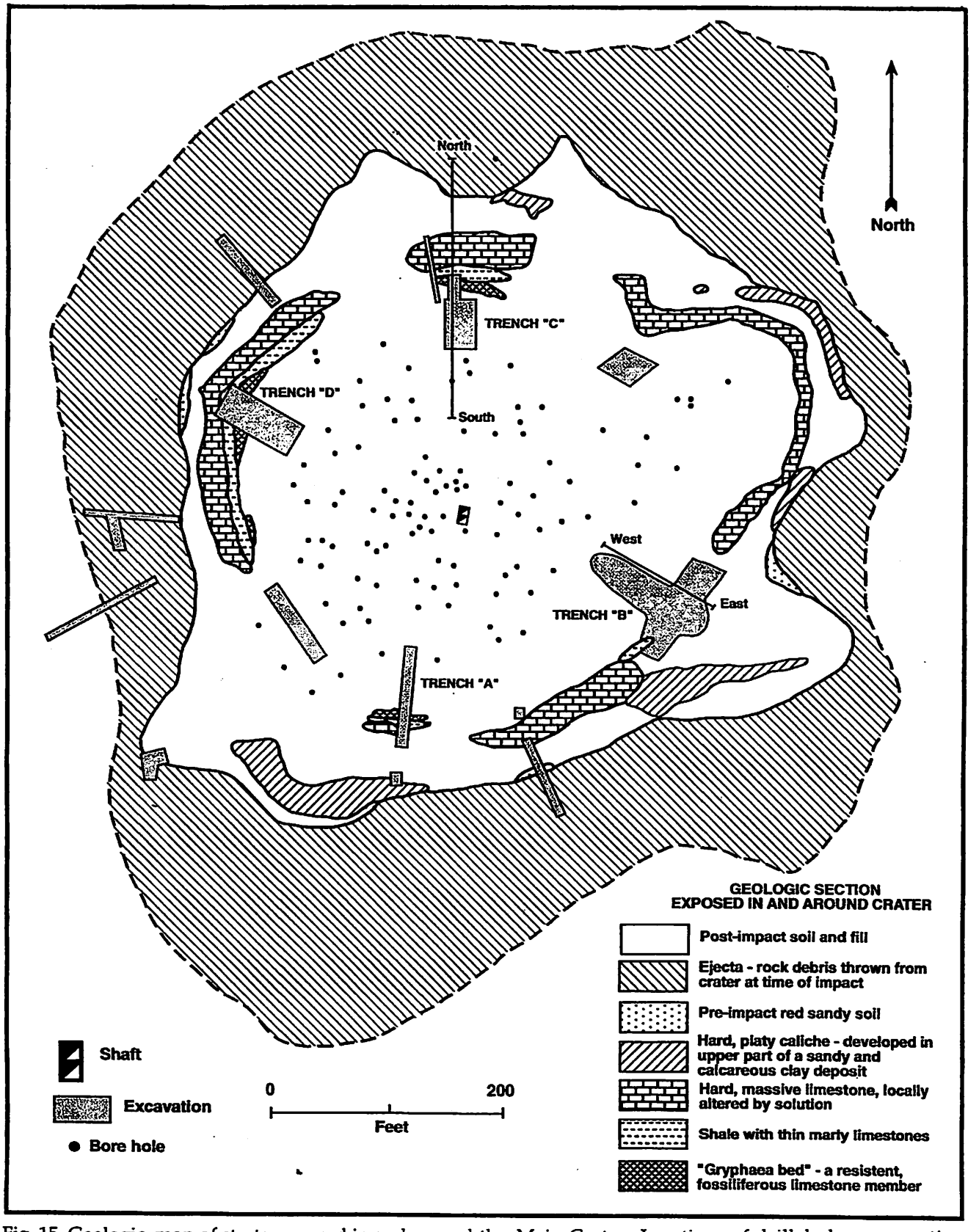

Fig. 15. Geologic map of strata exposed in and around the Main Crater. Locations of drill holes, excavation trenches, and the main shaft are noted. Drawing by the authors.

14

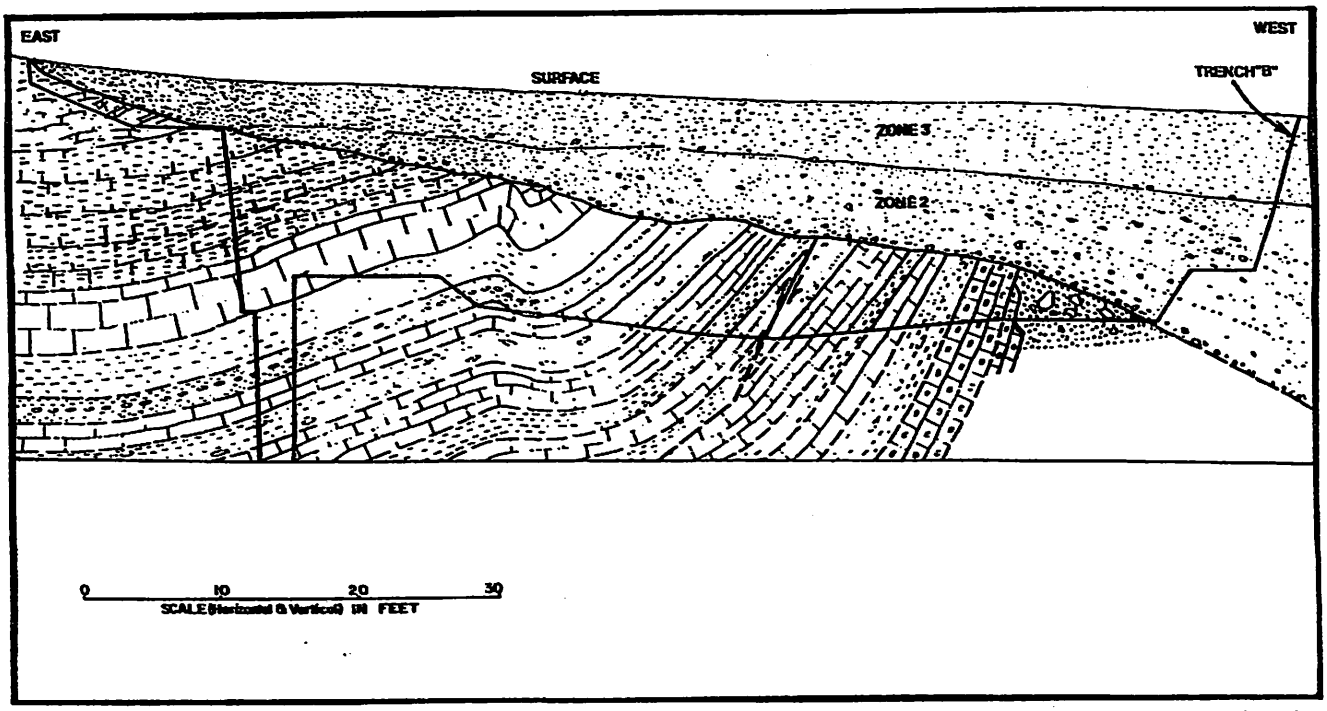

Fig. 17. East-West section through the eastern part of the Main Crater along Trench B. Drawing by the authors.

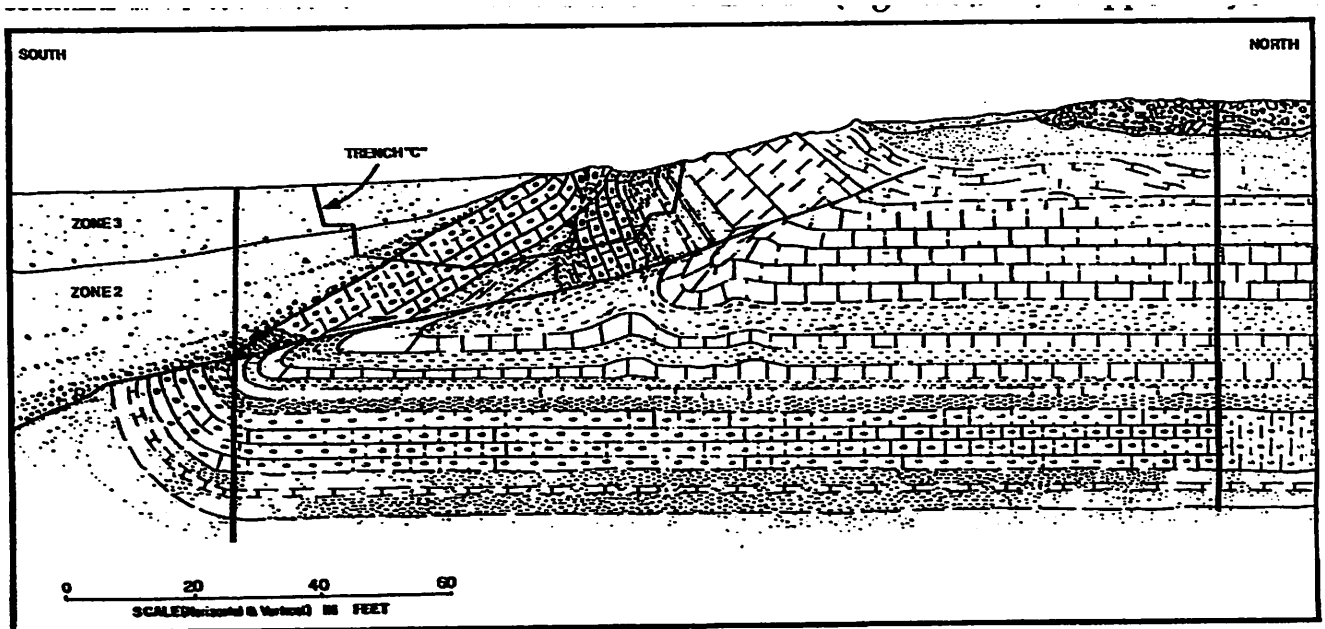

Fig. 16. North-South section through the northern part of the Main Crater along Trench C. Drawing by the authors.

15

Kilbourne Hole

Pete "The Invisible Fieldtripper" Lanagan

Introduction

The following discussion borrows heavily from a review article by Seager (1987).

Kilbourne Hole is located in the Potrillo volcanic field near several other maar volcanoes (Fig. 1). The diameter of the crater is approximately 2.3 x 3.3 km, and the crater floor lies 135 m beneath the surrounding terrain (Wood and Kienle, 1990).

Stratigraphy

From the bottom up...

1. The Camp Rice Formation, which is composed of early to middle Pleistocene sediments, comprises the lower half of the crater.

2. The Afton Basalt lies onto top the Camp Rice Formation. This flow is up to 5 m thick in places. Radiometric ages for the flow provides ages of 0.1-0.5 Ma.

3. Tuff ring ejecta comprises the upper half of the crater wall.

    a. basal unit: composed of angular basalt blocks up to 2 m in diameter in a matrix of unbedded, chaotic pyroclastic fall deposits

    b. upper portion: finer grained, thinly bedded pyroclastic surge and fall deposits; occasional sags from basalt blocks and xenolith bombs

4. Holocene crud (primarily blown sand).

Formation

According to Bates and Jackson (1984), a maar is "a low relief, broad volcanic crater formed by multiple shallow explosive eruptions." The term *maar* stems from the German word for lake, since in wet climates such craters fill with water.

Maar volcanoes occasionally form when a rising magma body contacts ground water. Heat transferred from the magma body to the water causes the water to flash to steam. The steam pressure rapidly exceeds the lithostatic pressure and the tensile strength of the overlying rocks, resulting in a phreatic explosion (where *phreatic* means "dealing with groundwater).

The precise behavior of how surface or near-surface water interacts with rising magma bodies depends on the relative ratio of magma to water (Fig 2). In the case of maars, little juvenile material is erupted, so the resulting crater primarily lies beneath the elevation of the surrounding terrain. Although the formation mechanisms are similar to maars, tuff rings and tuff cones result from the eruption of more juvenile material which build up cones and fill the early explosion crater.

In the specific case of Kilbourne Hole, it is thought that low energy strombolian eruptions ejected the Afton Basalt flow cap. Subsequent surtseyan eruptions ejected more material, excavating the main portion of the crater. As the surtseyan eruptions became weaker, ash beds were produced. On the basis of the presence of downfaulted masses of tuff-ring material at the base of the crater wall and beneath the crater floor, Seager (1987) suggests caldera-like collapse of the floor of the crater occurred soon after the eruptions ceased.

Chronology

The age of Kilbourne Hole is estimated to be between 24,000 and 500,000 years old.

The age of Kilbourne Hole is best constrained by the Afton Basalt, which has been dated at 100-500 ka. If Kilbourne Hole is the same age as nearby Potrillo maar, then an age of 180 ky is indicated. (Potrillo maar age is contrained by the presence of a basalt flow on its floor.) Pedogenic carbonate development on Kilbourne rim ejecta soils yield ages of 24,000 years.

The Planetary Connection

Maars on Mars: Data collected by the Opportunity rover have led to interpretations that water existed either on the martian surface as a shallow lake/sea or as shallow groundwater. Hodges and Moore (1994) have suggested some craters in the northern plains of Mars may be maar volcanoes.

Andy Rivkin Memorial Historical Trivia

Apollo astronauts trained near Kilbourne Hole.

References

Bates, R. L. and J. A. Jackson 1984. *Dictionary of Geological Terms.* Anchor Press.571 p.

Francis, P. 1993. *Volcanoes: A Planetary Perspective.* New York : Oxford University Press, 443 p.

Hodges, C. A. and H. J. Moore 1994. Atlas of Volcanic Landforms on Mars, USGS Professional Paper 1534, 194 p.

Hoffer, J. M.. 1976. *Geology of Potrillo Basalt Field, South-Central New Mexico,* New mexico Bureau of Mines and Mineral Resources.

Seager, W. R. 1987. Caldera-like collapse at Kilboune Hole, maar, New Mexico. *New Mexico Geology*, **9**, 69-73.

Wood, C. A. and J. Kienle, 1990. *Volcanoes of North America: United States and Canda.* Cambridge University Press, 354p.

Figure 1: Location map of Kilbourne Hole. From Hoffer (1976).

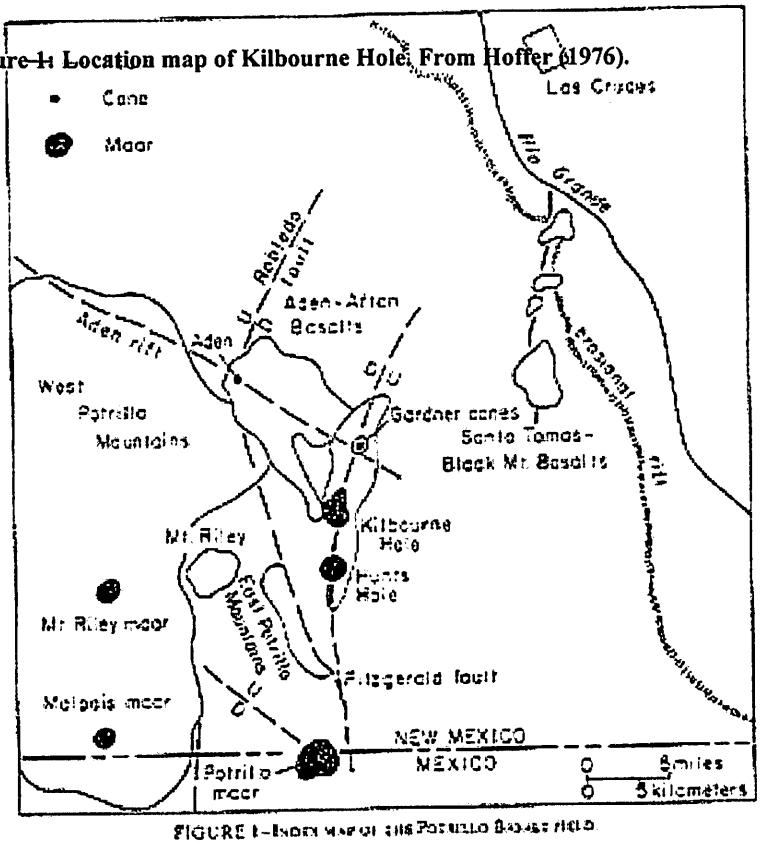

FIGURE 1—Index map of the Potrillo Basalt field.

18

Figure 2: Formation of volcanic edifices as a function of magma:water ratio. From Francis (1993).

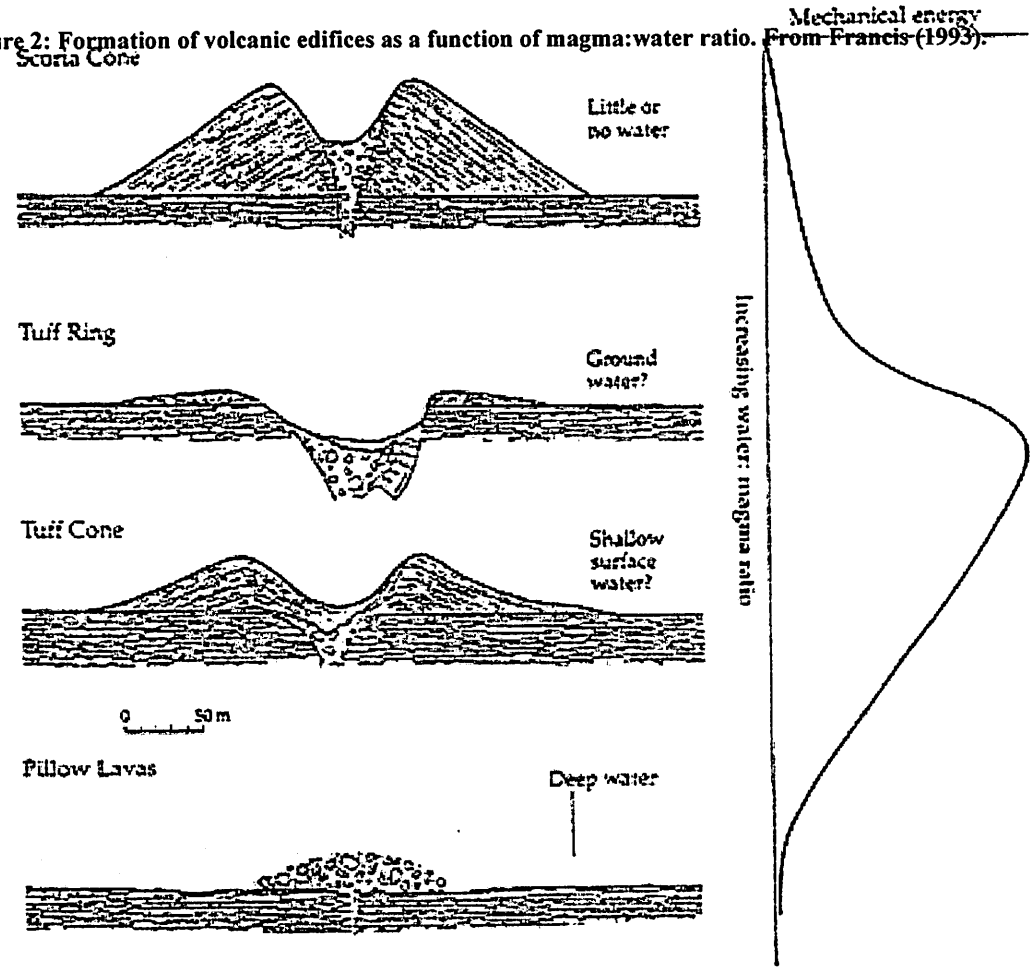

Crustal Xenoliths and Implications for Crustal Evolution

Mandy Proctor

What is a xenolith?

"The Greek root-word "xeno" means strange or foreign, and "lith" means rock. A *xenolith*, then, is a "strange rock" - one whose origin is unlike that of the rock in which it is found. For example, volcanic rocks can contain pieces of unrelated rocks usually found deeper in the Earth that were ripped out during an eruption. Those pieces are called *xenoliths*."

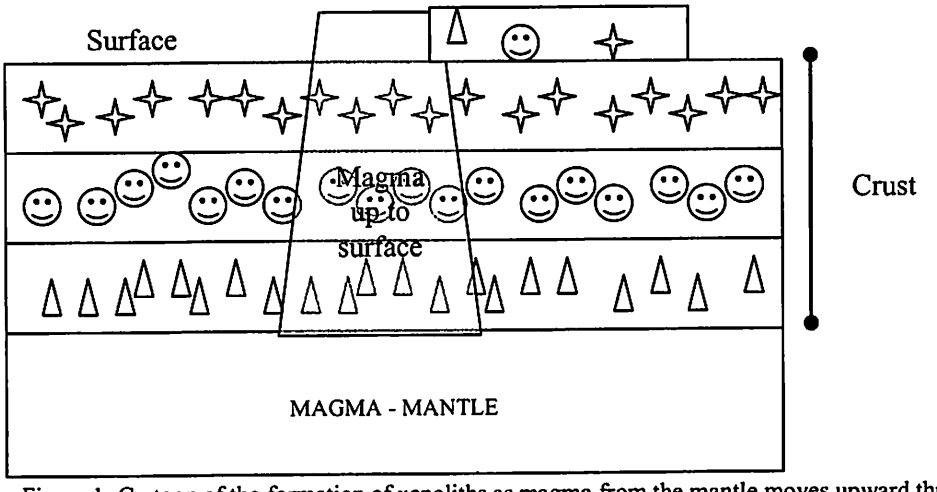

Figure 1: Cartoon of the formation of xenoliths as magma from the mantle moves upward through the crust. Notice that material from the various layers appear in the lava extruded onto the surface.

What can we learn from xenoliths?

It is difficult to probe the lower crust (given all that material on top of it). Two commonly used methods are: analyzing of sound waves and xenolith analysis.

- The presence of xenoliths in extruded surface rocks allow us to perform geological and chemical analysis of sub-surface crustal layers.
- It is possible to see fractionation effects in the material.
  - This may give hints as to the environment of formation. (i.e. open or closed system condensation).
- We can do age dating on the xenoliths (using radioactive isotopes) and date the lower crust.
- We can also ascertain if the rocks were exposed to any outside petrologic influences (i.e. interaction with magma) based on fractionation effects.

20

Effects of Magmatic Transport:

- Many xenoliths show melting as a result of contact with the magma.
- Have abundant cavities from segregation of CO_2-rich fluids while crystallizing.

Kilbourne Hole Xenoliths:

- What are they?
  - Garnet-bearing granulite xenoliths sample the lower-crust at ~ 28 km.
- What can we learn?
  - High $^{176}Hf/^{177}Hf$ ratios in KH xenoliths suggest that the lower crust has undergone open-system garnet growth.
    - Removal of partial melt in presence of garnet
    - Garnet accumulation
    - dehydration melting of amphibole or tolanite may be to blame.
  - Variations in $^{206}Pb/^{204}Pb$ suggest that some garnets were influenced by a mid- to late-Cenozoic basalt component.
    - Probably formed at the base of the crust.

Planetary Connection:

1. There have been some xenoliths found in chondrites, allow us to probe deeper into the parent body.
2. Xenoliths have also been found in some Martian meteorites.
3. May allow us to probe the lunar interior more deeply.

References:

Geologic Tour of UC – Berkeley, Glossary of Terms.
http://www.seismo.berkeley.edu/seismo/geotour/geoterms.html

Parsons, T., N.I. Christensen, & H.G. Wilshire (1995) Velocities of Southern Basin and Range
xenoliths: Insights on the nature of lower crustal reflectivity and composition. *Geology*, **23**, no. 2, 129-132.

Pasek, Matthew. Personal communication. 23 March 2004.

Scherer, E.E., K.L. Cameron, C.M. Johnson, B.L. Beard, K.M. Barovich & K.D. Collerson. (1997) Lu-Hf geochronology applies to dating Cenozoic events affecting lower crustal xenoliths from Kilbourne Hole, New Mexico. *Chemical Geology*, **142**, 63-78.

Mantle Xenoliths from Kilbourne Hole, NM

By Celinda A. Marsh

Xenolith- a foreign rock, a rock fragment that has a different origin than the host material.

Maar volcanoes often bring up fragments of material that have been transported to the surface by magma without those fragments undergoing melting. These materials retain their original (or close to their original) composition. This allows geochemist to perform a variety of measurements on them that reveal the temperature, pressure, and time of formation of the xenoliths.

Kilbourne hole is one such maar crater. Xenoliths from both the base of the crust and the mantle have been found within the volcanic deposits at this locality. I will be discussing xenoliths from the mantle.

There are two major types of mantle material: fertile and depleted. Depleted mantle material has undergone melting and produced basalts. Fertile mantle has not melted, and therefore retains the incompatible elements, pyroxene, spinel and other minerals that are removed by the melting process.

Both types of depleted and fertile material have been found at Kilbourne hole. In fact, three types of mantle xenoliths have been observed. The first group of mantle xenoliths is identified by its fine–grained texture and by its lherzolitic mineral composition. The second group are porphyroclastic lherzolites. Both lherzolite groups are fertile with a fair amount of clinopyroxene, the difference between the two groups are the fabric of the xenoliths. The fabric of the porphyritic lherzolites indicates that they formed under lower strain. The third group of xenoliths are olivine-rich peridotites. This group is less fertile than group the lherzolites and has less clinopyroxene. The temperatures measured for these three groups increases with each step between the fine-grained lherzolites, the porphyritic lherzolites, and the peridotites. [Silva, et al., 2004]

Peridotite - a plutonic, granular rock type that contains olivine and pyroxene but no feldspar or quartz. This rock type is therefore ultramafic in composition.

Lherzolite - a type of peridotite that is not dominated by any one type of pyroxene (i.e. orthopyroxenes or clinopyroxenes).

The following section was informed by reading a paper by Kopylova et al. (1999).
Temperature can be determined by examining the composition of orthopyroxenes and clinopyroxene in equilibrium with each other (as in Fig. 1). Other mineral equilibriums can be used as well.
Pressure can be determined by examining rocks that contain spinel and garnet in equilibrium with each other. Al abundance in orthopyroxenes is also used.

Each unique mineral equilibrium measurement conducted improves confidence in the results. Several of the minerals assemblages have multiple calibrations that have been calculated by various authors.

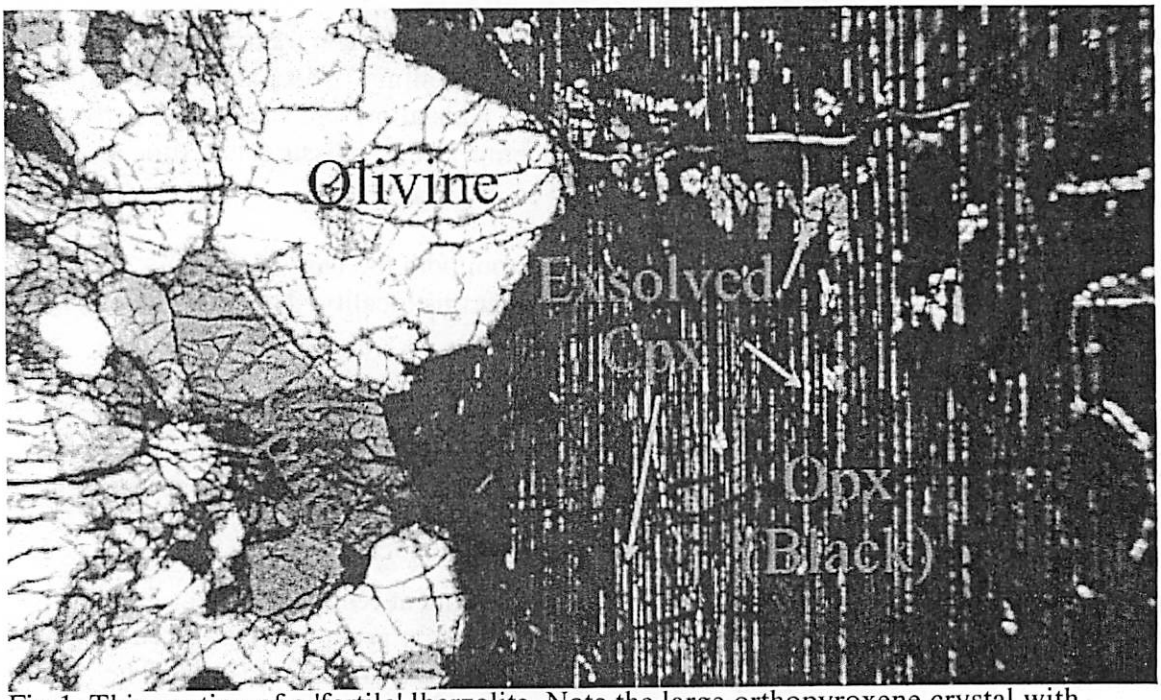

Fig 1. Thin section of a 'fertile' lherzolite. Note the large orthopyroxene crystal with lamellae and patches of exsolved clinopyroxene.

Mantle fragments from other planetary bodies

Vesta

Diogenites are hypothesized to represent mantle cumulates that were liberated from the asteroid Vesta by a large impact.

Mars

Nakhla is the only ultramafic martian meteorite, making it the meteorite most representative of the martian mantle. It also was probably liberated from its position at depth within Mars by an impact.

Reference:

Silva, A. et al. (2004) Thermometry and textures of Kilbourne Hole mantle xenoliths, New Mexico. *GSA Abstracts with Programs*, Vol. 36, No. 1, p. 9

Kopylova M. G., Russell J.K., and Cookenboo H. (1999) Petrology of Peridotite and Pyroxenite Xenoliths from the Jericho Kimberlite. Implications for the Thermal State fo the Mantle beneath the Slave Craton, Northern Canada. *Journal of Petrology*, Vol. 40, No. 1, p. 79-104.

Size of the Sierra Madera complex impact crater

by Gwen Bart

The Sierra Madera crater was formed in late Cretaceous or early Tertiary (~65 Ma; does K/T boundary sound familar?), and is very eroded. A fresh (recent, uneroded) complex crater would show a central uplift surrounded and partly burried by a lens of *breccia* that occupies a shallow crater, with a well developed crater rim. (Breccia consists of shattered blocks of underlying rock, some finely crushed and fused rock, and also meteoritic material in the form of fine spherules dispersed in glass. From Jay's book, p. 17.) At Sierra Madera, the entire crater depression, central peak, and all ejecta/breccia from the impact have been eroded away. Comparison of Sierra Madera stratography with other craters suggests that 2,000 ft (600 m) of material may have been removed by erosion.

The topography we see today is a central uplift 5 miles (8 km) diameter and 4,000 feet (1.2 km) high. Surrounding this central uplift there is a structural depression 1 - $1\,^1/_2$ miles wide, surrounded by a structurally high rim about 1/2 mile wide. This topography is a result of the way the underlying rock strata was deformed in the impact. The central peak is a result of the underlying rock that was pushed upward to form the central peak above it. The rim represents strata which folded upward beneath the original crater rim. Thus, the diameter of the present observable structure should be about the same as the original final crater diameter: **12.87 km (~8 miles)**.

The transient crater is the shape the crater had at the point when the crater stopped growing larger, and before gravatational collapse could begin. Because a complex crater is large and subject to a lot of post-cratering collapse, it is instructive to determine what the crater's diameter was before the collapse occured. For a simple crater, this calculation is fairly straight forward:

$$D_t = \left(1 - \frac{5}{4}\frac{H_b}{(H + H_b)}\right)^{1/3} D$$

If one assumes $H_b \simeq H/2$ then $D_t = 0.84D$. Complex craters are more complex, ☺ but

$$D_t \simeq 0.5 \rightarrow 0.65D$$

seems to work. This gives us a transient crater diameter for Sierra Medara of $\sim$ **6.25 km (4 miles)**.

Obviously impact cratering is a very important process on solar system bodies besides the Earth. Impact craters are observed on every other solid surface in our solar system, including the Moon, the other solid planets, their moons, the asteroids, and the comet Wild2. The Moon has lots of large impact craters with central peaks, for example, Copernicus (see figure). All lunar craters bigger than 15 miles have central peaks. In the past, studies of

Sierra Madera have allowed people to realize that lunar craters might expose the sub-surface and astronauts could therefore collect sub-surface samples without rigerous digging.

Most information taken from: Wilshire, H.G., T.W. Offield, K.A. Howard, and D. Cummings "Geology of the SierraMadera Cryptoexplosion Structure, Pecos County, Texas." U.S. Government Printing Office: 1973 O-477-953.

Also used crater program on Jay's website:
`http://www.lpl.arizona.edu/tekton/crater.html`

Transient crater information can be found in Jay's book: H.J. Melosh *Impact Cratering, a Geologic Process* Oxford University Press, (1989).

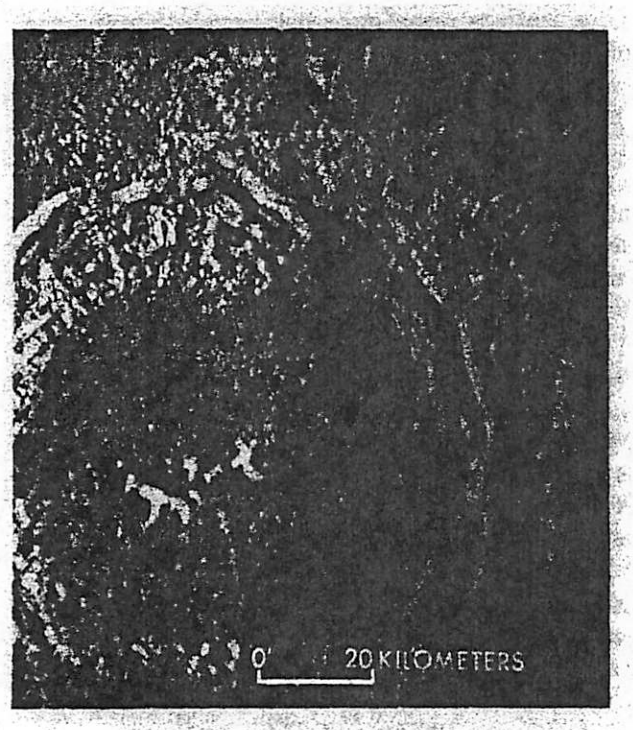

The lunar crater Copernicus. Orbiter IV photograph, courtesy of NASA.

Age of Sierra Madera Impact Crater

- Determining age of Terrestrial Craters
  - ◇ Fission Track Dating
    - i. Count the number of "tracks" left by spontaneous fission of Uranium in sample.
    - ii. Aging young rocks limited by probability ($8x10\text{-}17\ a^{-1}$) of ^{238}U fission.
    - iii. Aging old rocks limited by erosion of tracks.
  - ◇ Cosmogenic Nuclide Dating
    - i. Compare abundances of non-stable isotopes created by cosmic rays to stable isotopes.
    - ii. Limited to Myr time scales because of particle(^{10}Be, ^{14}C,^{26}Al,^{36}Cl) half life.
    - iii. Highly dependent on selected sample.
    - iv. Works very well if impactor can be dated directly.
  - ◇ Luminescence Dating
    - i. When heat is applied to a crystal which was originally exposed to ionizing radiation it emits light.
    - ii. Best for young craters <1Myrs

◇ Paleomagnetic Dating

i. Slowly cooling rocks retain information about the direction of the Earth's magnetic field at the time.

ii. Records exist for 100Myrs

iii. Lacks precision because of the possibility of tilting and rotation of rocks.

◇ Biostratigraphy

i. Finding fossil records in the post-impact sedimentation.

ii. Best for craters formed in shallow waters.

iii. Problems occur when sedimentation happened much later or there is a lack of marker fossils.

◇ Radioactive Dating

i. Similar to the cosmogenic nuclide dating, compare ratios of unstable to stable isotopes.

ii. Potasium-Argon dating used most frequently for impact melt rocks.

iii. Problems occur if either ^{40}Ar is lost to diffusion or if pre-existing ^{40}Ar is incorporated into the melt.

- Age of Sierra Madera
  - ◇ Exposed Rock ages: Lower Permian to Cretaceous
  - ◇ Central uplift age: Upper Permian
  - ◇ Rim age: Upper Permian and Lower Cretaceous
  - ◇ ~100 Myrs*

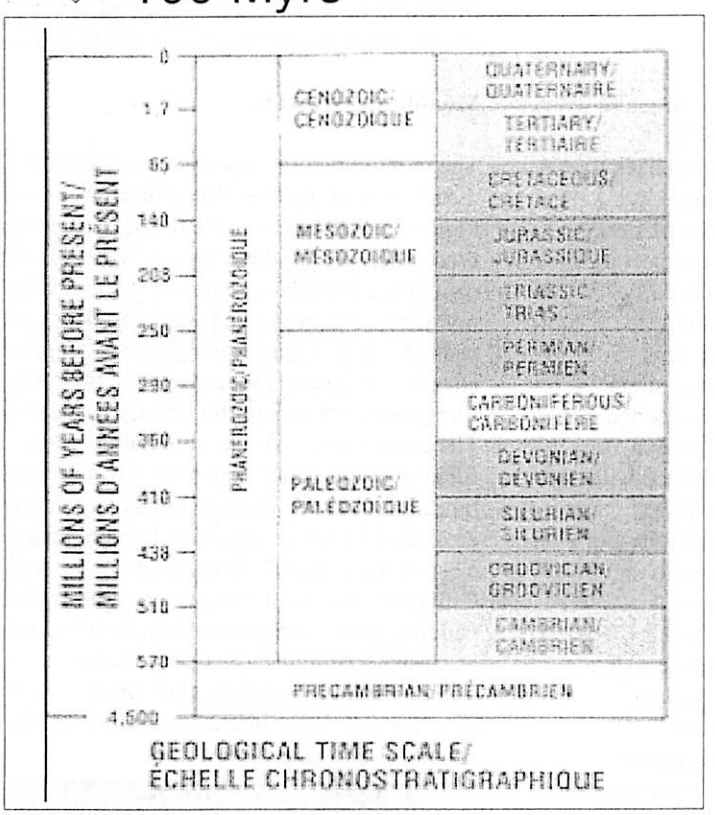

http://www.science.uwaterloo.ca/earth/geoscience/timescal.html

*http://www.lpl.arizona.edu/SIC/impact_cratering/World_Craters_Web/northamerica craters/Sierra_Madera.html

1) Alexander Deutsch and Urs Scharer: "Dating Terrestrial Impact Craters" Meteorite (29) 301-322 1994

2) H.G. Wilshire et. al : "Geology of the Sierra Madera Cryptoexplosion Structure, Pecos County, Texas" Contributions to Astrogeology

Impact breccias of the Sierra Madera impact structure, Texas.

Tamara Goldin

Introduction

The Sierra Madera impact structure consists of deformed sedimentary rocks. Brecciation, shatter cones, and deformation of quartz and carbonate minerals are ascribed to shock deformation during the impact event (Wilshire et al. 1973). The Sierra Madera structure differs from most known terrestrial craters, which involve some amount of crystalline basement rock, in that the target stratigraphy is entirely of sedimentary origin. Studies of the Sierra Madera breccias can improve our understanding of impacts in sedimentary targets.

Overview of Target Stratigraphy

The stratigraphy beneath the Sierra Madera structure is described in detail by Wilshire et al. (1973). Although wells revealed a sedimentary record back to the lower Ordovician overlying Precambrian crystalline rocks, the rocks exposed at Sierra Madera range in age from Early Permian to Early Cretaceous. The impact crater formed sometime after the early Cretaceous and before the consolidation of the youngest sediments, as evidenced by a lack of extensive brecciation of the lower Cretaceous strata.

Sierra Madera overlies a sedimentary sequence 18,000 feet thick (Figure 4). The Lower Permian Wolfcamp Series (7,000 feet thick) is associated with deposition in the Val Verde trough. These rocks consist of black shale interbedded with sandstone and some limestone and dolomite. This grades into the Hess Formation (2,400 ft), which is transitional between basin and shelf environments and is composed of interbedded clastic and carbonate rocks. The Hess Formation is overlain by the Cathedral Mountain Formation (<80 ft), which is a thin sequence of calcareous chert conglomerate, quartz and chert sandstone, and dolomite beds. Above this is the Word Formation (400-1000 ft), a shelf facies deposit of limestone, dolomite, and sandstone. Next is the Gillian Limestone (700-950 ft), which is composed of bedded dolomite with some sandstone. The Upper Permian strata consist of the Tessey Limestone (0-400 ft), which ranges from thin-bedded dolomite to block breccias. The coarser breccias are likely reef related and the widespread distribution of the breccias indicates a genesis unrelated to the impact.

The Triassic Bissett Conglomerate does not occur at Sierra Madera. Instead, Lower Cretaceous rocks (50-100 ft thick) unconformably overlie the Permian strata. These rocks, consisting of the Trinity, Fredericksburg, and Washita groups, are predominantly sandstones deposited during a period of marine transgression. Post-impact, Quaternary alluvium has been deposited in the impact basin.

BRECCIAS

The impact breccias at Sierra Madera were first described by Shoemaker and Eggleton 1961) and later by Wilshire et al. (1973). The latter divide the impact breccias observed at Sierra Madera into two categories: monolithic breccias composed of fragments of only one lithology and mixed breccias composed of fragments of several lithologies.

Monolithic Breccias

The monolithic breccias are most common. The distribution of the monolithic breccia is shown in Figure 3. Wilshire et al. (1973) describe the incipient brecciation of Permian strata at Sierra Madera as containing irregular veinlets (< 0.5 mm wide) of mylonite. The mylonite is composed of tightly packed, angular grains of carbonate. In more advanced stages of brecciation, the mylonite veinlets form a network separating unrotated clasts (Fig. 1). The clasts themselves are internally shattered and filled with mylonite. The most advanced stage of brecciation is seen in rocks displaying differential erosion of mylonite, resulting in more conspicuous clasts in the outcrop. Brecciation of the well-bedded Gilliam limestone shows preservation of the original bedding-planes, despite reorientation and size sorting of clasts. The impact breccias, in contrast to the Tessey breccias of sedimentary origin, are often flow-banded, show internal shattering of clasts, and consist of a range of grain sizes.

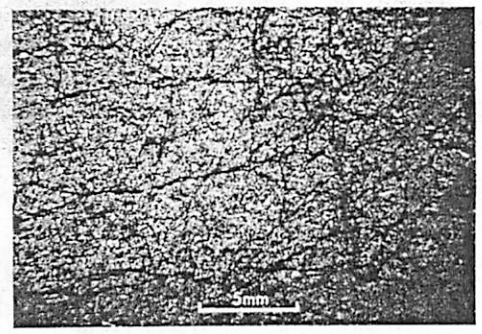

Fig. 1. Photomicrograph of monolithic breccia showing unrotated clasts surrounded by mylonite veins. From Wilshire et al. (1973).

Monolithic breccias occur in the same general areas as shatter cones and contain only small amounts of quartz. Planar deformation features are not observed in the quartz grains, although deformation of carbonate minerals has been observed. This indicates formation pressures below 200 kbars. Wilshire et al. (1973) explain the characteristics of these breccias as the result of tensile shattering due to the rarefaction phase of a shock wave.

Mixed Breccias

The mixed breccias in the Sierra Madera structure are composed of clasts of two or more lithologies (including clasts of monolithic breccia). They occur in all central uplift formations, although they are more prevalent in the older rocks (Fig. 3). These breccias form sheets up to 150 feet thick and 1,700 feet long and masses up to 1,100 feet across, often cross-cutting the country rock. These breccias show flow foliations, particularly in the tabular sheets, consisting of preferentially orientation and size sorting of clasts. Smaller clasts are found closer to breccia margins with larger clasts concentrated in the center of the breccia sheet (Fig. 2). This suggests emplacement as dense suspensions of clasts and rock debris in water or water vapor.

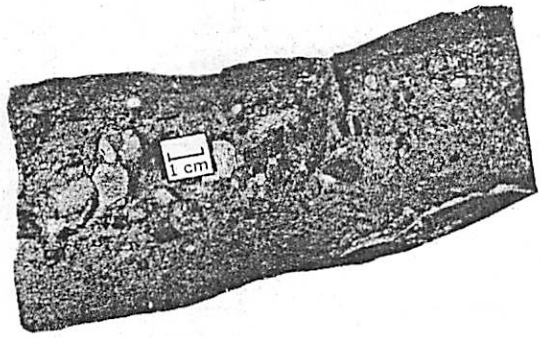

Fig. 2. A dike of mixed breccia showing the central concentration of large clasts with finer clasts outward. Note the varying lithologies of the clasts and compare with Fig. 1. From Wilshire et al. (1973).

The mixed breccia is hard and dense with rust-colored carbonate cement. The clasts themselves are often derived from the adjacent formation, but can also come from other formations both lower and higher in the stratigraphic section. A common clast in mixed breccias is white silty claystone composed of kaolinite, which has been deformed and foliated. The origin of clasts of this lithology is unknown. Fossiliferous chert nodules are another common clast. These appear to be products of the replacement of limestone clasts post-brecciation and are found in association with the replacement products of fluorite crystals. Chert clasts with developed flow structures are also observed.

Unlike the monolithic breccias, the mixed breccias contain shocked quartz with clear planar deformation features. This is consistent with formation at high pressure (>200 kbars). The structural occurrences of the breccias indicate an origin relating to the period of transient crater collapse and central uplift formation.

What about impact melt?

The previous descriptions of Sierra Madera lithologies do not mention any impact melt. Most studies of other terrestrial craters in predominantly sedimentary target rocks also do not recognize melt rocks. Recent work by Osinski et al. (2004), however, has demonstrated the existence of impact melt rocks associated with the Haughton impact structure, suggesting impacts in sedimentary targets may not be as different from those in crystalline targets as previously believed. Future analyses of the Sierra Madera impact breccias are needed to determine the true nature of the matrices and "mylonite veinlets".

References

Osinski, G.R., Spray, J.G., & Lee, P. 2004. Impactites of the Haughton impact structure, Devon Island, Nunavit, Canada. LPSC XXXV, No. 1004.

Eggleton, R.E & Shoemaker, E.M. 1961. Breccia at Sierra Madera. USGS Prof. Paper 424-D, p. D151-D153.

Wilshire, H.G., Offield, T.W., Howard, K.A., & Cummings, D. 1973. Geology of the Sierra Madera cryptoexplosion structure, Texas. Contributions to Astrogeology, p. H1-H42.

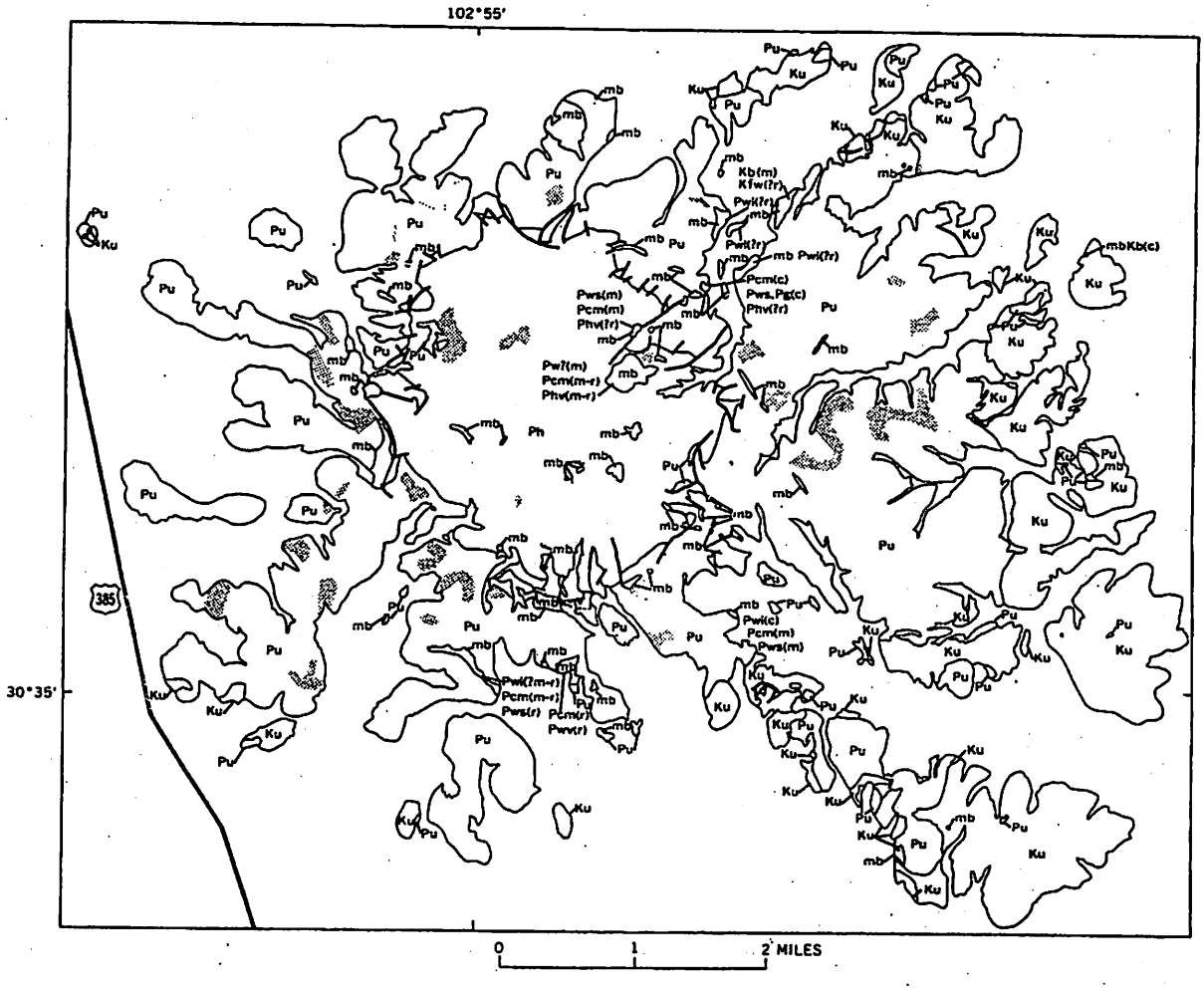

Fig. 3. Map of central uplift showing distribution of mixed breccias (mb) and monolithic breccias (stippled). Less obviously brecciated rock is more widespread on central uplift than illustrated. From Wilshire et al. (1973).

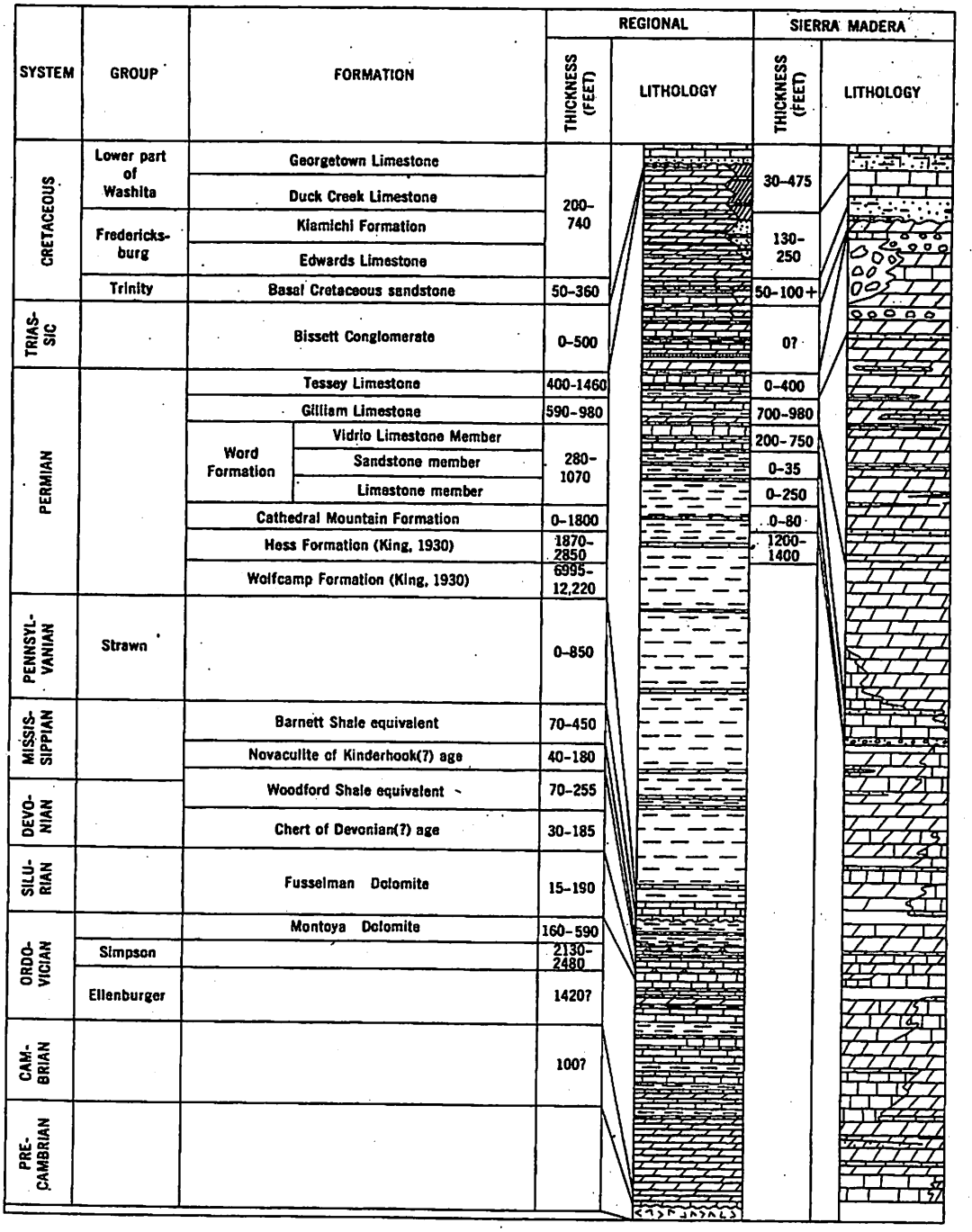

Fig. 4. Stratigraphic column of Precambrian to lower Cretaceous rocks at Sierra Madera (left column) and stratigraphic column of rocks exposed at Sierra Madera (right column). Thicknesses and lithologies are labeled. From Wilshire et al. (1973).

Shatter Cones at Sierra Madera Crater

Abby Sheffer

Description:

Shatter Cones are conical fracture surfaces with characteristic striations that fan outward from the apex, often called horsetail striations. They can range from less than 2 mm in cone height and side length to several meters, generally dependent on the lithology of the host rock. Shatter cones develop best in fine grained rocks, especially limestones, although they are found in all rock types. Incomplete cones are most common, especially at the larger sizes.
They are often used as definite indicators of an impact structure. Observations of natural shatter cones and shock experiments suggest a restricted range of pressures for their formation, 1 GPa to about 6 GPa. However, in one case they have been found at 20 GPa.

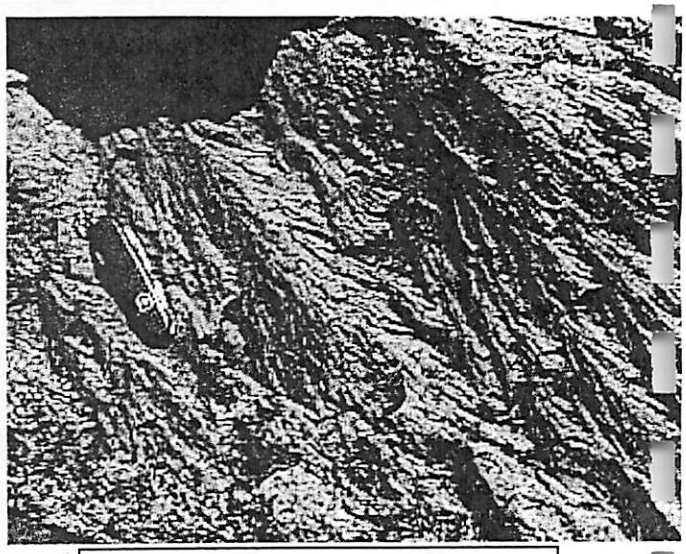

Shatter cones at Vredefort Dome, South Africa. Thanks, Ralph!

Formation: Summarized from Baratoux and Melosh, 2003, *EPSL*.

The Baratoux and Melosh model involves heterogeneities in the rock causing a scattered elastic wave to interfere with the spherical main stress wave.

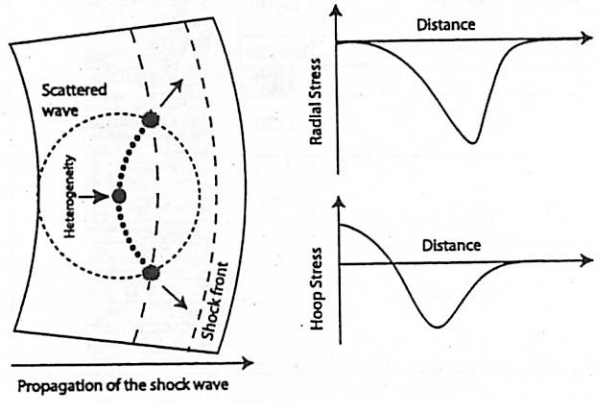

Fig. 2. Schematic representation of our model for the formation of shatter cones. Tensile fracture occurs at the intersection between the scattered tensile wave and the tensile hoop stresses in the main shock wave. When a critical value for the tensional stress is reached, the rock fractures in tension. The fractures accumulate on the surface of a conical region (indicated in the figure by filled circles and arrows).

At pressures lower than 2 GPa, tensional damage only accumulates in a small area at the edge of the heterogeneity and does not extend to form a full conical fracture.

Between 3 and 6 GPa, a shatter cone will form. At higher pressures, damage accumulates even inside the cone, which at lower pressures is mechanically isolated after fracturing.

The area around the heterogeneity is most damaged. In order for this to happen, the heterogeneity has to have a lower sound speed than the bulk material (higher density or lower bulk modulus). Otherwise the scattered wave is compressive.

At Sierra Madera: From Wilshire et al., 1968?, *Contributions to Astrogeology*.

Shatter cones can be found in all of the exposed Permian formations at Sierra Madera, mostly within 1-2 miles of the center of the structure (see figure). They also occur at depth, as seen from well cuttings, possibly up to 12,000 ft.

Aphanitic Dolomite (grains invisible to the naked eye) – shatter cones are most common, typically 5 cm long
Marly Dolomite (dense but crumbling?) – shatter cones are present, typically up to 12 cm long
Crystalline Dolomite, Siltstone, fine-grained Sandstone, and Chert – shatter cones are present, up to 20 cm long
Limestone – shatter cones are rare, up to 45 cm long
Coarse Sandstone – no shatter cones

The axes of the cones clusters have nearly the same orientation on an outcrop scale, but they do not all point inward and upward toward the center of the crater. However, much faulting occurred after the formation of the cones. After bedding is theoretically returned to horizontal, the estimated cone orientations do return to pointing inwards and upwards (87% towards, 13% away).

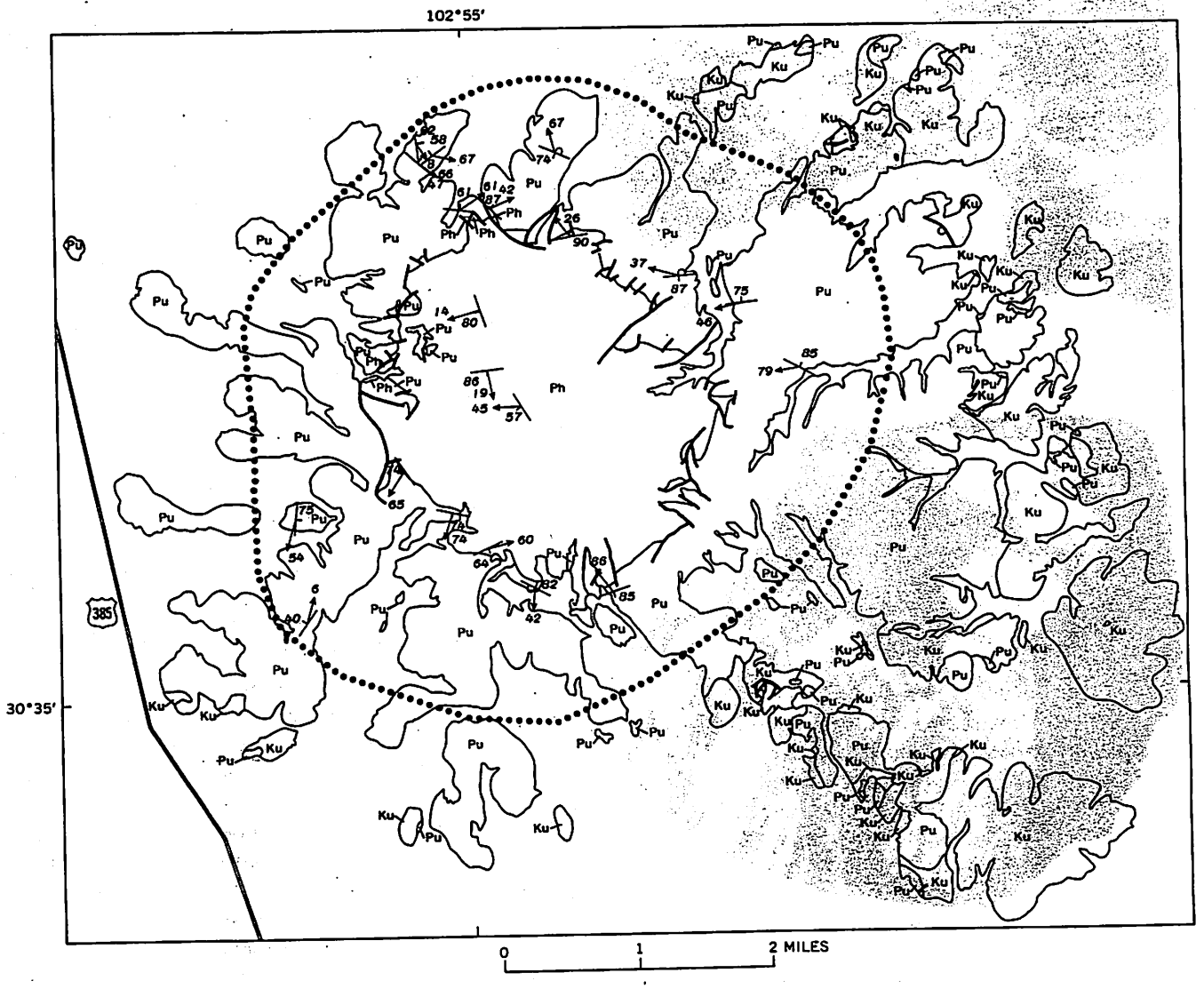

FIGURE 27.—Distribution of abundant shatter cones and orientation of shatter cones in place. Strike and dip of bedding shown by standard symbols. Direction of point of cones shown by arrows, with angle measured up from horizontal in degrees.

Central uplift formation at the Sierra Madera impact structure

by Gordon "Oz" Osinski

Background on central uplift formation:

Central uplifts are formed during the modification stage of complex impact crater formation (Fig. 1). The effects of the modification stage are governed by the size of the transient cavity and the properties of the target rock lithologies (Melosh 1989). For crater diameters <2–4 km on Earth, the transient cavity undergoes only minor modification resulting in the formation of a simple bowl-shaped crater (e.g., Meteor Crater, Arizona).

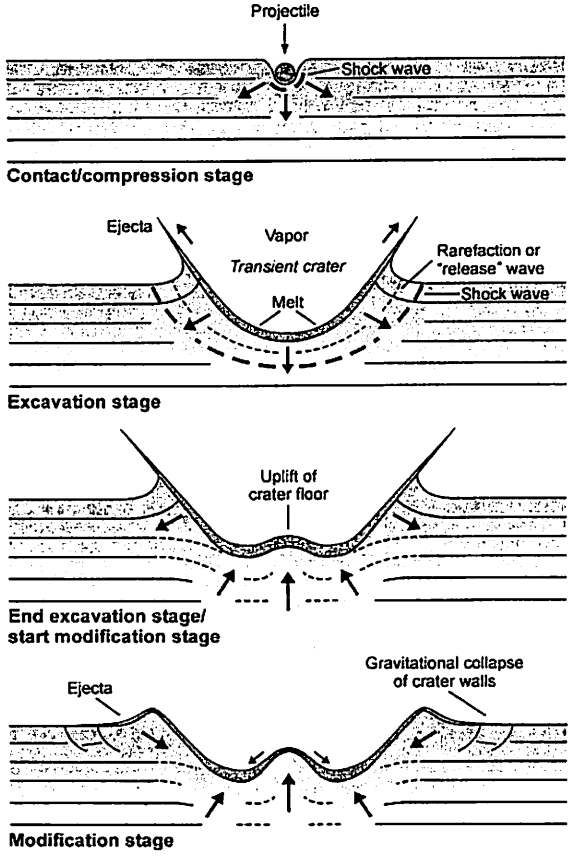

Fig. 1. Series of schematic cross sections depicting the formation of a terrestrial complex impact structure (i.e., diameter >2–4 km).

However, above a certain size threshold (>2–4 km diameter), the transient cavity is unstable and undergoes modification by gravitational forces, producing a so-called complex impact crater. There are two main competing forces that act during crater modification (Fig. 1):

1) Uplift of the transient crater floor leading to the development of a central uplift. This results in an inward and upward movement of material within the transient cavity.
2) Collapse of the initially steep transient crater walls due under gravitational forces. This induces an inward and downward movement of large (~100 m to km scale) fault-bounded blocks.

The diameter at which the transition occurs from simple to complex craters on Earth occurs at ~2 km for craters developed in sedimentary targets, and ~4 km for those in crystalline lithologies.

Sierra Madera impact structure:

- ~12 km diameter.
- Age: post Lower Cretaceous, pre-Quaternary.
- Target stratigraphy (Wilshire and Howard 1968):
  - ~6000 m of sedimentary lithologies.
  - Permian limestones and dolomites (Leonard Series, Word, Gilliam, and Tessey formations).
  - Lower Cretaceous limestones and marls, with a basal sandstone (Trinity and Fredericksburg groups, and the lower part of the Washita Group).

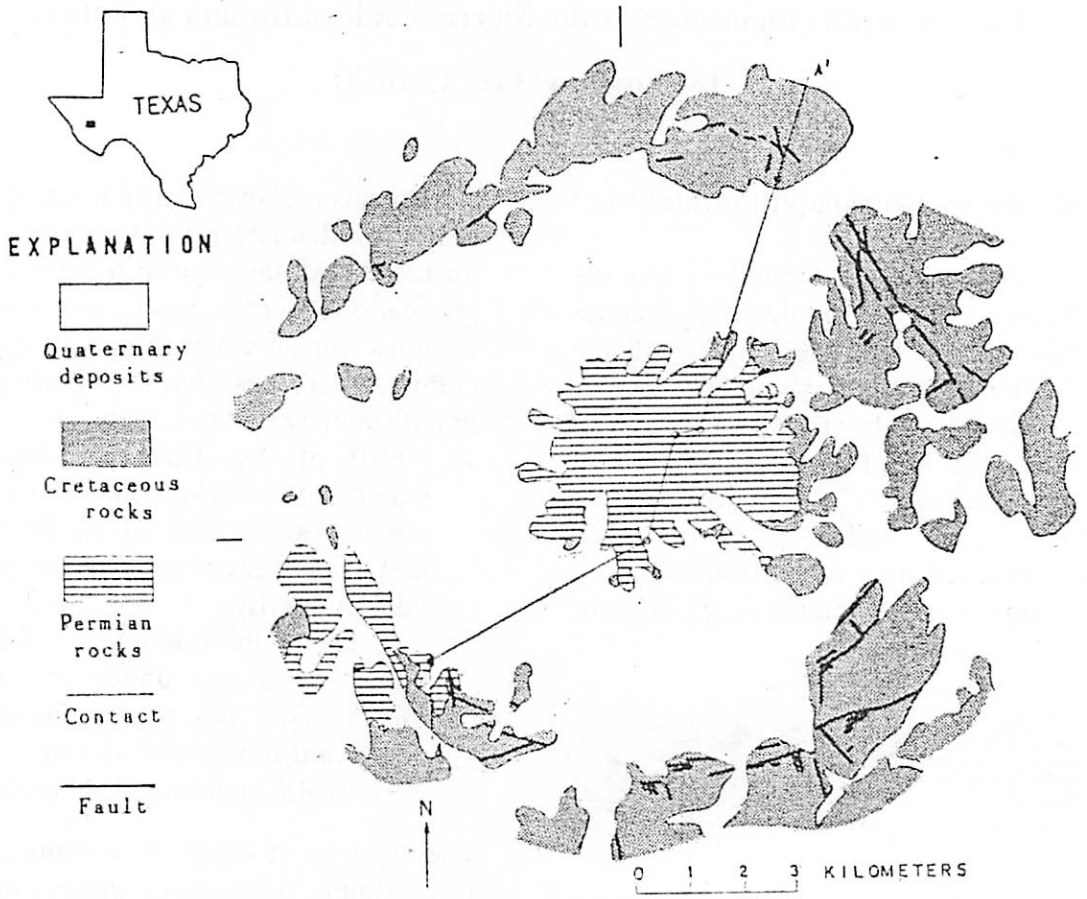

Fig. 2. Geological map of the Sierra Madera impact structure. Wilshire and Howard (1968).

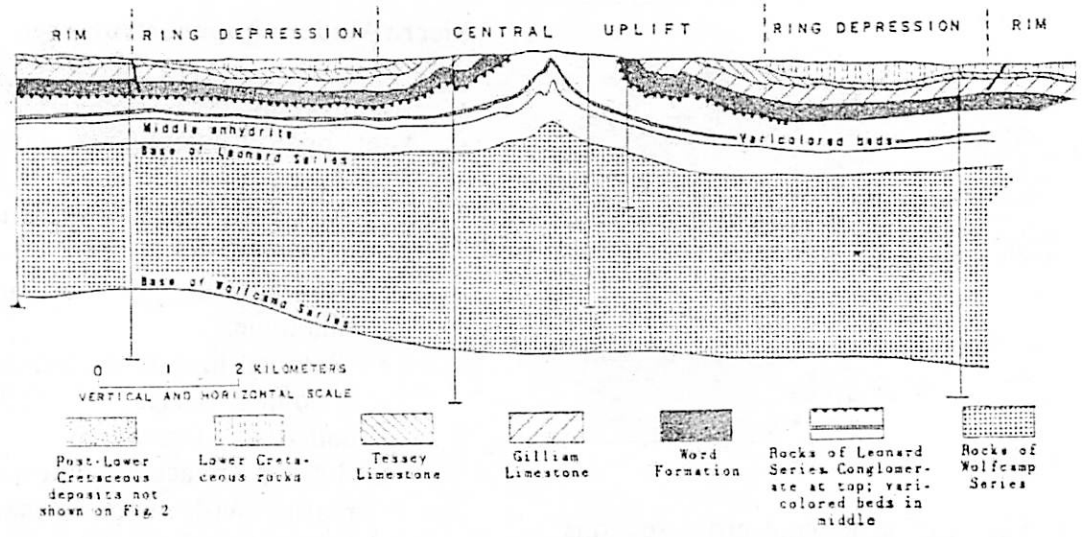

Fig. 3. Generalized cross section of the Sierra Madera impact structure. See Figure 2 for location of section. Wilshire and Howard (1968).

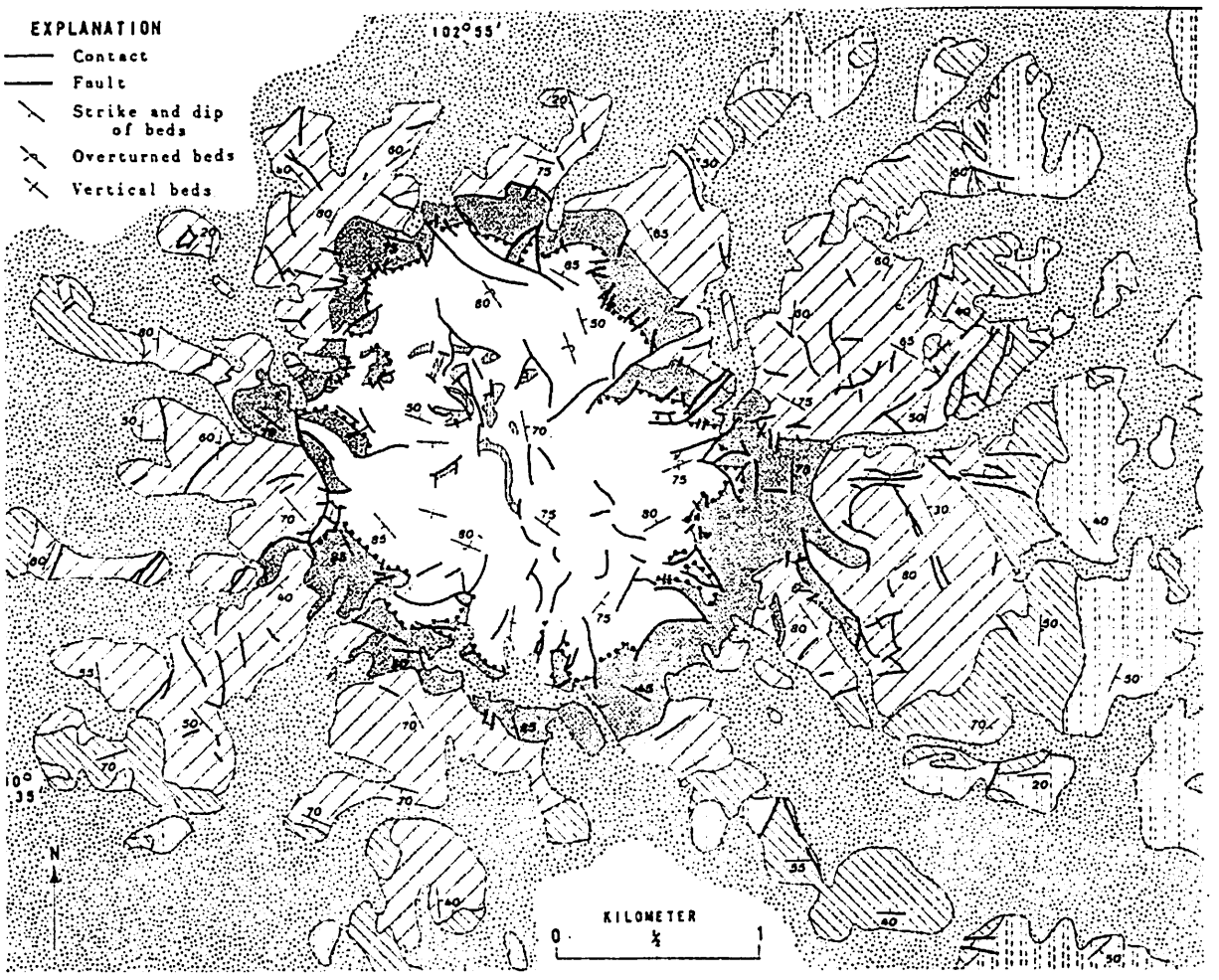

Fig. 4. Geological map of the central uplift at the Sierra Madera impact structure. Wilshire and Howard (1968). See Figure 2 for location.

Nature of the central uplift at Sierra Madera (Wilshire et al. 1972):

- ~5 km diameter (Figs. 2, 4).
- Deepest strata exposed are uplifted ~1200 m above pre-impact stratigraphic position (Figs. 2–4).
- Little if any deformation below 2–2.5 km under the crater center.
- Central 'core' ~1500 m in diameter comprising sub-vertical dips and radial fold plunges (Fig. 4).
- Permian rocks of the central uplift are extensively shatter-coned and brecciated.
- Distinctly different styles of deformation in the various different target lithologies.

- Geometry suggests that the central uplift formed by inward and upward movement of strata (Wilshire and Howard 1968) (cf., Wells Creek, Tennessee).
- Inward, converging movement results in a 'space' problem. This is accommodated by a series of deformation mechanisms (Wilshire and Howard 1968):
  - Steeply dipping radial faults and folds.
  - Duplication of beds by thrust faulting and folding.
  - Some lithologies (e.g., conglomerates) reported to have been 'highly mobile' during formation of the central uplift.
- It is apparent that to account for the observed dependence of final crater morphology on crater diameter, some type of extreme strength degradation must occur in the rocks surrounding the crater (Melosh and Ivanov 1999). Most common hypothesis is that of "acoustic fluidization" (e.g., Melosh and Ivanov 1999).

Questions to be discussed in the field:

- What is the nature of the central uplift at Sierra Madera? Is it a central peak?
- Is there field evidence that would support/discount acoustic fluidization?
- What is the effect of target lithology on central uplift formation? Why does the transition from simple to complex craters occur at 2 km and 4 km, respectively, in crystalline and sedimentary targets?
- How is the inward, converging movement during central uplift formation accommodated in the target rocks?
- How did the different target lithologies (e.g., limestones versus conglomerates) respond to crater collapse and uplift?

References:

Melosh H. J. 1989. *Impact Cratering: A Geologic Process*. New York: Oxford University Press. 245 p.

Melosh H. J. and Ivanov B. A. 1999. Impact crater collapse. *Annual Reviews of Earth and Planetary Science* 27:385–415.

Wilshire H. G. and Howard K. A. 1968. Structural pattern in central uplifts of cryptoexplosion structures as typified by Sierra Madera. *Science* 162:258–261.

Wilshire H. G., Offield T. W., Howard K. A., and Cummings D. 1972. Geology of the Sierra Madera cryptoexplosion structure, Pecos County, Texas. *US Geol. Surv. Prof. Pap.* 599–H, 42 p.

Breccias formed by Impact Cratering into Crystalline Target Rocks

John Moores

PTYS 594 Planetary Science Fieldtrip April, 2004

Background

When a planet is struck by another large object at astronomical speeds, the resulting impact leaves behind a very obvious mark on the landscape at the macroscopic scale in the form of an impact crater. However, the target rock is also affected on a much smaller scale depending mainly upon factors such as the amount of kinetic energy released (which depends on the size and speed of the impactor) and the distance of the rock from this point of release.

The cause of this dependence is due to a shockwave which propagates through the target material and whose strength falls off as it travels. Thus, if our rock was initially located sufficiently close to the point of impact it will be vaporized, while further from the impact the energy of the shockwave will be sufficient only to melt the rock. Still further from the point of impact the rock will be subject to large stresses causing it to break into shards and potentially undergo partial melting. This broken and reassembled rock is referred to as a breccia.

There is also a second means of manufacturing impact breccias. Since the surface of the planet is a free surface in terms of stress the induced stresses from the expanding shockwave will excavate material near the surface, breaking it apart and excavating it violently rather then doing much damage at the molecular level. Once this hot broken rock falls back to earth it can also fuse together to form a breccia.

Types of Breccias

Naturally, the specific morphology and mineralogy of brecciated rocks formed in this way depends to a great extent on the original morphology and mineralogy of the target rock. Specifically, this hand-out will discuss the observed morphology of breccias formed from principally crystalline target rocks.

However, before this topic is discussed it is necessary to discuss the distribution and characteristics of target rocks as well as to define some terminology. First breccias may be classified by the distribution of mineralogies found within a sample. If only one rock type exists in a particular sample it is referred to as a monomict whereas if shards of several different rock types are present it is termed a polymict.

Secondly, breccias may be classified according to provenance. Breccias which have been broken and reassembled without much displacement are called autochthonous. This is typical of brecciated rocks formed by the first mechanism. In contrast, Allochthonous Breccias are composed of shards which have been significantly transported (such as by stress-induced excavation of the transient crater) and corresponds to the second formation method discussed, although this could also

conceivably occur in post-impact collapse of the transient crater walls in the case of a large impact forming a complex crater.

As can be easily deduced from this terminology autochthonous breccias are much more likely to be monomicts then their Allochthonous counterparts, the inverse. Also, it is conceivable that breccias formed from the debris raining down following the excavation stage may be composed of parts of all the rocks initially located at the site of impact. However, whether or not these are monomicts or polymicts depends upon the initial distribution of rocks at the site of impact and how many geological layers have been excavated or otherwise affected by the impact.

Lastly the degree of shock sustained by individual elements of a brecciated rock should be defined. Here a five level scale (each with its own sublevels) is used ranging from stage 0 (unshocked) to stage V (vaporization). This system was first outlined by Stoffler in1974 and refined in 1978 both for crystalline rocks. The following chart shows the differences between the types:

TABLE 1. Stages of shock metamorphism of rocks of approximately granitic composition (Stöffler, 1974).

Stage	Shock effects	Shock pressure range (Gpa)	Postshock temperature °C
0	fragmentation, mosaicism, undulatory extinction, deformation bands in quartz, kink bands in biotite, shatter cones.	<10	<100
I	planar deformation lamellae in quartz, feldspar, amphibole, pyroxene, stishovite, coesite, kink bands in biotite.	10–35	100–300
II	diaplectic glasses of quartz and feldspar, planar deformation lamellae in quartz and feldspar.	35–45	300–900
III	selectively fused alkali feldspar, diaplectic quartz glass, thermal decomposition of biotite and amphibole.	45–60	900–1300
IV	complete fusion of rocks of granitic-granodioritic composition, impact melt.	60–80	1300–3000
V	vaporization.	>80	>3000

Target Rock

Logic dictates that the breccias found at a particular site must be composed of some combination of the various rock layers present at the site along with the impactor. For its part, the impactor sustains the bulk of the effects of the kinetic energy release and therefore very little in the way of fragments of the original object remain intact compared to the volume of solid material excavated and the even larger volume of heavily shocked material. As such, brecciated rocks are dominated by target rock.

This target rock may itself have several characters depending upon the geographic extent of sediments or crystalline basement rocks and the depths at which each layer may be found. One common (greatly simplified) configuration is a sedimentary layer which overlies crystalline basement rock.

Crystalline Targets

Even this crystalline basement rock is rarely homogenous. Deutsch et al (2003) for instance have found that impact melt and breccia from the Chicxulub structure on the Yucatan peninsula cannot be explained by a homogenous crystalline basement material – not surprising considering the large size of the structure. As a result the

same shockwave passing through this material has different effects on the differing grains of materials. An example of the observed characteristics from Metzler et al is given below:

TABLE 2. Observed shock effects in various minerals of basement rock clasts of the polymict breccia.

Shock effects	Quartz	Alkali-feldspar	Plagio-clase	Biotite	Amphi-bole	Pyrox-ene	Silli-manite	Garnet	Calcite	Apatite	Titanite
Coesite	X										
Vesiculated glass		X[1]									
Diaplectic glass	X	X	X								
Planar elements	X	X	X		X		X			X	
Planar fractures	X		X				X			X	
Mosaicism	X	X	X		X						
Kink bands				X							
Mechanical twinning						X			X		
Lowered pleochroism				X	X						
Shock-produced new phases				X[2]							
Irregular fractures				X		X[3]	X	X[3]		X	X
Recrystallization and alteration features											
Spherulitic crystallization	X	X	X								
Fan spherulitic crystallization		X									
Axiolitic crystallization	X		X								
Ballen structure	X										

[1] Vesicles filled with calcite and jarosite.
[2] Magnetite, hercynite, pyroxene, feldspar, glass.
[3] Network-like fractures.

Despite this, it is possible to draw some conclusions about the morphologies of breccias formed from crystalline target rocks. Firstly Metzler et al (1988) have noted that the crystalline breccias recovered from allochthonous polymict deposits on the rim and central peak of the Haughton structure showed a low degree of shock metamorphism (75% were type II or lower). This is possibly due to a reasonably deep basement of 1700m depth suggesting that at that depth the shockwave may have been insufficiently strong to melt the rock.

This is also consistent with values obtained by Engelhardt (1997) for the Ries structure in Germany in which 72% of polymict breccias were of type II or lower shock state. This is in spite of a particularly shallower basement depth of 600m and the suggestion by Engelhardt that the bulk of the kinetic energy of the projectile was transferred to the crystalline basement. Perhaps the low shock state of surface deposited breccias is due to a substantially smaller kinetic energy release (Ries is only 6-7km in diameter compared to about 25km for Haughton).

It is also important to note that complete melting and subsequent recrystallization to shock state 0 is common at many other sites such as Chicxulub (Schmitt).

[1] Metzler et al (1988) *Composition of the Crystaline Basement and Shock Metamorphism of Crystalline and Sedementary Target Rocks at the Haughton Impact Structure, Devon Island, Canada.* Meteoritics 23, 197-207.

[2] Stoffler (1974) *Deformation and Transformation of rock forming minerals by natural and experimental shock processes.* Fortscher. Mineral51 256-298.

[3] Deutsch et al (2003) *How homogeneous are impact melts? Sr-Nd case studies at Chicxulub and Popigai.* European Geophysical Union Conference Abstract.

[4] Schmitt et all (2003) *Shock metamorphism of impactite lithologies of the ICDP Chicxulub drill core YAX-1.* European Geophysical Union Conference Abstract.

[5] Engelhardt (1997) *Suevite breccia of the Ries impact crater, Germany: Petrography, Chemistry and Shock Metamorphism of crystalline rock clasts.* Meteoritics, 32 545-554.

Before and After: The Environment of an Impact

By Jade Bond

Pre-Impact

The impact that produced the Sierra Madera crater is believed to have occurred <100 million years ago (Ma). As the impact occurred after early Cretaceous sediments had been laid down in the area but quite likely before they solidified, the impact is believed to have occurred sometime in the Late Cretaceous or Early Tertiary period (Wilshire et. al. 1972). As such, a brief overview of the environment at the impact location in each period is provided.

Late Cretaceous 65-98.9 Ma:

- Geography – All of Texas was either the coast or the coastal shelf for an enlarged Gulf of Mexico. Specifically, at this time, the impact area was coastal lowland and relatively close to being at sea level (< 200m in elevation). The impact site has undergone only relatively minor changes in latitude but has experienced significant longitude changes in drifting from its Late Cretaceous position to its present day location.
- Geology – There were no significant, large scale deformation events occurring in the region. The Rockies had just begun to form, sea levels were falling and the inland sea of continental America was draining. The impact site had recently (geologically speaking) emerged from underwater and at this stage, fluviodeltaic sediments are likely to have been deposited in the region.
- Atmosphere – The global average temperature during the cretaceous period was approx. 6.5°C warmer than today (Barron et. al. 1995). Global average precipitation may have been 28% greater than today (Barron et. al. 1989). In general, the region was either at the tail-end of or beginning to recover from the Cretaceous Greenhouse event where global CO_2 levels rose to above 1,000 ppm (Ludvigson, 1999). This increased concentration resulted in global warming and possibly assisted the genetic boom observed at this time.
- Fauna – Every little kids dream!!!! Dinosaurs were common and fossils from this period that have been found in the broad area include Alamosaurus, Tyrannosaurus and Stegoceras (see Figure 1). Marine fossils are also common and include ammonites, rudists, oysters, corals and clams.

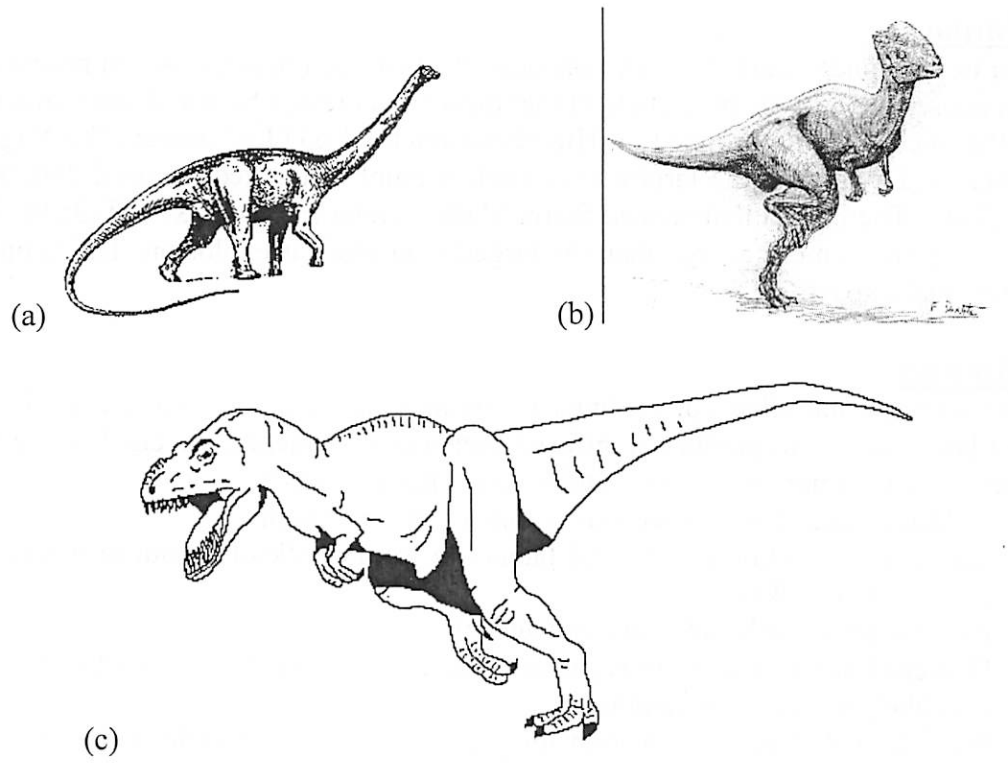

Figure 1: *Some of the larger fauna present in the impact region during the late Cretaceous. (a) Alamosaurus. Source: http://www.isgs.uiuc.edu/dinos/de_4/5cbe4d9.htm (b) Stegoceras. Source: http://www.isgs.uiuc.edu/dinos/de_4/5cbdbf2.htm (c) Tyrannosaurus. Source: http://www.isgs.uiuc.edu/dinos/de_4/5cb30f4.htm*

Early Tertiary (Paleocene Epoch) 58 – 64 Ma:

- Geography and Geology – No large change from the Late Cretaceous period. Interior USA continued to drain and drift towards its current position.
- Fauna and Flora – The K/T mass extinction wiped out many species previously seen in the impact area, such as the dinosaurs. We now begin to see the emergence of modern flora, with mammals later appearing in the Eocene Epoch.
- Atmosphere – It's likely that in the first few decades of the Paleocene that the area was still undergoing climate changes from the extinction event. The atmosphere began to warm towards the end of the Paleocene, leading in to the Eocene, the warmest period in geologic history (IMS, 1999).

The Impact

In order to fully understand the environmental effects of the impact, it is first necessary to gain an appreciation of the magnitude of the impact that created Sierra Madera crater. For scale, the nuclear bomb dropped on Hiroshima released 63TJ of energy, the Nagasaki bomb released 84TJ and the largest ever nuclear bomb detonated released 240, 000TJ (Elert, 2000). The impact that created Sierra Madera crater released $3x10^{19}$J ($3x10^{7}$TJ) of energy - 125 times more energy than the largest ever nuclear explosion. That's one big environmental impact!

Post-Impact

Global environmental effects of the impact were minimal. While the impact was large, it was not large enough to produce significant global environmental effects. Local effects, however, were common, widespread and severe. They included:

- Wildfires ignited within seconds within a radius of 90km
- Massive destruction and loss of fauna life from shockwaves out to 95km, trees felled out to 220km.
- Possible local earthquakes and/or tsunamis
- Darkened skies, leading to regional cooling for weeks, if not months. Acid rain also likely to occur for months.
- Possible global ozone depletion for years via chemical reactions with NO, soot and debris particles.
- Plant growth altered and disrupted for weeks to months

All effects based on Paine (2001) and Toon et. al. (1997)

In general, all of these effects were highly localized with the impact itself having little overall global impact. All of these effects were transient and lasted only a few years at most, unlike the effects of larger impacts, such as that associated with the K/T mass extinction event.

References:

Barron, E.J., Fawcett, P.J., Peterson, W.H., Pollard, D., and Thompson, S.L., 1995, A "simulation" of mid-Cretaceous climate, *Paleoceanography,* v. 10, no. 5, p. 953-962.

Barron, E.J., Hay, W.W., and Thompson, S., 1989. The hydrologic cycle, a major variable during Earth history, *Palaeogeography, Palaeoclimatology, Palaeoecology (Global and Planetary Change Section)*, v. 75, no. 3, p. 157-174.

Elert, G., 2000. Energy of a Nuclear explosion. Accessed online at: http://hypertextbook.com/facts/2000/MuhammadKaleem.shtml

IMS, 1994. Paleoclimatology: mapping the earth's past and future climate. *IMS News '94*. Accessed online at: http://ims.ucsc.edu/imsnews2.html

Ludvigson, G. A., 1999. Global Climate Change and the Cretaceous Greenhouse World, *Iowa Geology 1999.* Accessed online at: http://www/igsb.usiowa.edu/inforsch/greenhse/grnhouse.htm

Paine, M., 2001. Soirce of Australiasian Tektites?, *Meteorite*, February 2001.

Toon, O., Morrison, D., Turco, R.P. and Covey, C., 1997. Environmental Perturbations causes by the impacts of asteroids and comets, *Rev. Geophysics*, v. 35, no. 1, p. 41-78.

Wilshire, H.G., Offield, T.W., Howard, K.A., and Cummings, D., 1972, Geology of the Sierra Madera Cryptoexplosion structure, Pecos county, Texas: U.S. Geological Survey Professional Paper 599H, 42 p.

Impact-induced hydrothermal circulation at the Sierra Madera crater

Oleg Abramov

I. Introduction

Current research suggests that impact-generated hydrothermal systems may have played an important role on early Earth. Several lines of evidence point to a dramatic increase in the number of impact events at ~3.9 Ga, which coincides remarkably well with the earliest isotopic evidence of life at ~3.85 Ga. This period, often referred to as the Lunar Cataclysm, lasted 20 to 200 million years, during which time hydrothermal heat generated by impact events may have exceeded that generated by volcanic activity. These impacts would have resurfaced most of the Earth, and may have vaporized the Earth's oceans, virtually eliminating surface habitats. At the same time, an abundance of subsurface habitats in the form of large subsurface hydrothermal systems would have been created. These habitats could have provided sanctuary for existing life or perhaps the site of life's origin. Genetic evidence in the form of phylogenies that suggest that Archaea, Bacteria, and Eukarya have a common ancestor comparable to present-day thermophilic or hyperthermophilic organisms, further underscores the potential importance of hydrothermal systems in general, and impact-induced hydrothermal systems in particular, at the dawn of life.

Hydrothermal systems generated by an impact event have been identified at a wide range of terrestrial craters, such as Lonar (1.8 km), Haughton (~24 km), Manson (~35 km), Puchezh-Katunki (80 km), Chicxulub (180 km) and Sudbury (~150-250 km), based on an array of mineralogical evidence. Impact-induced hydrothermal activity at Martian craters has been suggested as well.

In order for hydrothermal circulation to occur, two things need to be present – a **heat source** and **presence of water**. The heat sources produced by an impact event are as follows:

- Shock heating: During an impact, a fraction of the kinetic energy of the impactor is converted into thermal energy by the shock wave that compresses the target material. This is the main heat source for a crater the size of Sierra Madera (~12 km original rim-to-rim diameter) and would have raised the temperature of the rocks in the central peak by several hundred degrees Celsius.

- Impact melt sheet: For large impactors, the resulting temperature increase melts the target material. However, no significant amount of melt is expected for a crater the size of Sierra Madera, and indeed, there is no evidence of a melt sheet.

- Central uplift: During large crater formation, warmer material from the lower crust is uplifted to the near-surface. At Sierra Madera, Permian rocks have been uplifted 1200 m, increasing the temperatures by ~25 °C.

Overall, there is little doubt that sufficient heat was deposited by the Sierra Madera impact to drive a hydrothermal system. Craters as small as the 1.8 km diameter Lonar crater in India show evidence of hydrothermal alteration (*Newsom et al.* 2004). However, the second parameter needed for a hydrothermal system, the presence and abundance of water, needs to be addressed in more detail.

II. Hydrologic conditions at the time of Sierra Madera's formation

Wilshire et al. (1972) suggested that the impact occurred some time after the Lower Cretaceous strata were deposited but before they were completely consolidated, thus, in Late Cretaceous or early Tertiary time.

During the Late Cretaceous period, the Sierra Madera site was most likely submerged in shallow water. In Early Cretaceous, the shallow Mesozoic seas extended inland, covering most of the state-as far west as the Trans-Pecos region and north almost to the state line. During most of the Late Cretaceous, much of Texas lay beneath marine waters that were deeper than the Early Cretaceous seas (*Spearing*, 1991). Local sedimentary strata from the late Cretaceous (the Washita group, the Woodbine group, the Eagle Ford Group, the Austin Group, and the Taylor Group) contain abundant marine fossils. This, among other lines of evidence, lead *Kelly* (1966) to suggest that the Sierra Madera crater formed as a result of impact into water.

The Late Cretaceous was the time of the last major seaway across Texas. At the end of the Cretaceous and the beginning of the Tertiary, major uplift and mountain building in the western United States during the Laramide Orogeny affected the southwestern and western border regions of Texas. This regional uplifting formed the Rocky Mountains, and large river systems draining from the young Rockies southeastward across Texas toward the Gulf of Mexico buried the older marine deposits. Major deltas fed by these rivers prograded the early Cenozoic coastline more than 100 miles seaward into the Gulf of Mexico (*Spearing*, 1991). While the Sierra Madera site was no longer submerged, there was abundant subsurface water replenished by the rivers draining from the Rocky Mountains. Thus, in both Late Cretaceous and early Tertiary time, the region was wet and the target rocks of the Sierra Madera impact were saturated with water.

III. Expected mineralogy

Where to look

At the crater the size of Sierra Madera, the hydrothermal fluids could have circulated through the central peak, the breccias on the floor of the crater, or through the faults of the modification zone near the outer rim. While the floor of the crater is covered by alluvial deposits and the rim of the crater is extensively eroded, the central peak is well-exposed and is a promising site to look for hydrothermal alteration. It was also the hottest region of the crater and most likely the region where the circulation was most vigorous and long-lived. Substantial hydrothermal alteration of the central peak has been observed in many terrestrial impact craters such as Manson (~35 km), Puchezh-Katunki (~80 km), and Siljan (~52 km) and is predicted by numerical modeling (Fig. 1)

What to look for

Hydrothermal alteration occurs when a hot fluid dissolves the minerals, allowing new minerals to form as a result of reactions within the fluid and between the fluid and the rock matrix. Upon cooling, the minerals precipitate out of the fluid, filling the voids in the rock. Signs of hydrothermal alteration can include unusual colors, such as green in the case of chloritization, halos around rocks, mineral veins, and inclusions. Specific examples of hydrothermal alteration are listed below:

- **Propylitic:** ***(Chlorite, Epidote, Actinolite)*** Propylitic alteration turns rocks green, because the new minerals formed are green. These minerals include chlorite, actinolite and epidote. They usually form from the decomposition of Fe-Mg-bearing minerals, such as biotite, amphibole or pyroxene, although they can also replace feldspar. Propylitic alteration occurs at relatively low temperatures. Propylitic alteration will generally form in a distal setting relative to other alteration types.
- **Sericitic:** ***(Sericite)*** Sericitic alteration alters the rock to the mineral sericite, which is a very fine-grained white mica. It typically forms by the decomposition of feldspars, so it replaces feldspar. In the field, its presence in a rock can be detected by the softness of the rock, as it is easily scratchable. It also has a rather greasy feel (when present in abundance), and its color is white, yellowish, golden brown or greenish. Sericitic alteration implies low pH (acidic) conditions.
  Alteration consisting of sericite + quartz is called "phyllic" alteration. Phyllic alteration associated with porphyry copper deposits may contain appreciable quantities of fine-grained, disseminated pyrite which is directly associated with the alteration event.

- **Potassic**: ***(Biotite, K-feldspar, Adularia)*** Potassic alteration is a relatively high temperature type of alteration which results from potassium enrichment. This style of alteration can form before complete crystallization of a magma, as evidenced by the typically sinuous, and rather discontinuous vein patterns. Potassic alteration can occur in deeper plutonic environments, where orthoclase will be formed, or in shallow, volcanic environments where adularia is formed.
- **Albitic**: ***(Albite)*** Albitic alteration forms albite, or sodic plagioclase. Its presence is usually an indication of Na enrichment. This type of alteration is also a relatively high temperature type of alteration. The white mica paragonite (Na-rich) is also formed sometimes.
- **Silicification**: ***(Quartz)*** Silicification is the addition of secondary silica (SiO2). Silicification is one of the most common types of alteration, and it occurs in many different styles. One of the most common styles is called "silica flooding", which results form replacement of the rock with microcrystalline quartz (chalcedony). Greater porosity of a rock will facilitate this process. Another common style of silicification is the formation of close-spaced fractures in a network, or "stockworks", which are filled with quartz. Silica flooding and/or stockworks are sometimes present in the wallrock along the margins of quartz veins. Silicification can occur over a wide range of temperatures.
- **Silication**: ***(Silicate Minerals +/- Quartz)*** Silication is a general term for the addition of silica by forming any type of silicate mineral. These are commonly formed in association with quartz. Examples include the formation of biotite or garnet or tourmaline. Silication can occur over a wide range of temperatures. The classic example is the replacement of limestone (calcium carbonate) by silicate minerals forming a "skarn", which usually form at the contact of igneous intrusions.
  A special subset of silication is a style of alteration called "greisenization". This is the formation of a type of rock called "greisen", which is a rock containing parallel veins of quartz + muscovite + other minerals (often tourmaline). The parallel veins are formed in the roof zone of a pluton and/or in the adjacent country rocks (if fractures are open). With intense veining, some wallrocks can become completely replaced by new minerals similar to the ones forming the veins.
- **Carbonatization**: ***(Carbonate Minerals)*** Carbonitization is a general term for the addition of any type of carbonate mineral. The most common are calcite, ankerite, and dolomite. Carbonatization is also usually associated with the addition of other minerals, some of which include talc, chlorite, sericite and albite. Carbonate alteration can form zonal patterns around ore deposits with more iron-rich types occurring proximal to the deposit.
- **Alunitic**: ***(Alunite)*** Alunitic alteration is closely associated with certain hot springs environments. Alunite is a potassium aluminum sulfate mineral which tends to form massive ledges in some areas. The presence of alunite suggests high SO4 gas contents were present, which is thought to result from the oxidation of sulfide minerals.
- **Argillic**: ***(Clay Minerals)*** Argillic alteration is that which introduces any one of a wide variety of clay minerals, including kaolinite, smectite and illite. Argillic alteration is generally a low temperature event, and some may occur in atmospheric conditions. The earliest signs of argillic alteration includes the bleaching out of feldspars.
  A special subcategory of argillic alteration is "advanced argillic". This consists of kaolinite + quartz + hematite + limonite. feldspars leached and altered to sericite. The presence of this assemblage suggests low pH (highly acidic) conditions. At higher temperatures, the mineral pyrophyllite (white mica) forms in place of kaolinite.
- **Zeolitic**: ***(Zeolite Minerals)*** Zeolitic alteration is often associated with volcanic environments, but it can occur at considerable distances from these. In volcanic environments, the zeolite minerals replace the glass matrix. Zeolite minerals are low temperature minerals, so they are generally formed during the waning stages of volcanic activity, in near-surface environments.
- **Serpentinization and Talc Alteration**: ***(Serpentine, Talc)*** Serpentinization forms serpentine, which recognized softness, waxy, greenish appearance, and often massive habit. This type of alteration is only common when the host rocks are mafic to ultramafic in composition. These types of rocks have relatively higher iron and magnesium contents. Serpentine is a relatively low temperature mineral. Talc is very similar to the mineral serpentine, but its appearance is slightly different (pale to white). Talc alteration indicates a higher concentration of magnesium was available during crystallization.
- **Oxidation**: ***(Oxide Minerals)*** Oxidation is simply the formation of any type of oxide mineral. The most common ones to form are hematite and limonite (iron oxides), but many different types can form, depending on the metals which are present. Sulfide minerals often weather easily because they are susceptible to oxidation and replacement by iron oxides. Oxides form most easily in the surface or near surface environment, where oxygen from the atmosphere is more readily available. The temperature range for oxidation is variable. It can occur at surface or atmospheric conditions, or it can occur as a result of having low to moderate fluid temperatures.

(from *http://www.dmtcalaska.org/course_dev/explogeo/class08/notes08.html*)

IV. References

Abramov, O. and D. A. Kring, Impact-Induced Hydrothermal System at the Sudbury Crater: Duration, Temperatures, Mechanics, and Biological Implications, *Lunar Planet. Sci., XXXV*, abstract 1697, 2004.

Newsom, H. E., M. J. Nelson, C. K. Shearer, F. J. M. Rietmeijer, R. Gakin, and K. Lee, Major and Trace Element Variations in Impact Crater Clays from Chicxulub, Lonar, and Mistastin, Implications for the Martian Soil, *Lunar Planet. Sci., XXXV*, abstract 1087, 2004.

Kelly, A.O. 1966 A water-impact hypothesis for the Sierra Madera structure in Texas, *Meteoritics,* **3**, 79-82, 1966.

Spearing, D., *Roadside Geology of Texas*, Mountain Press Publishing Company, Missoula, Montana, 418 pp., 1991.

Wilshire, H.G., Offield, T.W., Howard, K.A. and Cummings, D., Geology of the Sierra Madera cryptoexplosion structure, Pecos County, Texas, *U.S. Geological Survey Professional Paper* 599-H, 42 pp, 1972.

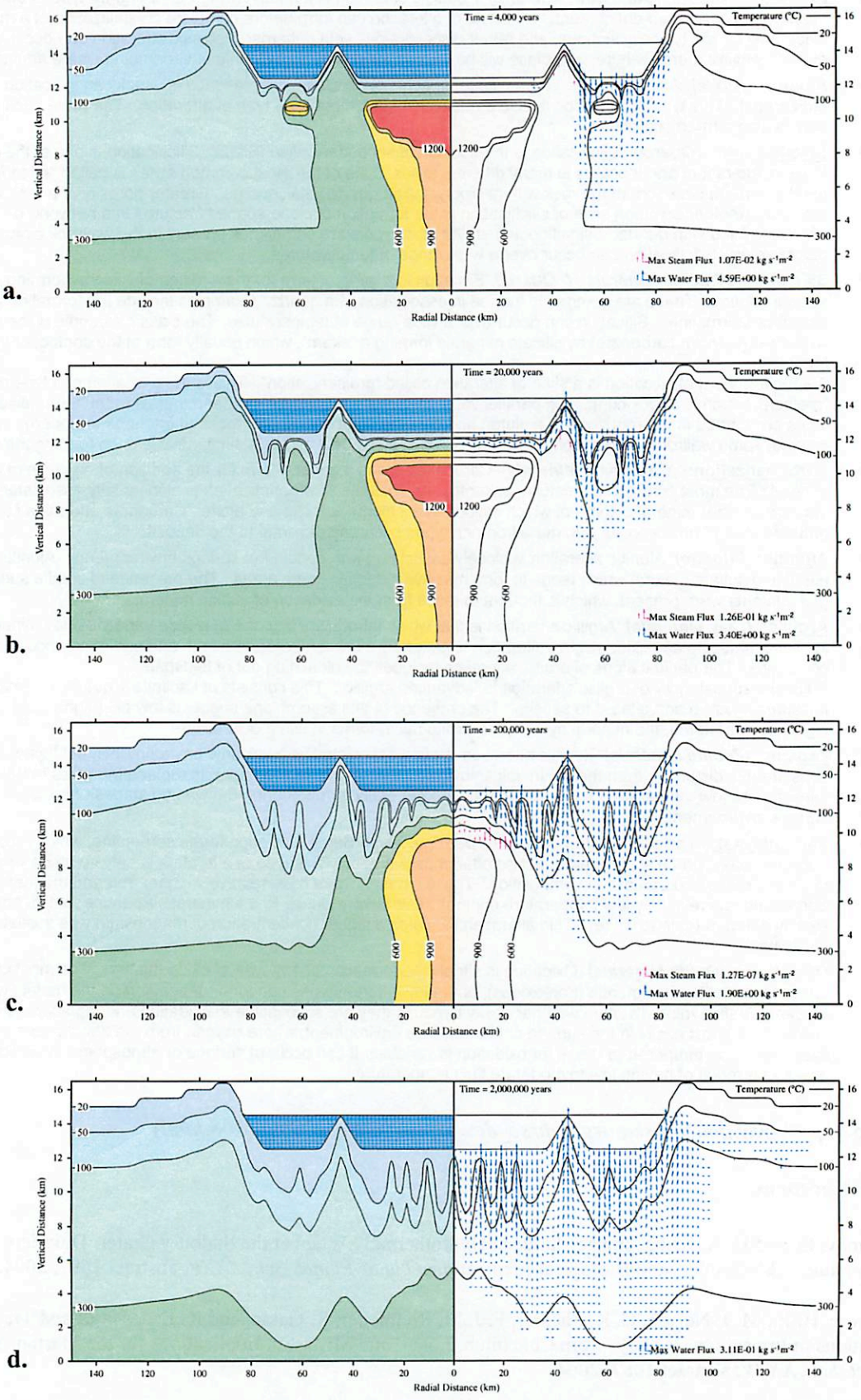

Figure 1. A numerical model of impact-induced hydrothermal circulation at the Sudbury crater. While this crater is an order of magnitude larger than Sierra Madera, some parallels can be drawn. Note, for example, the strong, long-lived upwelling in the peak ring, which is similar to Sierra Madera's central peak.

The Monahans Meteorite

Presented by Carl W. Hergenrother
Spring 2004 Field Trip
West Texas – Kilbourne Hill - Sierra Madera – Odessa

A short time before sunset on 22 March 1998, a fireball was observed to pass over the Odessa-Midland region of Texas. Traveling from the ENE to WSW, the fireball terminated and dropped fragments near the town of Monahans, Texas (located in the west Texas Big Bend area) (Fig. 1). [1] The orange and green fireball left a smoky train that was visible for 2 minutes. A series of sonic booms was heard over the course of 5 seconds. Two stones were recovered (Fig. 2), one fell within 40' of a group of boys playing basketball; the other piece was recovered by a Sheriff's deputy imbedded in asphalt. The first piece weighed 1243 grams and was transported to Johnson Space Center (JSC) within 50 hours of its fall. The second larger piece weighed 1344 grams and was found a day after the fall. This meteorite is now named the Monahans (1998) meteorite. Confusingly, an earlier iron meteorite find in the region from 1938 also goes by the name Monahans. [1]

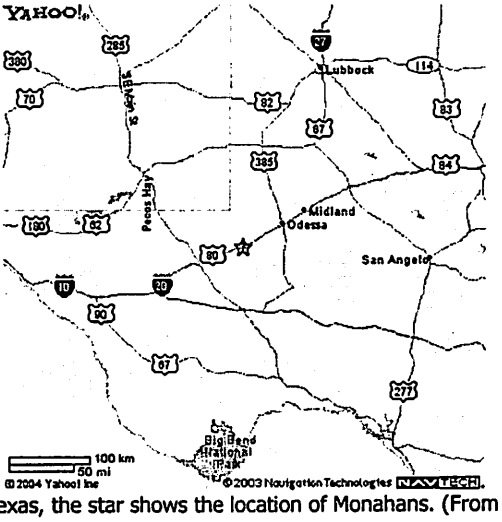

Fig.1 – Map of the west Texas, the star shows the location of Monahans. (From http://maps.yahoo.com)

The Monahans meteorite is a regolith breccia consisting of light and dark clasts within an intermediate gray matrix. The hue is related to the shock level. The lightest clast corresponds to a shock level S2 (5 to 10 GPa), the gray matrix to S3 (10 to 15 GPa) and the dark clast to S4 (15 to 30 GPa). [4] The light colored clast made up ~65 vol%, the dark clast ~5 vol% and gray matrix ~35 vol% of a small sample; though these proportions may not represent the entire rock. [3] All of the lithologies are H5. Large aggregates of purple halite (NaCl) crystals (up to 3 mm in diameter) were contained in the gray matrix. This marked the first occasion in which large non-microscopic halite have been observed in meteoritic samples. Crystals of sylvite (KCl) are present within the halite crystals, which is also common in terrestrial evaporates. A second unrelated fall in 1998 was also found to contain large halite crystals, the Zag (Morocco) fall. [2]

Some of the halite crystals contained fluid inclusions that formed when the halite originally precipitated. A number of secondary fluid inclusions were the result of the breaking of halite crystals by hypervelocity impacts on the regolith surface. The relative lack of vapor bubbles within the inclusion fluid suggests the halite precipitated at low temperatures (≤ 100 °C) (Fig. 3).

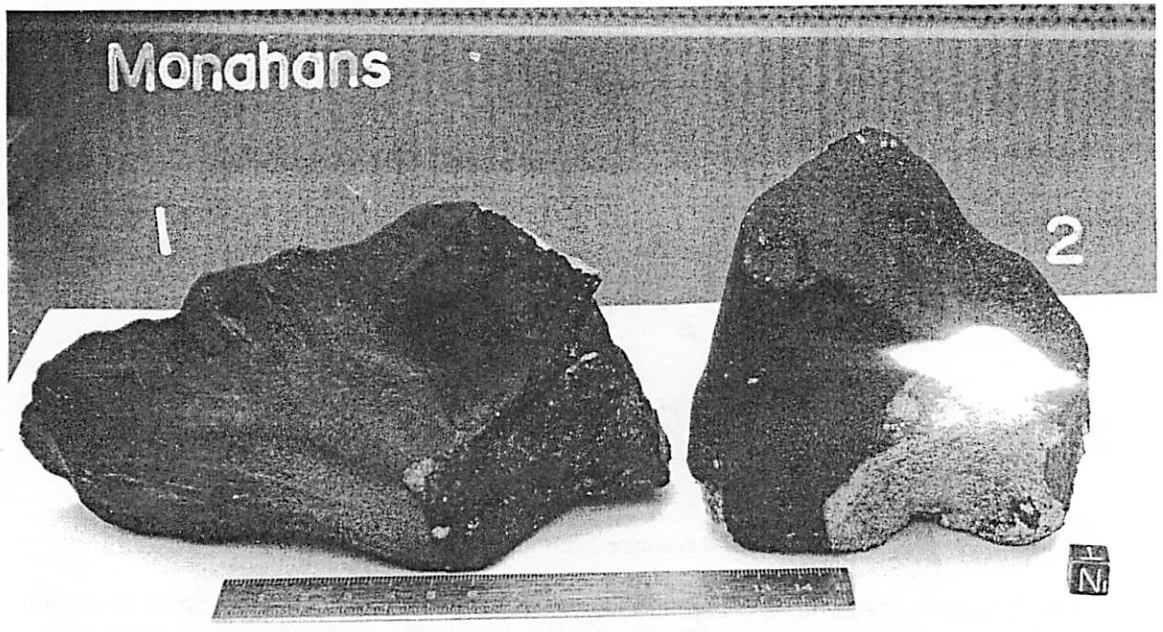

Fig. 2 – Image of the two stones that compose the Monahans fall. (From http://www-curator.jsc.nasa.gov/astromaterials/specialfeatures/monahans/)

The great abundance of halite on the surface of the Earth begs the question of terrestrial contamination. Rubin *et al.* (1998) make a number of arguments for a preterrestrial origin of the halite. Monahan was a fresh fall and picked up within minutes. The Monahan area is in a desert and there was no precipitation on the date of the fall. Within 3 days, the sample was opened by hammer and chisel at JSC. The halite was found throughout the matrix region of the meteorite. Terrestrial fluids could not have permeated the extent of the rock in the short amount of time exposed to the elements. The color of the halites strongly suggests that it was exposed to ionizing radiation. The majority of terrestrial halites are clear while Monahan's are bluish purple. The color is due to electron trapping in Cl^- vacancies. Finally, the Ar-Ar ages of the halite crystals produce a minimum age of 4.33 ± 0.01 Ga, much too old for terrestrial halites.

Both Monahan and Zag have shed light on the complex series of modifications that took place on the H-chondrite parent body. A summary of parent body process is presented in Rubin et al. (2002). After agglomeration, the H-chondrite parent was comprised of unequilibrated primitive nebular materials. A phase of heating to 600-950 °C produced the light colored metamorphosed H chondrites. This heating was either due to collisions or the decay of ^{26}Al. Following the period of thermal metamorphism, the rocks were shocked causing metallic Fe-Ni and troilite to be melted and mobilized. The result was the production of the dark clasts. A continuous rain of impactors pulverized the surface producing the clastic regolith. The impacts also created small droplets of chondritic melt that were incorporated into the regolith. During the entire process, solar-wind noble gases bombarded the regolith and were implanted into the regolith. The light and dark color clasts, on the other hand, do not absorb a large concentration of particles due to their low porosity. The ancient ages of the halite grains in both Monahans and Zag indicate that aqueous alteration occurred in the early days of the solar system within a few million years of accretion. Since the fluid inclusions suggest a cold temperature (< 100 °C) at trapping, the halite formed in a region of the parent body that was not significantly heated. In order to account for the amount of water-soluble Cl measured, a large amount of rock must have been leached (minimum of 2 to 600 kg, and probably a lot more due to inefficient leaching at low temperatures). Finally, an impact event ejected Monahans from the H-chondrite body. Cosmic-ray dating dates this event to 6.0 ± 0.5 Ma ago.

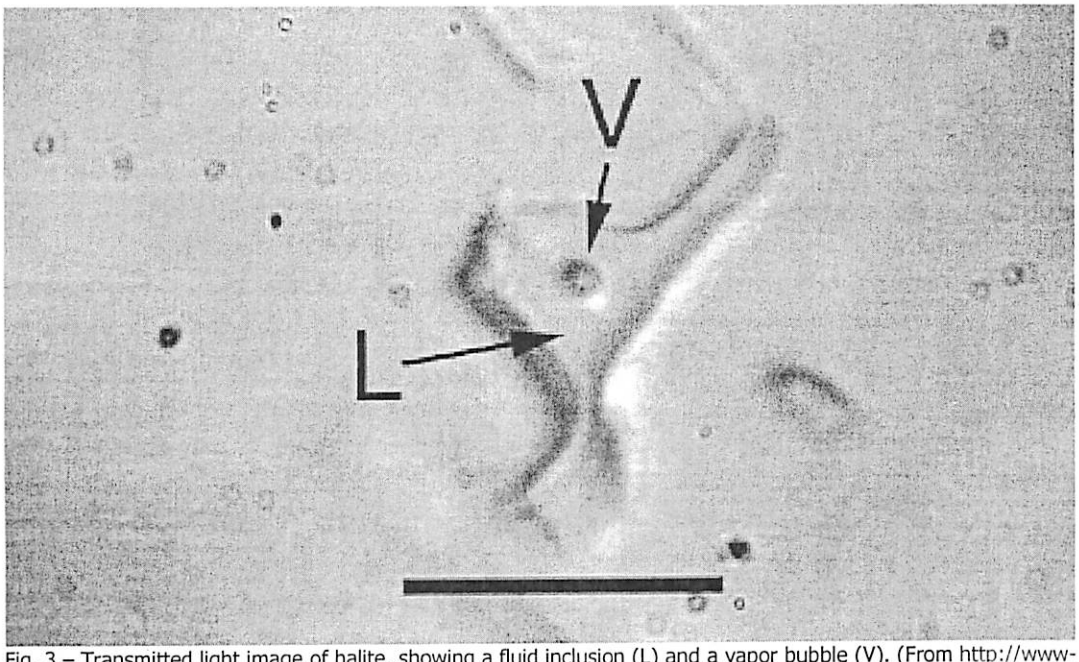

Fig. 3 – Transmitted light image of halite, showing a fluid inclusion (L) and a vapor bubble (V). (From http://www-curator.jsc.nasa.gov/astromaterials/specialfeatures/monahans/)

References

[1] Bogard, D. D., D. H. Garrison and J. Masarik. 2001. The Monahans chondrite and halite: argon-39/argon-40 age, solar gases, cosmic-ray exposure ages, and parent body regolith neutron flux and thickness. *Meteorit. Planet. Sci.* **36**, 107-122.

[2] Gibson, E. K., M. E. Zolensky, G. E. Lofgren, D. J. Lindstrom, R. V. Morris, S. D. Schmidt and S. V. Yang. 1998. Monahans (1998) H5 chondrite: an unusual meteorite fall with extraterrestrial halite and sylvite. *Meteorit. Planet. Sci.* **33**, A57.

[3] Rubin, A. E., M. E. Zolensky and R. J. Bodnar. 2002. The halite-bearing Zag and Monahans (1998) meteorite breccias: shock metamorphism, thermal metamorphism and aqueous alteration on the H-chondrite parent body. *Meteorit. Planet. Sci.* **37**, 125-141.

[4] Zolensky, M. E., R. J. Bodnar, E. K. Gibson Jr., L. E. Nyquist, Y. Reese, C. –Y. Shih and H. Wiesmann. 1999. Asteroidal water within fluid inclusion-bearing halite in an H5 chondrite, Monahans (1998). *Science* **285**, 1377-1379.

The Odessa Impact Crater Complex

Jim Richardson

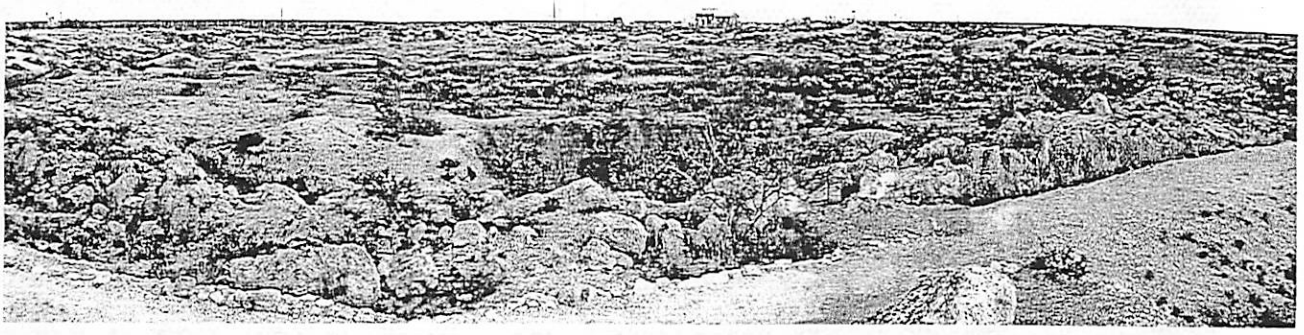

Figure 1: Panoramic view of the main Odessa impact crater, as seen from the western rim of the ~550 ft. diameter structure. Note the man-made trench in the foreground, and the visitor's center on the far (northeast) side.

Introduction

The Odessa impact crater complex is a set of five simple craters formed coincidentally about 50k-100k years ago from the impact of a fragmented, small, iron asteroid body into sedimentary country rock (colluvium, limestone, shale, & sandstone) near what is currently Odessa, Texas. Rough estimates for the original diameter of the impactor are on the order of a few meters. The main impact crater (see *Figure* 1) is about 550 ft (168 m) in diameter and was originally about 77 ft deep, but post-impact crater fill has reduced this depth to just a few feet below the surrounding plains. Total relief on the main crater is now only about 15-20 ft vertical, from crater-center to crater-rim. The next largest crater (crater "No. 2") lies about 100 ft to the west of the main crater, is about 50 ft in diameter, was originally about 15 ft deep, but has been completely filled by post-impact deposition such that virtually no surface relief remains (excluding man-made excavations). Three even smaller (completely filled) craters lie scattered a bit further to the west. Hundreds of kilograms of heavily weathered iron meteorites (coarse octahedrite) have been recovered from the craters and surrounding area, in addition to iron "shale" (rust flakes) and iron spherules.

Local Area Geology

The local area geological stratigraphy is described in the following table, as determined by five bore-holes drilled around the crater site during a 1939-1941 investigation. The impact is estimated to have occurred sometime during the late Pleistocene, at a time when the local climate was more moist and the local soil, now at ~2-4 ft depth, was a reddish sandy-loam with an underlying hard (Ogallala) caliche. In places along the north rim of the main crater, this "event horizon" is sandwiched between massive limestones of the Fredericksburg Group, marking the crater overturn flap.

Table 1: Geological stratigraphy in the Odessa area

DEPTH	THICKNESS	AGE	NAME	DESCRIPTION
0-22 ft	22 ft	Cenozoic		wind-blown sand, semi-arid soils, caliche
22-71 ft	49 ft	Cretaceous	Fredericksburg Group	limestones, shales, sandstones
71-200 ft	129 ft	Cretaceous	Antler Formation	sandstones, gravels, conglomerates
>200 ft		Triassic-Permian		"red beds" (primarily sandstones)

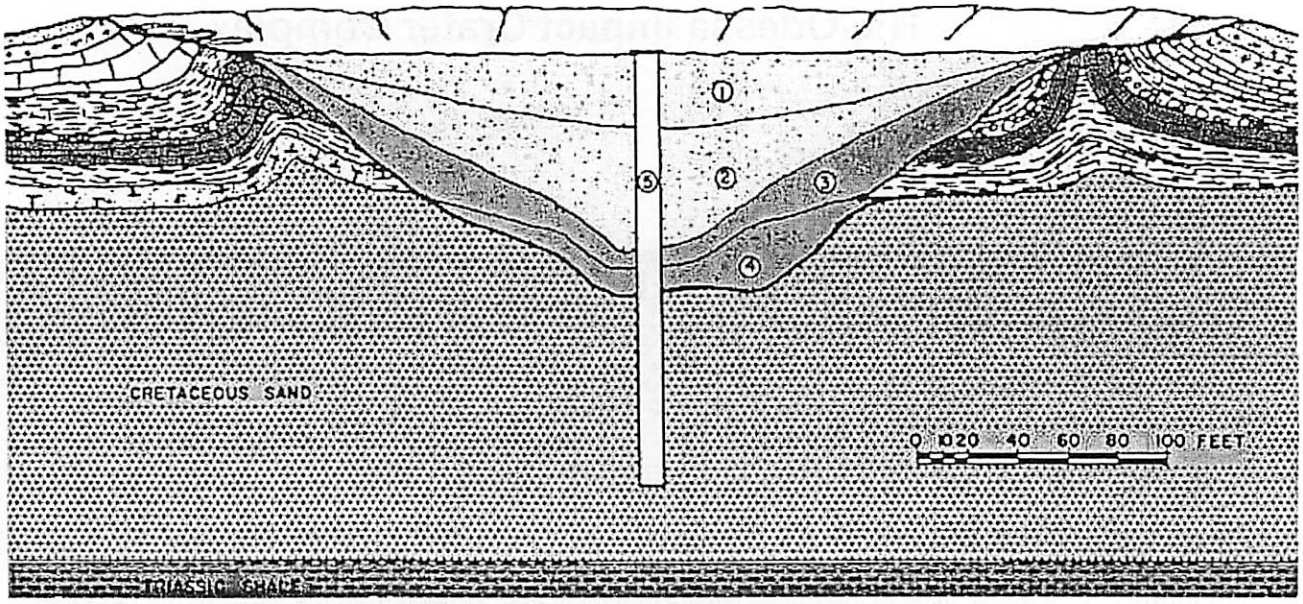

Figure 2: Cross-sectional view of the main crater, showing five material zones: (1) dry-deposition colluvium and aeolian silt, (2) wet-deposition silt, clay, and gravels, (3) crater collapse breccia lens, (4) fragmented bedrock, and (5) 165 ft deep exploratory shaft. Note the sharp anti-cline in the upper massive limestone beds, indicating radial thrust-faulting during crater formation (see diagrams at booklet front).

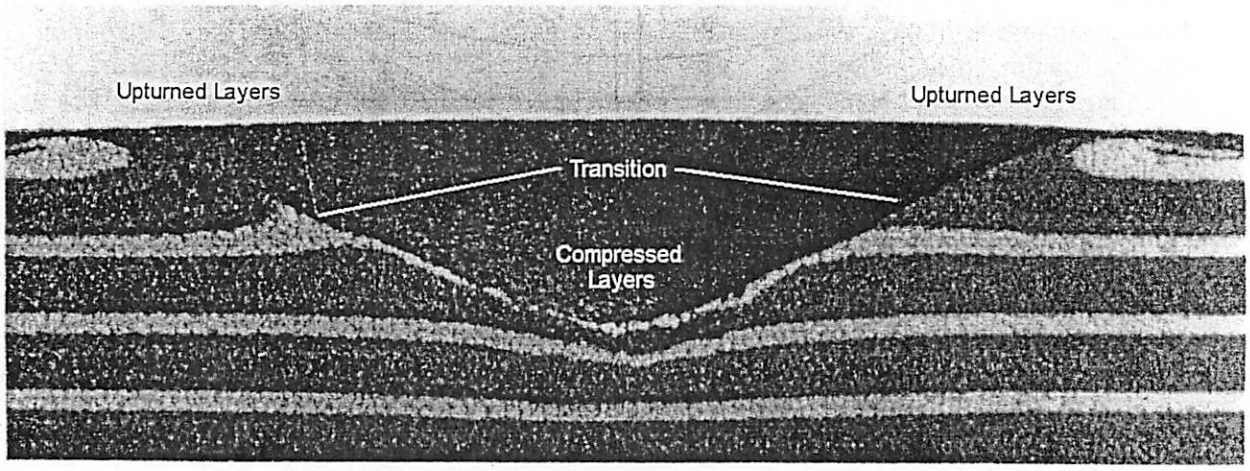

Fig. 5.14 Cross-section of a small-scale impact crater produced in a layered noncohesive sand target. The overturned flap near the rim, uplift of beds near the rim, and downwarp of beds beneath the crater are clearly seen. A white sand layer whose top is about one-third of the transient crater depth below the surface marks the transition between excavation and displacement. *Photo courtesy of P. H. Schultz.*

Figure 3: A similar cross-sectional view of a simple crater formed in the laboratory. Note the clear demarcation between layers which were compressed downward and layers which were thrust upward (with some overturning at the lip of the crater). Note also that the depth of crater excavation is only about 1/2-1/3 the transient crater depth or about 1/4-1/6 the transient crater diameter.

Main Crater Structure & Geology

The geological structure of the Odessa impact craters were extensively investigated in a 1939-1941 expedition headed by the University of Texas. The basic structured is shown in *Figure 2*, as well as in the more detained geological map and trench-cut diagrams provided in the front material of this booklet. *Figure 3* shows the cross-section of a simple crater created in the laboratory. The 165 ft deep main shaft in the center of the crater revealed the following geological stratigraphy:

Table 2: Geological stratigraphy of the main crater central shaft

DEPTH	THICKNESS	AGE	DESCRIPTION
0-25 ft	25 ft	Pleistocene-Holocene	dry colluvium and aeolian deposits (*vertebrates*)
25-77 ft	49 ft	Pleistocene	pond deposited clays, silts, gravels (*invertebrates*)
77-94 ft	17 ft	Pleistocene	highly fractured & shocked breccia lens infill
94-165 ft	71 ft	Cretaceous	Antler Formation sandstone & shale

The rock strata forming the wall of the main crater were lifted, broken, folded, and faulted (see *Figure 2*). The most highly effected layers were those of the Fredericksburg Group, most conspicuously its upper hard, massive limestone layers, originally at a depth of ~22 ft, but which were subsequently uplifted to about 25 above the level of the surrounding plain. Another fossiliferous limestone layer which originally lay at a depth of 50-55 ft below the plain now stands nearly vertically in the crater walls at a depth of only 3-5 ft below the surrounding plains. The impact ejecta blanket, emplaced above the uplifted strata, is now a heavily eroded breccia layer, such that most of the present day rim is due only to the uplifted layers.

An interesting feature of the Odessa main crater are the thrust faults which formed roughly parallel to the crater walls and along which the Cretaceous limestones where pushed upward and outward. As a result, intense folding and a severe anticline appear in these layers, with layers inside the anticline dipping strongly inward and layers outside of the anticline dipping strongly outward.

Simple Crater Excavation and Modification

Figure 4 shows the basic series of events that occur during the excavation and modification stages in the formation of a simple impact crater. The most important point illustrated here is the difference between the *transient crater*, which is the extent of the crater at the time of maximum excavation (point *(c)* in the left hand series), and the *final crater*, which is the extent and composition of the crater following the modification stage (point *(c)* in the right hand series).

The Odessa crater is noteworthy for three reasons: (1) its rather shallow penetration depth, having a transient crater depth-to-diameter ratio of about 1/5 as opposed to the more typical 1/3-1/4, (2) the amount of breccia crater fill that occurred during the modification stage is rather light, leading to (3) a conical shape (see *Figure 2*) rather than a parabolic shape. The contours of the final crater at Odessa was extensively investigated during the 1939-1941 hunt for the main body of the impactor, which was (of course) never found. Curiously, the smaller members of this crater complex also seem to display (according to the published geological cross-sections) the same odd conical shape, even though they did not penetrate beyond the Cenozoic soil and caliche layers.

Impactites at Odessa

Impactites at Odessa primarily originate from the local sandstone layers, in the form of shock modified and metamorphosed quartz grains. The Evans (2000) report identifies "rock flour" and Coesite within the main crater breccia lens (from the borehole investigations). Stishovite might also be expected in this regime. A single shatter cone was also provisionally identified in limestone in the north main crater rim (further investigation?). Note that like the Winslow impact crater (AZ), no forms of impact melt were identified in the 1939-1941 investigation.

Table 3: Expected & found impactites at Odessa

PRESSURE	NAME	PRESENT	REPORT NOTE
2-6 GPa	Shatter cones	perhaps	one located in limestone, north rim
5-35 GPa	Planar deformation features (PDFs)	yes	called "rock flour" (shocked quartz)
15-40 GPa	Stishovite	???	not identified in report
30-50 GPa	Coesite	yes	found in breccia lens

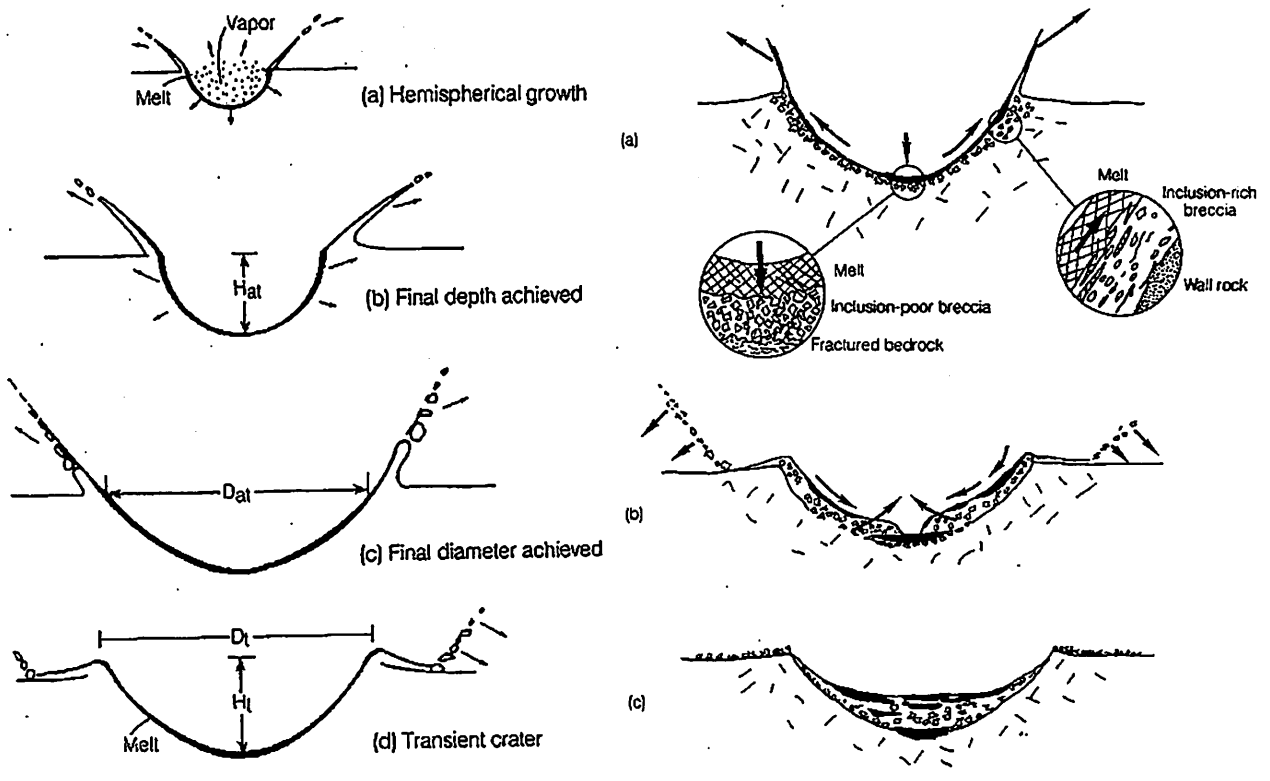

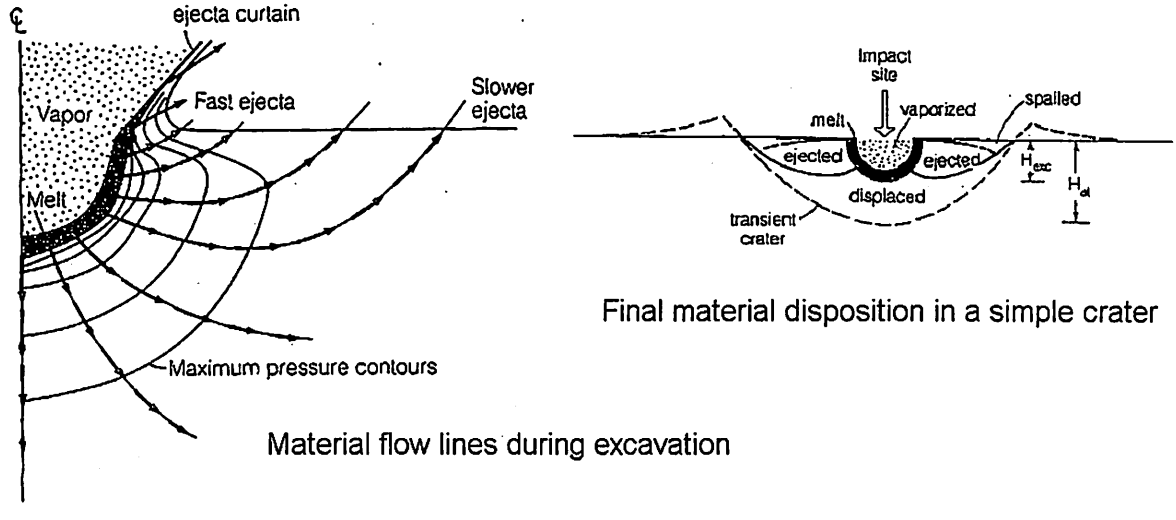

Figure 4: Various figures from *Impact Cratering* (Melosh, 1989), showing details of the excavation *(upper left)* and modification *(upper right)* stages of simple crater formation. The illustration at *lower left* shows typical material flow paths ("stream tubes") during the excavation stage, while the illustration at *lower right* shows the typical final disposition of all materials which originally filled the transient crater.

Primary Reference

Evans, G.L. & Mear, C.E. (2000). The Odessa meteor craters and their geological implications, *Occasional Papers of the Strecker Museum, No. 5.*

Fragmentation of an iron asteroid in the atmosphere

By
C.S. Cooper

1. Odessa Crater Field

The site near Odessa, Texas was identified as a meteorite impact crater site by Daniel Moreau Barringer, Jr., in 1926.[1] As Figures 1-2 show, the site is marked by one large crater having a diameter of ~167 m and depth of 30 m.[2] There is a secondary smaller crater having a diameter of ~21 m and depth of 5 meters (Figure 3, next page). The smaller circle in Figure 1, which is a blow-up of Figure 4 (next page), shows the location of the 21 m secondary crater relative to the large crater; the little x's are locations where one or more meteorites or meteorite fragments from Odessa have been found.

Figure 1: Close-up of Odessa site layout. A blowup of Figure 4 and the legend that shows the primary and secondary craters and nearby meteorite occurrences.

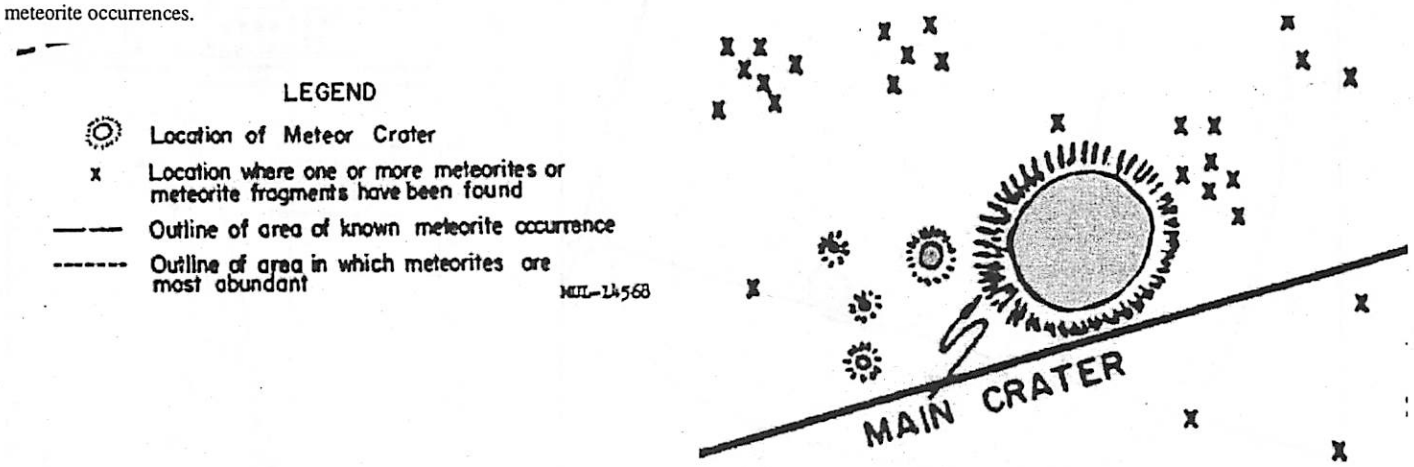

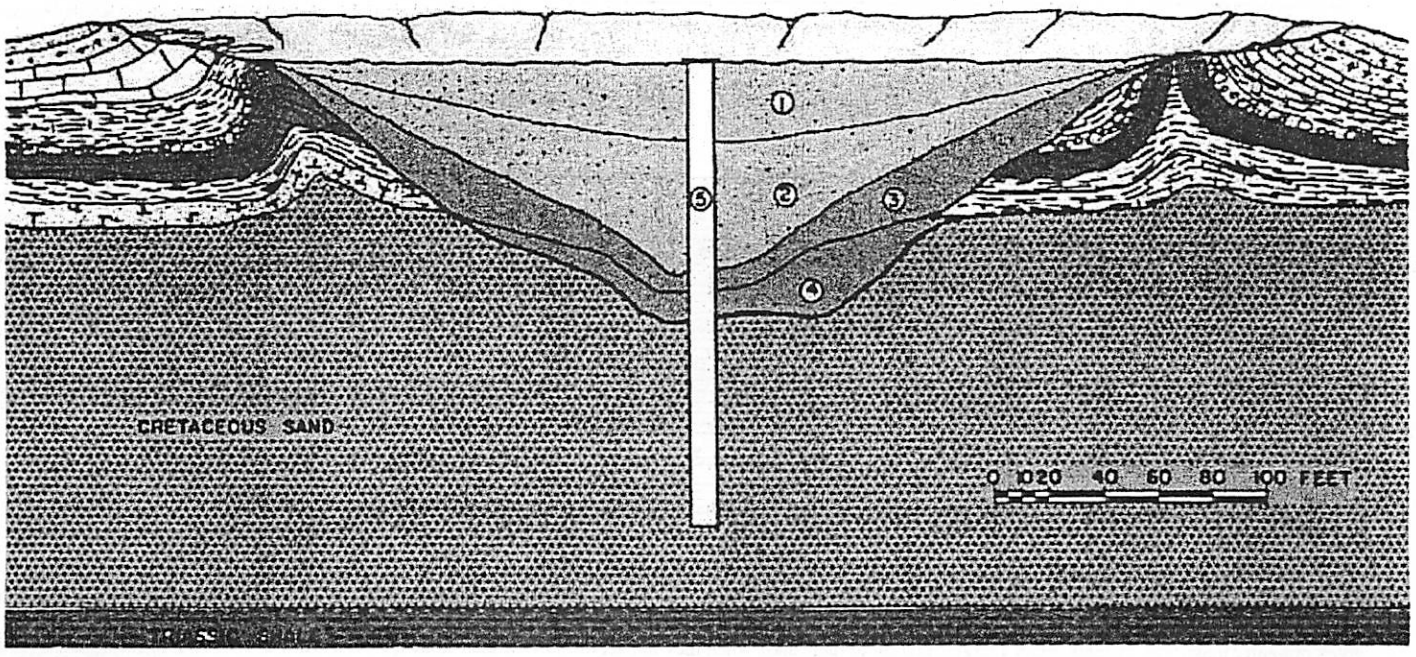

Figure 2 (above): Cross-section of the large crater. The little circled numbers show stratigraphic sections.

Figure 4 (left). Odessa meteor crater site. Shows the relative locations of the primary and secondary craters. Also shows the perimeter (dotted line) of the most abundant meteorite finds and the total region of meteorites found at the site (bold dashed line).

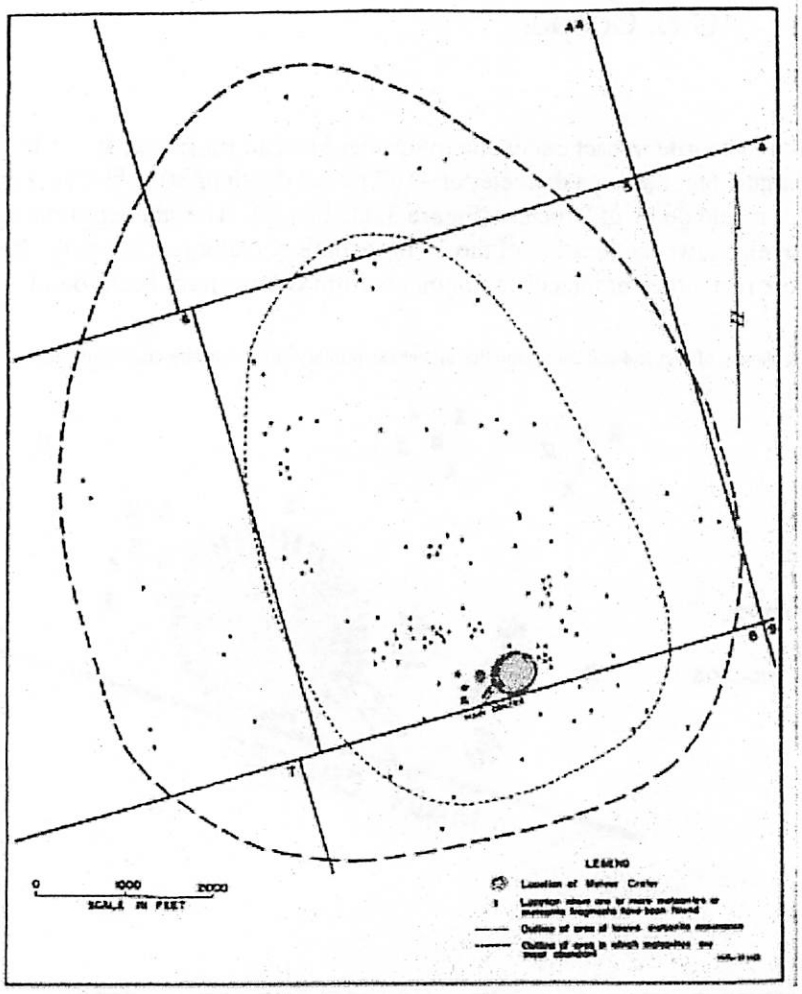

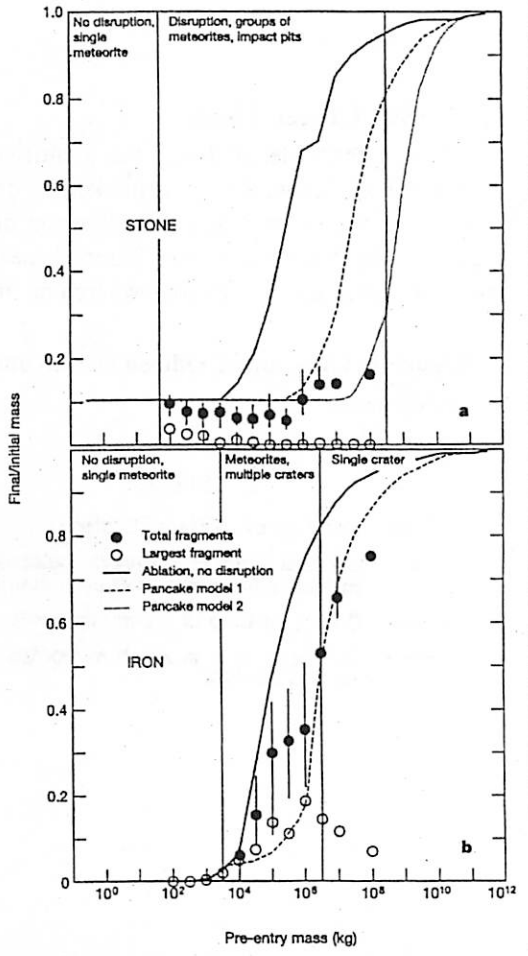

Figure 1 Results of SF and 'pancake' model simulations for stone and iron impactors. The SF model is described in detail elsewhere[3,4]. The model takes into account successive fragmentation and ablation of individual fragments, and simulates the evolution of a meteoroid consisting of a variable number of solid fragments. Early attempts were made at modelling separated fragments[23,24], but most subsequent numerical approximations have taken the form of the more common 'pancake' model[1,2]. While 'pancake' models treat the disrupted meteoroid as a deformable continuous liquid, the SF approximation allows us to define a mass- or velocity-distribution at the surface for fragments that create craters (high final velocity) or occur as meteorites (fragments with low final velocity). The production of crater fields by small fragmented asteroids may therefore be simulated. Two types of projectile are principally considered: irons with density of 7,800 kg m^{-3}, ablation coefficient of 0.07 s^2 km^{-2} and strength of 4.4 × 10^8 dyn cm^{-2} (for 1-kg samples)[3], and stones with density of 3,400 kg m^{-3}, ablation coefficient of 0.014 s^2 km^{-2}, and 10 × lower strength. The parameters for stones were chosen to define approximate upper limits on strength and density: larger stony bodies in the atmosphere, and carbonaceous bolides, may well have significantly lower strength and density. All simulations were at average asteroidal impact velocities and entry angles: 18 km s^{-1} and 45°, respectively. The figure portrays the ratio of final mass (both the combined mass of all surviving fragments >100 g, and the largest single surviving fragment) to initial mass for stone (a) and iron (b) impactors. The 'pancake' model results are also shown: 'pancake model 1' is based on spreading to twice initial radius; 'pancake model 2', spreading to four times initial radius.

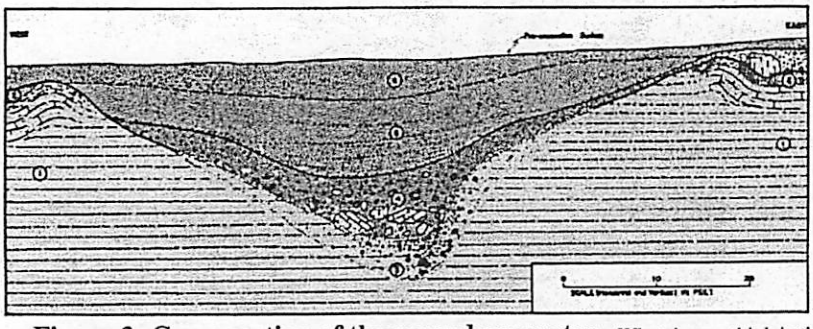

Figure 3: Cross-section of the secondary crater. What do you think is the cause of the asymmetrical shape?

Figure 5 (right): Comparison of the results of a modern numerical model with semi-analytic "pancake" models. This graph is taken from the Nature article by P.A. Bland and N.A. Artemieva [3]. The goal of their research project was to use the separated fragments model to simulate the fragmentation and ablation of an asteroid impacting the Earth's atmosphere both for stone and iron impactors. These new models 1) show that for a given pre-entry mass, iron meteors retain a larger fraction of their mass when they impact the surface than stone meteors. They 2) furthermore show that "over the mass range 103 – 107 kg, iron impactors transfer to the surface about three orders of magnitude more energy per unit area than stones." Finally, note that the simulations shown by these authors indicate more effective fragmentation of asteroids in the planetary atmosphere than the semi-analytic "pancake" models. The authors suggest that perhaps impact hazards to the Earth's surface are considerably lower in likelihood than previously thought.

2. Basic concepts of asteroid fragmentation

As was thoroughly explained around the campfire in Death Valley in October 2000,[7] several factors determine the fate of a meteoroid entering the Earth's atmosphere:

1. Sufficient mass to survive atmospheric passage.
   - Several kg is the minimum mass necessary for meteoroid survivability.
2. Sufficient structural strength and density to survive atmospheric passage.
   - Crudely speaking, a meteoroid must have ~1900-2100 kg/m^3 or greater to survive atmospheric passage.
3. Sufficiently slow meteor geocentric speed.
   - This depends on the direction of approach to the Earth and typically varies from 11.2 km/s up to ~70 km/s.

A meteor shower occurs when an asteroid breaks up in flight near the surface. These fragments hit the ground at different locations in a roughly elliptical pattern called a **strewn field**. The long axis of the ellipse corresponds to the trajectory of the original impactor before it began to fragment. The strewn field of the Odessa site is shown in Figure 4 (previous page). In general, since the massive fragments carry greater linear momentum relative to their cross-sectional surface area, their trajectories will be less affected than their low-mass counterparts by atmospheric drag, both in the vertical and horizontal directions. It is therefore common to find more massive meteorite samples near the edge of the elliptical meteoritic field. This effect is manifest in the Odessa site, as shown in Figure 4, because the large craters that formed by the two most massive fragments are near the periphery of the strewn field.

3. Semi-analytic physical models of asteroid fragmentation

Simple analytical models of impactor fragmentation employ the Newtonian momentum equation for an object in flight. The total linear momentum of the meteor gets smaller with time as it imparts its initial momentum at the top of the atmosphere to the air column underneath it, which is proportional to its cross-sectional area. A bow shock forms in front of the projectile with the atmospheric air compacted at high pressure near the meteor's bottom surface. Since momentum is conserved, the momentum decrease of the meteor is equal to the momentum transferred to the cylindrical column of air swept out by the meteor's path, which in turn depends on the atmospheric integrated column density. The column mass to which the last portion of the impactor penetrates is approximately equal to the mass of the impactor at the top of the atmosphere.[5]

Momentum considerations are combined with a straightforward model for **ablation**, which is the process of melting or evaporation of meteor material as it heats up in the atmosphere. The energy balance here is not as simple as the momentum balance. The heat generated in this highly dissipative process is split between atmospheric heating and heating of the projectile. Temperatures of thousands of degrees are typical for high-velocity impactors. The structure of the ablation in semi-analytical approaches is often assumed to be well-represented by the so called "pancake model," which considers the impactor as a strengthless liquid-like object. In pancake models, the object typically spreads to twice its initial radius.[3]

4. Modern models of asteroid fragmentation in planetary atmospheres

Of course, the simple model outlined above is not adequate for predicting the exact distribution of stony versus iron meteorite finds on Earth. Various research groups worldwide have been steadily improving numerical models of projectile motion through the planetary atmosphere.[3, 4, 5] These calculations involve complex models of asteroid structure and strength and attempt to incorporate realistically the fluid dynamics of the incoming object's interaction with the shocked atmospheric column beneath it. Significant uncertainties remain in the appropriate material equation of state to use for the impactor.[5]

Although it is beyond the scope of this talk to describe the details of numerical models, I was able to find a particularly interesting recent paper on this subject in the July 2003 issue of Nature by P.A. Bland and N.A. Artemieva.[3] They use a "separated fragments" (or SF) model to describe the motion of both stony and iron meteors through the atmosphere. As I show in Figure 5 (page 2), Bland and Artemieva (2003) show that the separated fragments model predicts effective atmospheric disruption of much larger asteroids than previously thought. Given the well-constrained flux of pre-atmospheric asteroids with diameters less than 1 km, they proceed to predict using the SF model the total flux of small bodies striking the Earth surface. They estimate that bodies >220 m in diameter will impact the Earth's surface on average

once every 170,000 years.

Figure 5 also elucidates the relative durability of iron asteroids to stony asteroids, which is in general agreement with meteorite data. The proportion of stony meteorites decreases steadily at higher masses because at low mass, iron asteroids hold a larger fraction of their initial energy intact before striking the surface at high velocity, where they form small craters. Hence, small craters like the Odessa crater are often associated with iron impactors.

5. Other solar system planets

On Venus, where the atmospheric pressure at the surface is roughly two orders of magnitude higher than here on Earth, meteors are very effectively slowed by the atmosphere. Hence, you would expect to find many small meteorites intact on Venus that were slowed by the atmosphere enough to remain intact after they hit the surface.

Neglecting variations in the gravitational acceleration with height, the integrated column density of a hydrostatic atmosphere at the surface of a planet is proportional to its surface pressure and inversely proportional to the acceleration of gravity. Therefore Titan, which has an atmospheric pressure near the surface of ~1.5 bars—comparable to the terrestrial value—but a comparitively lower self-gravity, has a much higher integrated column density of atmosphere than on Earth. Per unit area of the surface, therefore, the mass of atmosphere above you will be an order of magnitude greater on Titan than on the Earth. (Thus, among other reasons, Titan's atmosphere is optically much thicker than Earth's atmosphere, even though they are both composed mostly of nitrogen gas). Like Venus, Titan's atmosphere is much more effective than Earth's atmosphere at slowing down high-velocity asteroids.

Mars, on the other hand, would be expected to have relatively fewer intact meteorites at the surface because its thin atmosphere does note effectively slow incoming objects, which disintigrate when they impact the planet's surface at high velocity.

References

[1] Barringer, Brandon, "Historical Notes on the Odessa Meteorite Crater", 1967Metric...3..161B.

[2] Center for Energy and Economic Diversification, URL: http://www.utpb.edu/ceed/GeologicalResources/West_Texas_Geology/Links/odessa_meteor.htm

[3] P.A. Bland and N.A. Artemieva, "Efficient disruption of small asteroids by Earth's atmosphere," Nature, **424**, 07/17/2003.

[4] Hills, Jack G. and M. Patrick Goda, "The Fragmentation of Small Asteroids in the Atmosphere," AstronomicalJournal, **105** n. 3, 1114-44.

[5] D.G. Korycansky and Kevin J. Zahnle, "High-resolution simulations of the impacts of asteroids into the venusian atmosphere III: further 3D models, Icarus **161** (2003), 244-261.

[6] H.J. Melosh, "Impact Cratering", © 1989 by Oxford University Press, New York.

[7] Richardson, James, "The Gold Basin Meteorite Strewn Field," **Field Guide** to Fall 2000 PtyS Trip to Death Valley, CA.

Impact Melt

Jason W. Barnes
Department of Planetary Sciences, University of Arizona, Tucson, AZ, 85721
jbarnes@c3po.barnesos.net

ABSTRACT

A significant fraction (54%) of the kinetic energy of an impacting bolide is eventually used to melt (14%) and to vaporize (40%) target rock. Impact melt affects the subsequent lithographic, morphological, and thermal evolution of the crater, while some vapor condenses into microtektites that are strewn about either locally (if $D_{\text{crater}} < 15$km for Mars) or globally (for larger craters). The Blueberries found by the Opportunity rover inside Eagle Crater on Mars are not impact spherules.

Subject headings:

1. MELTING AND VAPORIZATION

Crater-forming collisions between planets and other bodies can be thought of as the nearly instantaneous deposition of $\frac{1}{2}mv^2$ of kinetic energy into the outer layers of the planet's crust. In the end, nearly all of the initial energy gets converted to heat. As the shock wave generated by the collision propogates through target material, some the shock's energy dissipates, heating the material that it propogates through. The amount of heating is greatest for the target rocks closest (in a 3D radial sense) to the impact point, and diminishes for those farther away. The target rock closest to the impact point has enough heat applied to vaporize the rock. This vaporized material becomes a plume of gas that expands as a function of time (see Section 2 for more on what happens to the plume).

At a certain radial distance from the point of impact, the shock begins to deposit an amount of heat insufficient to vaporize the target rock, but sufficient to melt it. At a larget radial distance, the rock is heated but not enough to melt. Thus a hemispherical shell exists where the majority of target rock gets melted (see Figure ??).

The mass of target material melted relative to

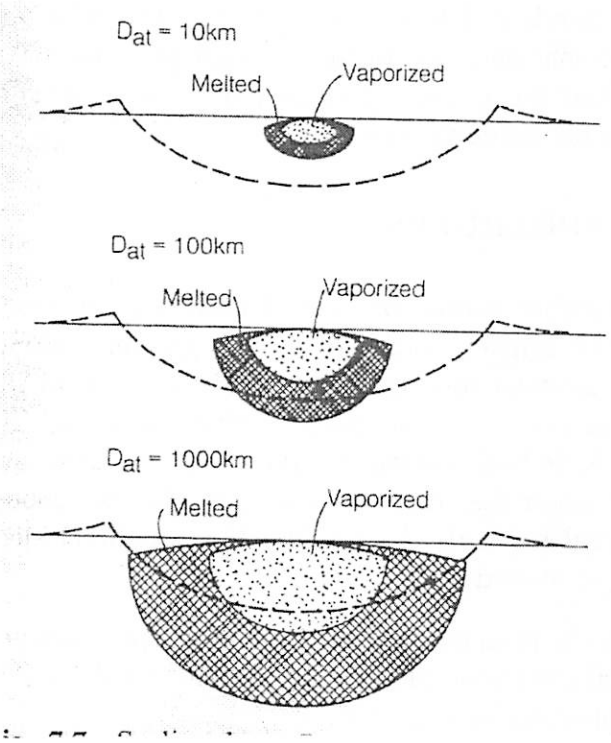

Fig. 1.— Sample volumes of vapor and melt from target material for impact craters on Earth of the listed diameters, assuming $v = 35$ km/s. Totally ripped off from Melosh (1989)

the mass of the impactor is a strong function of the collision velocity, v (Melosh 1989):

$$\frac{M_{\rm melt}}{M_{\rm bolide}} = 0.14\ \frac{v^2}{\epsilon_{\rm m}}.$$

Melosh (1989) also furnishes an expression for the mass of vaporized material:

$$\frac{M_{\rm vapor}}{M_{\rm bolide}} = 0.4\ \frac{v^2}{\epsilon_{\rm v}},$$

where $\epsilon_{\rm m}$ and $\epsilon_{\rm v}$ are the specific heat of melting and vaporization respectively. $\epsilon_{\rm m} = 3.4 \times 10^6$ J/Kg and $\epsilon_{\rm v} = 5.7 \times 10^7$ J/Kg for gabbroic anorthosite (whatever THAT stuff is – sounds like a rock to me). The first expression is only valid for $v > 14$km/s, the second for $v > 35$km/s (see p122 of Melosh (1989) for more info).

However, these expressions imply that $0.14mv^2 + 0.4mv^2$ is the total amount of energy used to both melt and vaporize target rock. This seems highly unlikely to me, seeing as the total amount of energy had better only be $0.5mv^2$ – for the rest of this handout I have assumed that the 0.14 and 0.4 coefficients are both too high by a factor of 2. Thus the actual values may differ substantially from my made-up one.

2. SPHERULES

Another source of melted material generated by the impact comes from the gaseous plume. The gaseous rock condenses as it cools into little melted balls of magma that later solidify into little balls variously called microtektites, impact spherules, or microkrystites (Lorenz 2000). Spherules can also be produced by the direct ejection of melted target material.

In the presence of an atmosphere, spherules get distributed around the crater. The total volume of spherules produced is:

$$V_{\rm spherules} = 3.8 \times 10^{-4} R_{\rm crater}^{-3.38}$$

for $R_{\rm crater}$ in km (Lorenz 2000). Large enough impactors (¿ a few hundred meters in diameter for Earth and Mars) can blow off the atmosphere and globally distribute the spherules (Lorenz 2000).

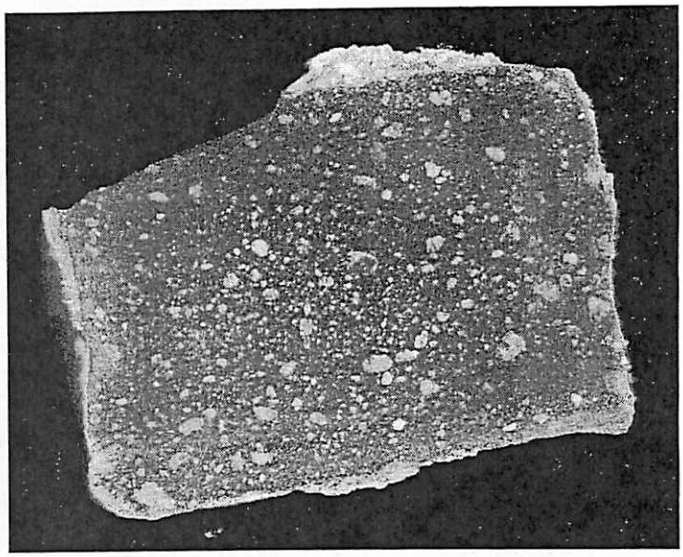

Fig. 2.— Polished section of impact melt from Vredefort. From `http://www.impact-structures.com/melt/impactmeltpage.html`

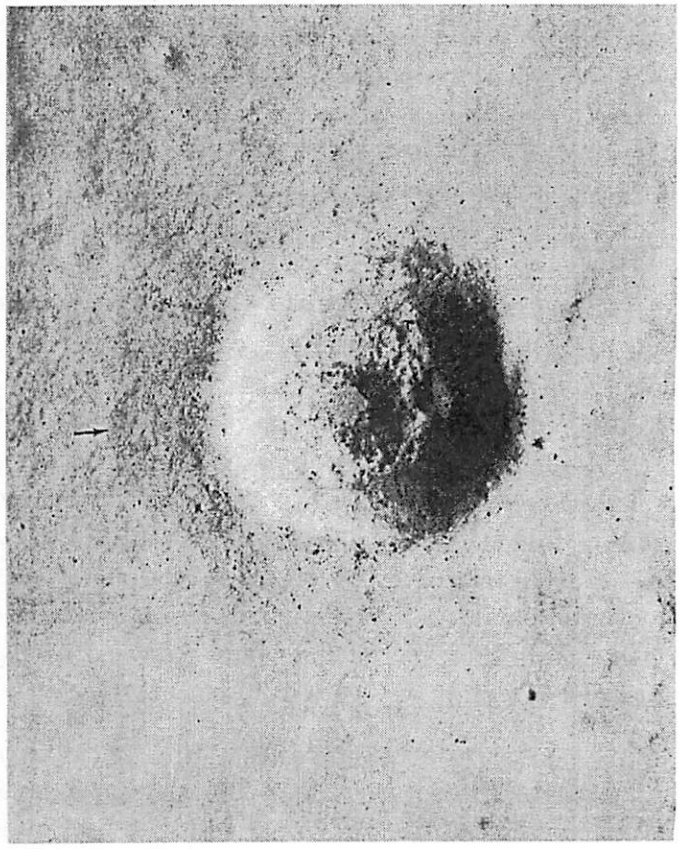

Fig. 3.— 1.2 km impact crater on the Moon as viewed from Apollo 16. Jay thinks that the flat, dark, smooth part in the middle may be impact melt. NASA AS15-9287.

There had been some speculation (on flame anyway) that the Blueberries (Figure 6) discovered by the MER-B rover Opportunity might in fact be impact spherules. Their size and presence on Mars are certainly consistent with this hypothesis. The rover team has recently ruled out impact spherules, however, in favor of hematite-rich undersea concretions on the basis of their chemical composition and their scattered presence in the bed – you would expect spherules to exist preferentially in horizon layers, barring extremely rapid bed deposition or extremely long-lived spherules.

3. MELT IN SIERRA MADERA AND ODESSA CRATERS

To my [wholly inadequate] knowledge, no impact melt has been found in or around Sierra Madera crater, possibly because of the highly eroded nature of the structures that are left at this point. However, some impact breccias around Odessa have been found to contain a small fraction of melted material. The craters themselves are small enough that the total volume of melt produced should have also relatively small in total, such that it is not as surprise that the Odessa craters lack melt lakes.

REFERENCES

Lorenz, R. D. 2000, Icarus, 144, 353

Melosh, H. J. 1989, Impact cratering: A geologic process (Research supported by NASA. New York, Oxford University Press (Oxford Monographs on Geology and Geophysics, No. 11), 1989, 253 p.), 45–+

This 2-column preprint was prepared with the AAS LaTeX macros v5.2.

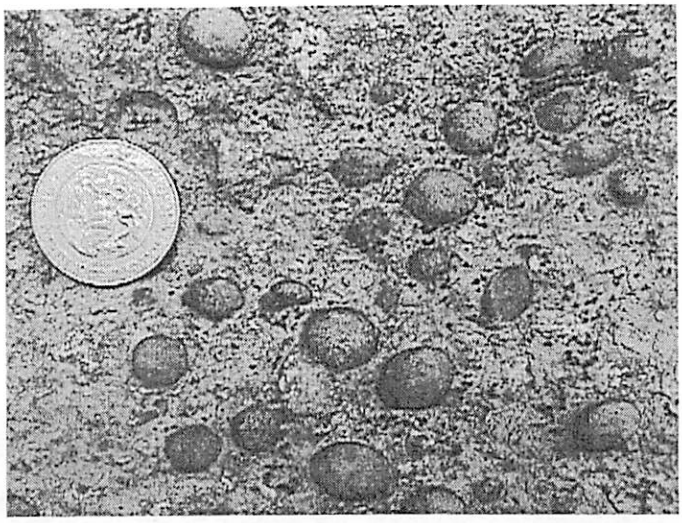

Fig. 4.— Impact spherules on the Earth, from distal K/T boundary layer sediments. The chemical composition of the spherules is similar to that expected to have condensed from the impact vapor plume. From `http://www.ehu.es/ gpplapam /congresos/bioeventos/claeys.html`

Fig. 5.— Magellan radar image of a Venusian impact crater. Ralph thinks that the parabolic curve of black material is a layer of spherules at least ~ 5 cm thick. Shamelessly stolen from Lorenz (2000).

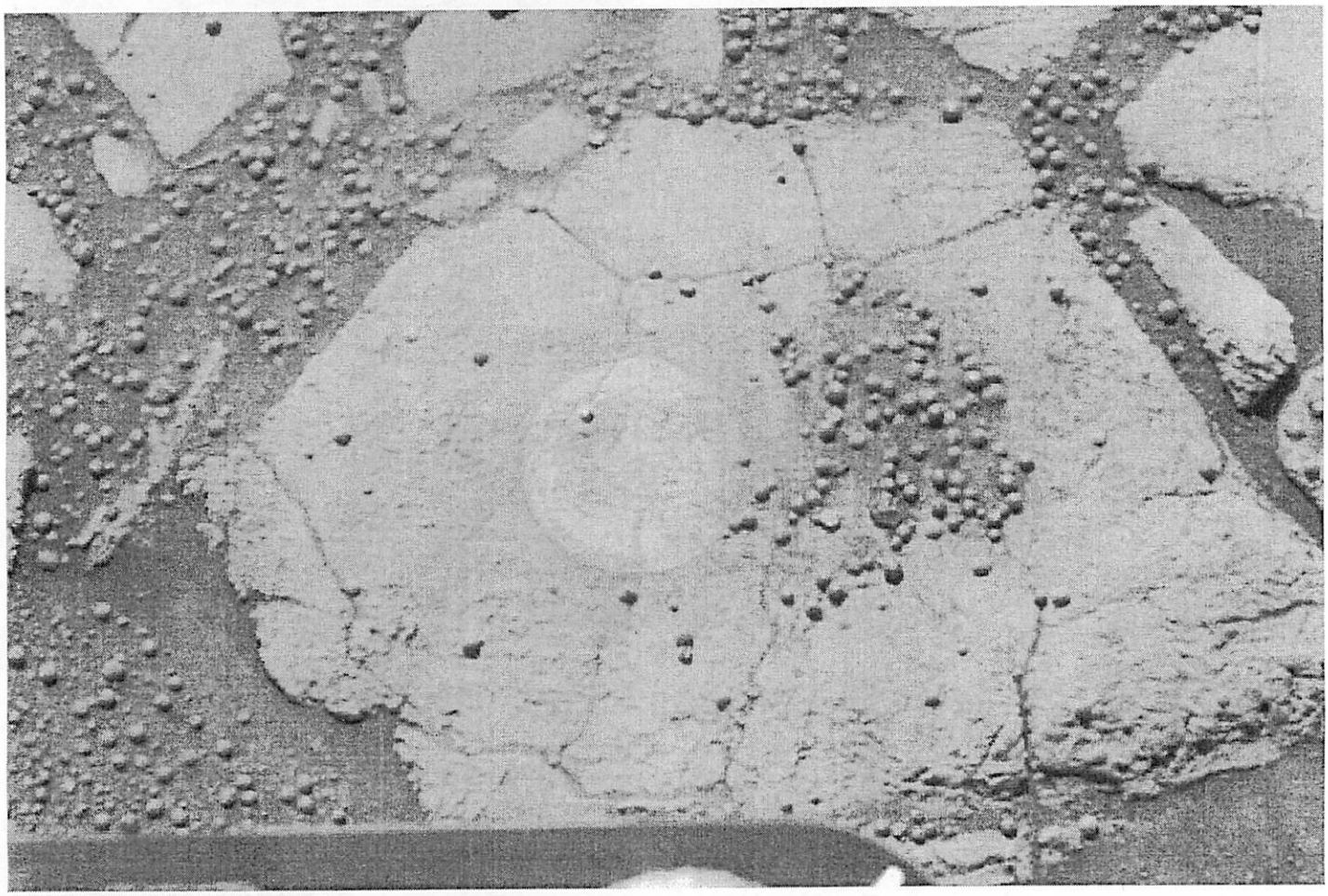

Fig. 6.— Blueberries detected by Opportunity at Eagle Crater, Terra Meridiani, Mars. They are each a few mm across.

LPLGrad Rover goes to Planet Texas!

A study plan for Odessa Crater (minor)
Jani Radebaugh

We will be touching down in the middle of the small crater adjacent to Odessa Meteor Crater in West Texas on April 3, 2004. What should we study? How can we maximize our time (1 short Earth day!) on Texas' surface? We use the tour of Opportunity Rover in the similar-sized Eagle Eye Crater (22 m or 72 feet in diameter), Mars, for comparison.

What do we want to learn?

A. Composition of soil and current/recent ability of region to be habitable –or--
B. Composition of bedrock and past processes - use impact crater as an excavator

For A:

Do what Opportunity did! Stay within crater, dig trenches in various locations and conduct detailed soil surveys. See how soils inside the crater relate to soils on the surrounding plains and near contacts (near the rock layers within the crater).

View from rover on crater rim, looking back at landing platform

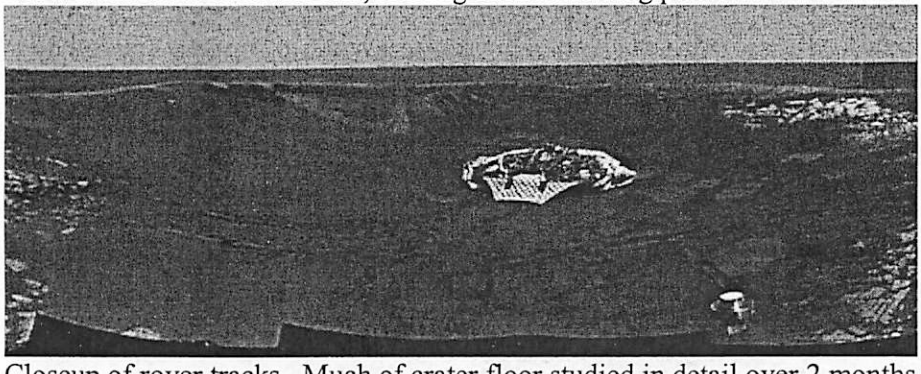

Closeup of rover tracks. Much of crater floor studied in detail over 2 months.

If you were to find:

1. Soils on crater floor are similar to surrounding rock layers (or evaporite-rich in Eagle Eye Crater)
    a. = erosion of surrounding layers yielded current soils, through water, wind, impact gardening, slumping
2. Soils on crater floor are unlike the composition of surrounding layers
    a. = Dust has blown in from surrounding regions, and may find similar composition to the soils on plains

Opportunity digs in soil with wheels to determine soil color, cohesiveness, grain size

3. Soils have carbonates and…fossils!
    a. = Jackpot! But were these carried in by other processes, or did your crater form a small lakebed in the past? Look for layering to your deposits.
4. Look carefully, you may find some chunks of the impactor! Would you be able to differentiate between these and lithics in the soil?

For B: (more preferable, in my opinion, so it's our course of action!)

First, take a careful look at the rock layers exposed in the crater on your way out, these are a natural "road-cut" down into layers that represent past time. Look at these layers carefully in different sections to watch for similarities and differences.

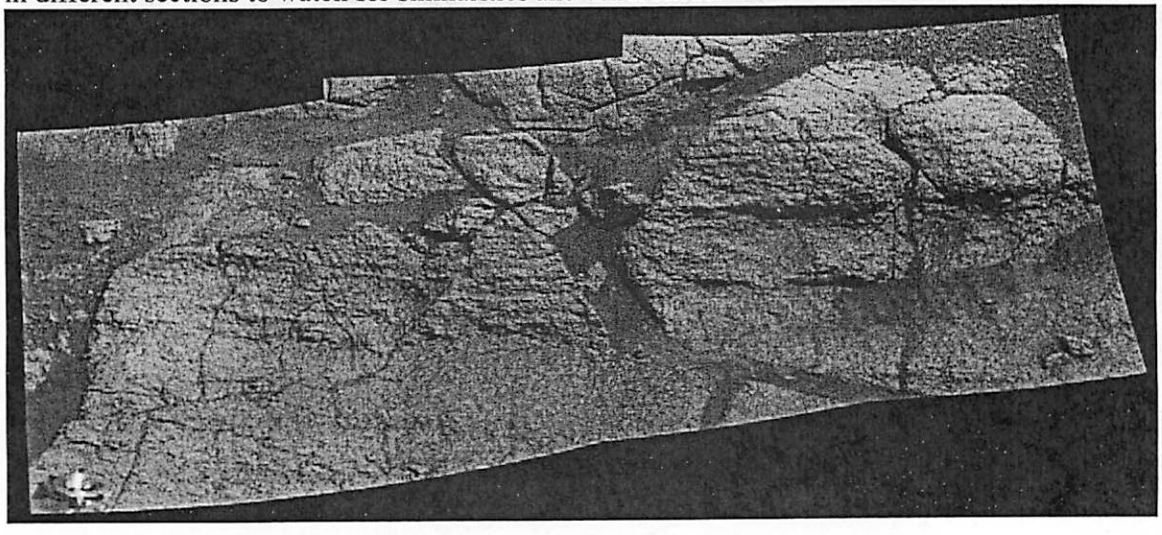

If you see:

1. Tilted layers
    a. = disruption of original horizontality (most likely) by impact process
    b. If tilting seems to have a more regional orientation, it may have predated the crater, and will give you information about the tectonics of the region
    c. Look for cross bedding, indicating wind or water effects at time of deposition
2. Repeated layers
    a. = overturning of beds by impact process, similar to Meteor Crater, AZ
    b. = transgressions/regressions of shallow sea (possible here on Texas!)

What are their compositions?? Use your abrasion tools and spectrometers to tell you the rock chemistries.

It is flat in this part of Planet Texas, and slopes gently down to the current shoreline. Therefore, we could be on part of an ancient seabed (perhaps the Cretaceous Interior Seaway?) so we should see limestones and other shallow sea deposits. In fact, we are in a Permian basin, so we should expect marine deposits (and evaporates!). What if there were volcanic ash beds? We can use those to help us date the events (topaz fission-track, Rb-Sr in plagioclase).

Now, get out of the crater!

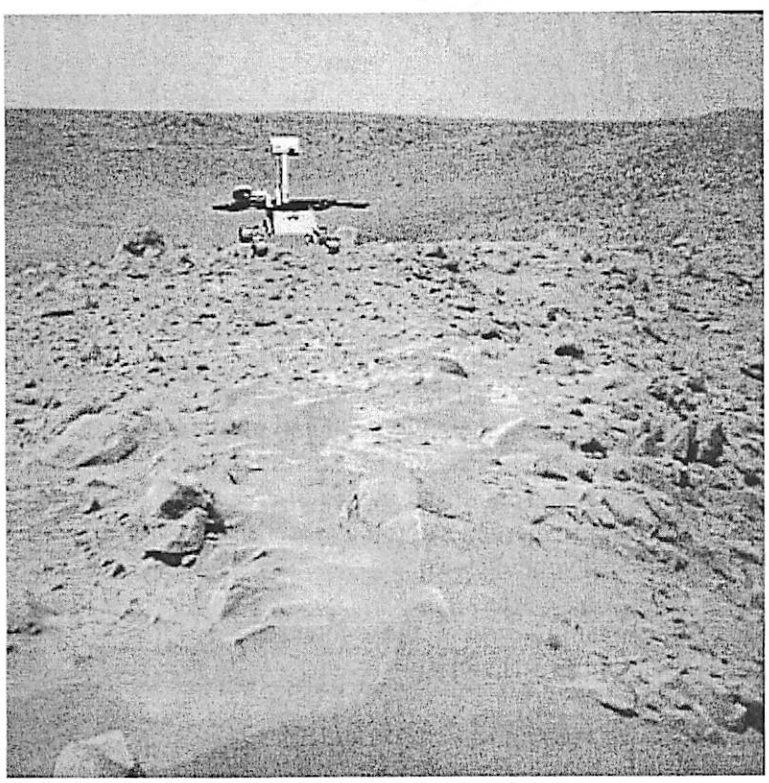

The impact process has done your excavating for you, so now go look at the ejecta for clues to underlying compositions. Whole large blocks and boulders must have been excavated from the crater (and not brought in by water or wind later, as much of the dust is likely to have been), so look at these for compositions of rocks below.

Lastly, a "sol-by-sol" survey of Odessa Crater Minor:
(One Texas sol is about 30 Earth minutes)

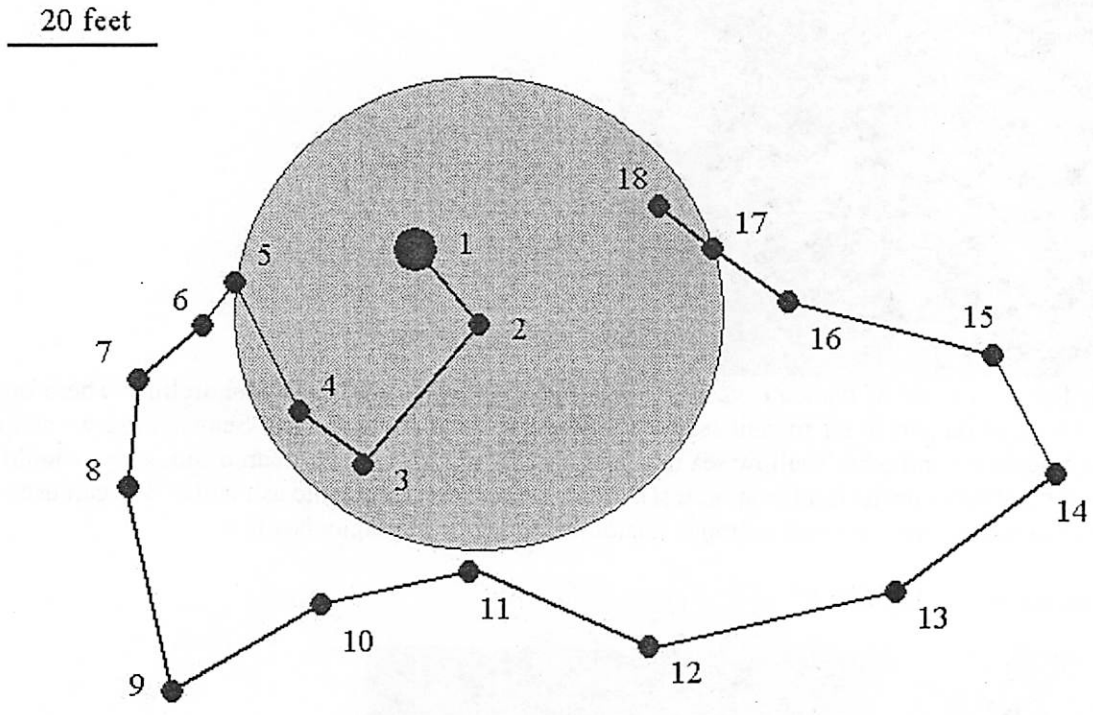

Sols:
1 – Touch down! Take pictures, sample atmosphere, roll off and sample soil
2 – Sample soil near crater center, dig with wheels
3 – Study layers near rim – APXS, Mini-TES, hi-res imager
4 – Move across section in layers, do comparative study with location 3
5 – Move up section in layers to crater rim, do same as 3 and 4, take panoramic images
6 – Sample near-rim ejecta, look at soil and boulders, compare with soil and rocks in crater
7-9 – Sample increasingly more distant ejecta, target facies changes, or different soil colors
9-11 – Move back toward crater rim, sampling ejecta from different side of crater
11-14 – Rove to most distant point away from crater margin, sampling ejecta and recording size change, differences in soil and rock compositions, wind directions
14-16 – Move back toward crater rim
17 – Sample layers and ejecta on crater rim comparatively with those found at 5
18 – Sample layers inside crater, compare with those at 3 and 4.

References:
Images from http://www.jpl.nasa.gov
Information about Odessa Crater from the University of Texas of the Permian Basin, http://www.utpb.edu/ceed/

10